Some Unpleasant Tropical Nights: Nighttime Heat, Commuting Accidents, and Climate Damages*

RAÚL BAJO-BUENESTADO

Department of Economics & NCID, University of Navarra

Baker Institute for Public Policy, Rice University

October 2, 2026

Abstract

Climate change is increasing the frequency of abnormally hot nights (*tropical nights*), which disrupt sleep and impair cognition, exposing workers to risks the following day. I examine one measurable example of these risks—commuting road accidents—using data on the universe of such accidents in Spain and exploiting granular variation in weather. Tropical nights increase this risk by about 15%, accounting for roughly one in eight commuting accidents the following day, with the magnitude varying with adaptation. Patterns across accident timing and trip purpose are consistent with sleep disruption. The increase is disproportionately concentrated among women—with evidence pointing to gendered time use as an underlying mechanism—and is higher in lower-income areas. Using projections from 11 climate models, I estimate annual social costs exceeding 1€ million, even allowing for adaptation. These findings speak to potential benefits of flexible start times and working from home arrangements, particularly for working mothers.

Keywords: Climate change; Nighttime heat; Commuting accidents; Climate adaptation; Workplace flexibility; Sleep disruption; Labor-market gender gaps.

JEL Classification Numbers: J16, J22, J28, Q51, Q54, R41.

*Department of Economics, Edificio Amigos, University of Navarra, 31009 Pamplona, Spain; Navarra Center for International Development (NCID), University of Navarra; and Baker Institute for Public Policy, Rice University. Email: rbajo@unav.es. Part of this paper was written while I was visiting the University of Pennsylvania. I thank Guillermo Caruana, Natalia Fabra, Gerard Llobet, Jisung Park, and Paul Stainier for helpful conversations. I also thank seminar participants at CEMFI (FIRMS seminar), the University of Navarra (NCID seminar), and the 2026 World Congress of Environmental and Resource Economists (Nova Lisbon) for their comments. I gratefully acknowledge financial support from Fundación Ramón Areces and the Ministry of Science, Innovation, and Universities (grant PID2023-153142OB-I00). All errors are my own.

1 Introduction

Climate change is making nights warmer around the world. While much attention to extreme heat focuses on record high temperatures, an increasingly consequential but less visible dimension of global warming is the rapid and widespread increase in minimum temperatures (Alexander et al., 2006; Donat et al., 2013). This shift has raised the frequency of abnormally warm nights, commonly referred to as *tropical nights*—defined as nights during which temperatures remain above 20°C (WMO, 2009).[1] This matters because nighttime is when the body recovers: elevated nighttime temperatures reduce sleep duration and quality, especially when households lack access to cooling infrastructure (Obradovich et al., 2017; Minor et al., 2022). Poor sleep, in turn, impairs cognitive function, reaction time, and executive performance, with consequences for tasks requiring attention and rapid decision-making (Gibson and Shrader, 2018; Jagnani, 2024). This paper studies whether these consequences appear in a routine but high-stakes activity: commuting to work.

Understanding these implications speaks to the climate-economics literature on the costs of rising temperatures and to labor research on worker safety. A large body of evidence links extreme heat to mortality, health, labor supply, and productivity (Graff Zivin and Neidell, 2014; Barreca et al., 2016; Somanathan et al., 2021), while related studies show that environmental conditions also shape workplace safety and accident risk (Dillender, 2021; Drescher and Janzen, 2025; Lavy et al., 2025). Yet much less is known about whether increasingly prevalent nighttime heat generates economic costs through impaired rest. Commuting accidents provide a natural setting to study this margin because driving to work is a widespread,[2] routine, time-constrained, and attention-intensive activity that cuts across occupations. Moreover, the stakes are high: these accidents generate substantial human and economic costs (Smith, 2016; Sager, 2019)—existing evidence suggests that commuting accidents can involve more severe outcomes than workplace accidents (Vargas-Garrido et al., 2021).

To examine this question, I rely on confidential administrative records from Spain's traffic authority covering the universe of commuting traffic accidents in Spain from January 2014 to December 2019. Commuting accidents are recorded as a separate category due to their distinct legal status under Span-

[1] This trend is visible in Spain (the setting studied here) and also in the broader European context. Long-run historical records show a marked rise in the frequency of tropical nights, and climate projections point to sizable further increases over the twenty-first century (see Figures A.1 and A.2, Appendix A).

[2] More than one-quarter of passenger journeys in the European Union (EU) are commuting trips (Salminen, 2012).

ish law. The dataset reports the timing and location of each accident and the municipality of residence of each driver. I aggregate the accident records by municipality-day and merge them with daily municipality-level weather measures obtained from the Spanish Meteorological Agency's national station network; this allows me to link nighttime temperature exposure in the municipality of residence to accident risk on the following day. The analysis focuses on the pre-pandemic period, when remote work remained limited in Spain; commuting trips were therefore largely non-discretionary, leaving workers with limited scope to avoid or reschedule travel after unpleasantly warm nights.

I show that tropical-night days, on which minimum temperatures exceed 20°C—a threshold linked to shorter sleep duration and poorer sleep quality (Teyton et al., 2022; Bigler and Janzen, 2024)—substantially increase commuting accident risk. Specifically, exploiting granular variation in minimum temperatures and controlling for other weather conditions and a rich set of temporal and geographic fixed effects, I find that the number of commuting drivers involved in traffic accidents rises by about 14-16% relative to otherwise comparable days. This effect is stable across increasingly demanding specifications and a range of robustness checks, including alternative outcome definitions and exposure-assignment restrictions. Additional empirical tests rule out same-day daytime heat as a potential explanation and lend support to the interpretation that sleep disruption is a key mechanism: the effect is larger for early-day commuting accidents and appears for other routine work- and school-related trips, but disappears for more discretionary travel.

My estimates imply that roughly one in eight commuting-driver accident involvements following a tropical night during my sample period is causally attributable to nighttime heat. This translates into approximately 103 excess casualties and an aggregate social cost of about 4.6€ million in the sample municipalities alone, excluding direct costs to firms. The magnitude of this toll indicates that nighttime heat generates substantial human and economic costs along a margin that has received little attention in climate-damages research and remains largely unexplored in the labor literature, shedding light on a novel channel through which climate change affects workers and may reduce labor productivity.

While the estimates above reflect an average effect, the costs of nighttime heat are not evenly distributed. I leverage the richness of the data to examine heterogeneity across places and workers, identifying where and among whom the burden of rising nighttime temperatures is likely to be most concentrated and where targeted policies may be most valuable. First, consistent with adaptation to repeated

heat exposure, the estimated effect is largest in municipalities with cooler nighttime climates and attenuates as municipalities with warmer nighttime climates enter the sample. This pattern suggests that historically cooler areas may face larger short-run damages as climate change exposes them to more tropical nights, while adaptation remains limited.

Second, I uncover pronounced gender disparities, with tropical nights increasing female drivers' accident involvement by about 30%, while the estimates for men are smaller and statistically imprecise. Part of this pattern may reflect differential physiological vulnerability to heat; consistent with this channel, the effect among women is largest around the menopausal transition—when heat sensitivity tends to intensify. Beyond physiological vulnerability, the larger accident risk among female drivers also appears to reflect gendered time constraints and unequal childcare responsibilities. Three pieces of evidence point in this direction: *(i)* the share of commuting drivers involved in accidents traveling with a minor is 80% higher for women than for men; *(ii)* the female-male gap disappears among drivers under 30, for whom child-related responsibilities are likely less prevalent; and *(iii)* the gap is more pronounced for speed-related accidents, consistent with women facing tighter time constraints. These results reveal an underexplored gendered dimension of climate damages and suggest that flexible-work policies may help mitigate the unequal work-related risks I document—complementing evidence on the role of workplace flexibility in shaping gender gaps in labor-market outcomes (Wiswall and Zafar, 2018).

Third, motivated by socioeconomic differences in access to cooling infrastructure and housing insulation (Barreca et al., 2016; Memmott et al., 2021; Doremus et al., 2022), I examine heterogeneity by local income. My results indicate that the accident burden from tropical nights is larger in lower-income municipalities, with systematically higher point estimates than in high-income municipalities and implied excess accidents roughly 1.5-2 times larger under a conservative calculation. This pattern is consistent with the broader climate-adaptation literature showing that economically disadvantaged households are less able to shield themselves from extreme heat, and points to the value of targeting cooling and housing-improvement policies to lower-income communities.

To assess how the accident burden may evolve as nights become warmer, I combine my estimates with station-level projections of tropical-night exposure from 11 state-of-the-art global climate models, spanning four emissions scenarios and three 30-year horizons. I show that, absent further adaptation, excess casualties rise under all emissions scenarios; by the long term, they increase more than fourfold

under the high-emissions scenario and more than sixfold under the very-high-emissions scenario, with annual social costs reaching about 3.4€ million and 5.0€ million, respectively. I then use the heterogeneity documented above to construct an adaptation-adjusted projection. Even with adaptation, the burden remains sizable: annual social costs reach approximately 1.2-1.4€ million across the four scenarios, remaining about 50-80% above the present-day benchmark.

These projections highlight policy responses along two dimensions. First, adaptation policies that improve sleeping conditions during hot nights (e.g., access to cooling technologies or better housing quality) can weaken the link between nighttime heat, impaired sleep, and next-day risk, especially for lower-income households. Second, the results point to a labor-market policy margin: flexible start times or temporary work-from-home (WFH) arrangements can reduce exposure to routine work-related activities, such as commuting, when impaired rest may make them riskier.[3] Given the gender heterogeneity documented above, this margin may be especially valuable for female workers with childcare responsibilities, complementing evidence on the role of WFH and flexible work in reshaping gender differences in commuting costs, working time, and earnings (Le Barbanchon et al., 2021; Arntz et al., 2022).

The contribution of this paper is threefold. First, it identifies nighttime heat as an economically relevant but understudied source of climate damages by documenting an important labor-market margin through which these damages materialize. Whereas much existing work studies heat through contemporaneous exposure while people work (Dillender, 2021; Cabral and Dillender, 2024; Lavy et al., 2025; Drescher and Janzen, 2025), I show that hot nights can generate sizable next-day costs by impairing rest, with implied damages reaching millions of euros in the setting of commuting accidents alone and projected to grow as climate change makes nights warmer. This result points to a channel through which climate change may affect workers and reduce labor productivity even when direct heat exposure on the job is limited, complementing earlier studies on the role of sleep in labor-market and human-capital outcomes (Gibson and Shrader, 2018; Bessone et al., 2021; Giuntella et al., 2026) and evidence that sleep shapes cognition and decision-making (Carrell et al., 2011; Escobar Carias et al., 2024).

Second, much of the literature on heat-induced productivity losses and worker safety focuses on specific sectors where workers are physically exposed to extreme temperatures, such as agriculture,

[3]This labor-market policy margin is already present in employer and policy discussions during heat episodes. For example, UK guidance emphasizes flexible working patterns (Health and Safety Executive, 2026), and employer groups, unions, and officials have discussed WFH or flexible schedules during heatwaves (The Guardian, 2022; CIPD, 2024).

construction, and manufacturing (Graff Zivin and Neidell, 2014; Zhang et al., 2018; Somanathan et al., 2021). By contrast, I broaden the scope of labor-market climate damages beyond highly exposed sectors by studying nighttime heat, which can affect workers regardless of occupation. I document this broader margin by studying commuting accidents, a widespread and high-stakes but largely overlooked form of work-related risk that is often more severe than workplace accidents (Vargas-Garrido et al., 2021).

Finally, the paper contributes to research on the distributional incidence of climate damages by showing that this toll is not borne equally, pointing to where and for whom targeted adaptation policies may be most valuable. The estimates reveal large gender differences, with the burden overwhelmingly concentrated among female workers and effect sizes roughly twice as large as the average estimate. This gender pattern connects the paper to recent work on the gendered costs of commuting and the role of workplace flexibility in improving women's labor-market outcomes (Petrongolo and Ronchi, 2020; Le Barbanchon et al., 2021; Borghorst et al., 2024). The burden is also larger in historically cooler areas, consistent with adaptation to repeated heat exposure (Barreca et al., 2016; Carleton et al., 2022), and in lower-income places, consistent with evidence on unequal household capacity to protect against extreme temperatures (Doremus et al., 2022).

The rest of the paper proceeds as follows. Section 2 describes the data and empirical strategy. Section 3 presents the main estimates, mechanism tests, and robustness checks, while Section 4 examines heterogeneity by local climate, gender, and income. Section 5 uses climate-model projections to quantify future damages under alternative scenarios. Finally, Section 6 concludes.

2 Empirical framework

To examine how nighttime heat affects commuting accident risk on the following day, my analysis combines administrative records on traffic accidents with high-frequency, station-level weather data and municipality-level socioeconomic data. I first describe these data sources and the construction of the sample, and then turn to the empirical strategy.

2.1 Data and sample

Commuting accident data. I use a confidential dataset provided by the Directorate-General for Traffic (DGT), the agency within the Spanish Ministry of the Interior responsible for road safety and traffic

regulation. The dataset covers the universe of commuting traffic accidents in Spain between January 1, 2014, and December 31, 2019. For each accident, it records the time and location and provides detailed information on drivers, vehicles, and accident circumstances, including driver gender and age, the presence of minor passengers, and recorded contributing factors.

Commuting accidents—technically called *in itinere* accidents—involve drivers traveling to or from work and are recorded as a distinct category by the DGT. This is because, under Spanish law, *in itinere* accidents are legally recognized as work-related accidents despite occurring outside the workplace. As a result, they fall under the same legal and insurance protections as on-site occupational accidents.[4] This legal status requires police officers and investigators to determine whether an accident occurred while commuting, supporting the consistent and accurate classification of the accident records that I use in the analysis.

The sample period ends in December 2019, before the COVID-19 pandemic disrupted commuting patterns through lockdowns and the subsequent diffusion of remote work. This timing is important because, prior to the pandemic, remote work remained limited in Spain: the country had one of the lowest rates of remote work in the EU, with the vast majority of workers commuting in person (Jerbashian and Vilalta-Bufí, 2024; Rubino et al., 2024). The 2011 Spanish Population and Housing Census—the last national population census before the pandemic—provides a benchmark for the importance of driving: an estimated 7.40 million employed people reported usually driving to work, representing 53.3% of employed respondents with a reported commuting mode. My analysis therefore captures commuting behavior under pre-pandemic conditions, when trips to and from work were largely non-discretionary, leaving workers with limited scope to avoid or reschedule travel in response to disruptions such as poor sleep the previous night.

The dataset comprises 73,735 commuting drivers involved in 57,505 traffic accidents, or just over 26 accidents per day on average (see Table A.1, Panels A and B). These accidents resulted in more than 82,500 casualties, including 1,241 fatalities. A potential concern is that commuting drivers are not necessarily the party at fault in every accident in which they are involved. For example, in a multi-driver collision, a commuting driver may be affected even if responsibility lies with a non-commuting driver. This concern is mitigated by the fact that more than two-thirds of all drivers involved in these accidents

[4] In several other European countries, labor-insurance systems similarly extend coverage to commuting accidents (Pecillo, 2012).

are commuting, and about half of the accidents involve only commuting drivers. I nonetheless report results restricting the sample to this subset, which ensures that any driver-side responsibility necessarily lies within the commuting-driver population.

The dataset records each driver's municipality of residence. I use this information to construct municipality-day counts of commuting drivers involved in traffic accidents, which I then merge with daily municipality-level weather data—allowing me to link drivers' residential exposure to nighttime temperatures with subsequent accident risk. A potential concern, however, is that some drivers may have spent the night preceding the accident outside their municipality of residence, creating measurement error in exposure assignment. For example, a worker may temporarily commute from a location other than her usual residence. To address this concern, I also report results restricting the sample to accidents occurring in close proximity to the driver's municipality of residence, thereby reducing potential exposure misclassification.

Weather data. I also use daily station-level weather records from the Spanish Meteorological Agency (AEMET).[5] The dataset covers 858 weather stations distributed across Spain and is available from May 2013 to May 2023. The empirical analysis uses the January 2014 to December 2019 period, corresponding to the overlap with the traffic accident records—the full weather series is used only for auxiliary descriptive figures. For each station-day, the data report minimum and maximum temperatures in degrees Celsius (°C), the exact time (hour and minute) at which these temperatures are recorded, daily precipitation in millimeters, and maximum wind speed in kilometers per hour.

The station network provides broad coverage of populated areas in Spain, spanning 784 municipalities of which 23 have populations exceeding 200,000. Overall, municipalities with at least one station account for more than half of the total national population. Figure A.3 (Appendix A) maps the station network alongside municipal population in 2019. Because Spanish municipalities are small local administrative units, I assign weather conditions to each municipality using the station located within it. Two exceptions arise. First, when multiple stations are available within a municipality, I average weather conditions across stations. Second, municipalities without a weather station are assigned weather conditions from the closest station (as the crow flies). These municipalities are mostly small (typically with populations below 10,000) and, individually, they generally account for few commuting accidents—the

[5]The data was curated by https://datosclima.es/Aemet2013/Datosporestacion.html, and cannot be publicly redistributed.

main results are virtually unchanged when they are excluded from the sample.

A tropical night is commonly defined by meteorological and environmental agencies such as the World Meteorological Organization (WMO, 2009), the European Environment Agency (EEA, 2020), and the UK Met Office (Met Office, 2025) as a night in which temperatures remain above 20°C. European climate-risk monitoring classifies tropical nights as a high-priority extreme-heat index with particular relevance for human health (Crespi et al., 2020; European Environment Agency, 2021)—in part through sleep disruption, which is itself associated with adverse health outcomes and higher mortality (Cappuccio et al., 2010; Zheng et al., 2024; Zhang et al., 2025).[6] Direct evidence on sleep from both wearable-measured and self-reported outcomes confirms that temperatures near and above 20°C reduce sleep duration, increase the probability of trouble sleeping, and worsen perceived sleep quality relative to lower temperature ranges (Teyton et al., 2022; Wang et al., 2023; Bigler and Janzen, 2024).

I therefore follow this standard definition (and its well-documented relevance for sleep and rest) and classify a municipality as experiencing a tropical night on any day for which the minimum temperature recorded during the 24-hour period (from midnight to 11:59 p.m.) exceeds 20°C. This classification is supported by the timing of daily minimum temperatures in my dataset: as shown in Figure A.4 (Panel A), the daily minimum is recorded during late-night or early-morning hours in the vast majority of cases (about 85%). In these instances, the recorded minimum closely reflects nighttime thermal conditions.

In a smaller share of observations (approximately 12%), however, the daily minimum is recorded late in the evening (after 11:00 p.m.), reflecting cooling conditions during the following night.[7] Still, when the recorded daily minimum exceeds 20°C in these cases, the classification remains valid, since temperatures must also have exceeded the tropical-night threshold during the preceding night. The relevant concern instead involves false negatives: if the minimum falls below 20°C late in the evening, the procedure may fail to classify the preceding night as tropical even if temperatures remained above the threshold overnight. I therefore also report a robustness check excluding observations for which the daily minimum is recorded after 11:00 p.m.

[6]The health relevance of tropical nights is also supported by epidemiological evidence linking the same 20°C threshold to adverse health outcomes (Royé et al., 2021; Rippstein et al., 2023). Physiological and review evidence further links heat exposure during sleep to disrupted rest and poorer sleep quality (Okamoto-Mizuno et al., 1999; Okamoto-Mizuno and Mizuno, 2012; Chevance et al., 2024).

[7]This share is below 5% among tropical-night days; in approximately 93% of tropical-night observations, the minimum temperature occurs during late-night or early-morning hours—see Figure A.4 (Panel B).

Sample construction. A distinctive feature of my empirical setting is Spain's pronounced climatic diversity: the country is among the most climatically heterogeneous in Europe, with substantial spatial variation in nighttime temperatures—and, consequently, in the prevalence of tropical nights—driven by factors such as proximity to the coast, elevation, and insularity (Comín et al., 2019). Figure A.5 (Appendix A) illustrates this variation by mapping average monthly minimum temperatures across municipalities by quarter of the year. The spatial differences are large, with some municipalities experiencing average minimum temperatures above 15°C even during spring and fall, while others record average minimum temperatures below 10°C even during the summer months.

Given this spatial heterogeneity, my baseline empirical analysis focuses on municipalities where tropical nights are relatively uncommon. Specifically, I restrict the main sample to municipalities whose monthly average minimum temperatures remain below 19°C—over 76% of Spanish municipalities are included in this sample.[8] The rationale is that in municipalities where tropical nights occur frequently, residents are presumably more likely to be acclimatized or better equipped to cope with nighttime heat, including through air conditioning (AC) ownership.[9] In Section 4.1, I explicitly examine the effect across samples defined by alternative thresholds of monthly average minimum temperature. Specifically, I show that the estimated effect becomes larger when the sample is further restricted to municipalities with cooler nighttime climates, and becomes progressively attenuated as municipalities with warmer climates enter the sample—a pattern consistent with adaptation to repeated nighttime heat exposure.

Income and auxiliary data. I also obtain municipality-level income data from the Spanish National Statistics Institute (INE). The INE reports annual average net and gross household income at the census-block level for 2015-2019. I aggregate this data to the municipality level and average it across years to construct a cross-sectional measure of local income for the heterogeneity analyses. In addition, I use data from Idealista on the share of homes equipped with AC across Spanish provincial capitals to provide descriptive evidence on adaptation to nighttime heat. Finally, additional DGT records on non-commuting traffic accidents allow me to compare routine, time-constrained trips with more discretionary travel categories in auxiliary analyses.

[8] Figure A.6 (Appendix A) maps the municipalities included in this sample. The sample includes Madrid and other municipalities in its metropolitan area and several large metropolitan areas in northern and inland Spain, including the three main metropolitan areas of the Basque Country, the two major metropolitan areas in Galicia, Asturias, and Valladolid, among others.

[9] Figure A.7 (Appendix A) provides suggestive evidence of this by showing that places with higher average nighttime temperatures also exhibit higher rates of AC ownership.

2.2 Empirical strategy

I examine how nighttime heat affects commuting accident risk by regressing daily municipality-level counts of drivers involved in *in itinere* traffic accidents—that is, accidents occurring while traveling to or from work—on bins of daily minimum temperature. The specification includes a separate indicator for tropical-night days, defined as days on which the minimum temperature exceeds 20°C. As discussed above, this cutoff is not only the standard tropical-night definition (WMO, 2009; EEA, 2020), but also a sleep-relevant threshold above which nighttime temperatures are associated with shorter sleep duration and poorer sleep quality (Teyton et al., 2022; Bigler and Janzen, 2024).

Given that the outcome is a non-negative count variable, I estimate Poisson fixed-effects models by pseudo-maximum likelihood (PPML). This approach accommodates the large number of zero-accident municipality-days while providing a flexible way to model the conditional mean of accident risk. Specifically, I estimate variants of the following regression model:

$$\mathbb{E}\left[Y_{it} \mid X_{it}\right] = \exp\left(\sum_{j \in \mathcal{J}} \alpha^j T_{it}^j + \boldsymbol{Z}_{it}'\boldsymbol{\beta} + \gamma_i + \nu_w + \mu_{pm} + \lambda_d\right), \tag{2.1}$$

where Y_{it} denotes the number of drivers residing in municipality i who are involved in a commuting traffic accident on day t, with each day defined as the 24-hour period from midnight to 11:59 p.m. As a robustness check, I also estimate the model using only early-day commuting accidents (7:00 a.m. to 2:59 p.m.), when most commuting accidents occur and when drivers are most likely to be affected by heat exposure during the preceding night.[10]

On the right-hand side (RHS), T_{it}^j denotes a set of indicators for bins of daily minimum temperature in municipality i on day t. As discussed above, daily minimum temperatures typically occur during nighttime hours and therefore capture nighttime thermal conditions (see Figure A.4, Appendix A). The robustness checks below assess the sensitivity of the results to the small share of observations that deviate from this pattern.

Following common practice in the climate-economics literature (Dell et al., 2014; Hsiang, 2016; Bigler and Janzen, 2024; Kuruc et al., 2025), I discretize the daily minimum-temperature distribution into 5-degree bins, ranging from temperatures below 0°C to temperatures above 20°C. The coefficient of in-

[10] Figure A.8 (Appendix A) reports the distribution of commuting accidents by time of day.

terest is $\alpha^{>20}$, corresponding to tropical-night days. In the Poisson model, $\left[\exp(\hat{\alpha}^{>20}) - 1\right]$ captures the estimated proportional change in commuting accident risk on tropical-night days relative to the omitted reference bin, which I define next.

In my baseline specification, I use the 15°C–20°C bin as the omitted category. This is because prior research identifies this temperature range as conducive to high-quality sleep for most adults (Wang et al., 2015), as the body requires relatively little thermoregulatory effort; colder temperatures may also impair sleep quality, particularly in poorly insulated homes. A potential concern, however, is the "knife-edge" nature of the tropical-night classification around the 20°C threshold. For example, a night in which the minimum temperature briefly falls to 19.9°C would be assigned to the reference bin even if temperatures remained close to 20°C for most of the night, making its thermal conditions similar to those of tropical nights. To address this concern, I also present estimates using a more conservative reference category. Specifically, I define the omitted bin as nights with minimum temperatures between 15°C and 18°C—a range aligned with the physiological optimum for restorative sleep (Wang et al., 2015)—and exclude the 18°C-20°C interval from the estimation sample. This specification removes borderline nights just below the tropical-night threshold from the comparison group, while providing a cleaner benchmark of favorable nighttime thermal conditions.

Next, $\boldsymbol{Z}'_{it}$ is a vector of weather controls that may affect accident risk, including precipitation, maximum temperature, and maximum wind speed. Equation (2.1) also includes a rich set of spatial and temporal fixed effects. The baseline specification includes municipality fixed effects (γ_i), which control for time-invariant differences across municipalities, and week-by-year fixed effects (ν_w), which absorb shocks and seasonal patterns common across municipalities. I also include province-by-month fixed effects (μ_{pm}), allowing seasonal patterns in accident risk to differ across provinces. Across specifications, I replace μ_{pm} with progressively more demanding spatial-seasonality controls: province-by-week, municipality-by-month, and municipality-by-week fixed effects. Some specifications also include day-of-the-week fixed effects (λ_d), which account for systematic variation in accident risk across the week.[11]

[11]Standard errors are clustered at the municipality level to allow for arbitrary serial correlation within municipalities. To address potential spatial correlation across nearby municipalities, Appendix B.1 reports the main results using spatially corrected Conley standard errors under alternative distance cutoffs.

3 Empirical results

3.1 Main results

Table 1 reports the estimated temperature-bin coefficients from equation (2.1). All specifications include the weather controls described above ($\boldsymbol{Z}'_{it}$) as well as municipality and week-by-year fixed effects. The table tests the robustness of the estimated coefficients to progressively more demanding controls for spatially varying seasonality. Column (1) adds province-by-month fixed effects; in this specification, identification comes from daily variation in nighttime temperature across municipalities within the same week-year, after netting out province-specific monthly seasonality. Columns (3), (5), and (7) replace these controls with province-by-week, municipality-by-month, and municipality-by-week fixed effects, respectively. The even-numbered columns add day-of-the-week fixed effects.

The estimates reveal a sharp increase in the number of commuting drivers involved in accidents on tropical-night days: the coefficient ranges from 0.128 to 0.147 and is statistically significant at the 1% level in every specification. This corresponds to a 13.7% to 15.8% increase relative to days with minimum temperatures in the reference category.[12] By contrast, the coefficients on all other temperature bins are small and generally statistically indistinguishable from zero.

The magnitude of the tropical-night effect is stable across columns, even though the more demanding fixed-effect specifications progressively drop additional singleton observations—observations that do not contribute to identifying the coefficient of interest once the fixed effects are absorbed (Correia, 2015; Correia et al., 2020). This attrition shifts the estimation sample toward municipalities with more frequent commuting accidents (fewer zero-accident days), raising the mean of the municipality-day outcome. At the aggregate daily level, however, the accident base is unchanged: mean accidents per day is 10.67 in every specification, and the implied increase associated with a tropical night ranges from 1.45 to 1.69 accidents per day. This stability suggests that the main result is not driven by the changing composition of municipalities retained by the fixed-effect structure.

To put these estimates in context, nighttime heat accounts for approximately one in eight commuting drivers involved in traffic accidents on tropical-night days in the baseline sample. Given the casualty profile of commuting accidents in this sample, the estimates imply approximately 103 excess casualties

[12] Percentage effects are computed as $100 \times [\exp(\hat{\alpha}^j) - 1]$, where $\hat{\alpha}^j$ is the estimated coefficient for temperature bin j.

Table 1. The impact of minimum nighttime temperature on commuting accidents

	(1)	(2)	(3)	(4)	(5)	(6)	(7)	(8)
≤ 0°C	0.0516	0.0758	0.0606	0.0889	0.0459	0.0712	0.0433	0.0729
	(0.0597)	(0.0618)	(0.0600)	(0.0619)	(0.0603)	(0.0626)	(0.0606)	(0.0628)
0–5°C	0.0054	0.0307	0.0115	0.0399	0.0014	0.0275	-0.0013	0.0280
	(0.0467)	(0.0469)	(0.0465)	(0.0467)	(0.0485)	(0.0488)	(0.0481)	(0.0485)
5–10°C	0.0282	0.0548	0.0359	0.0651*	0.0229	0.0508	0.0266	0.0572
	(0.0377)	(0.0383)	(0.0378)	(0.0384)	(0.0396)	(0.0405)	(0.0399)	(0.0409)
10–15°C	0.0255	0.0432	0.0276	0.0459	0.0154	0.0341	0.0146	0.0329
	(0.0352)	(0.0342)	(0.0350)	(0.0332)	(0.0376)	(0.0365)	(0.0376)	(0.0356)
$>$ 20°C (tropical night)	0.142***	0.135***	0.134***	0.128***	0.147***	0.139***	0.139***	0.132***
	(0.0487)	(0.0457)	(0.0502)	(0.0467)	(0.0494)	(0.0463)	(0.0514)	(0.0481)
Weather controls	✓	✓	✓	✓	✓	✓	✓	✓
Mun. & week-year FE	✓	✓	✓	✓	✓	✓	✓	✓
Prov. × month FE	✓	✓						
Prov. × week FE			✓	✓				
Mun. × month FE					✓	✓		
Mun. × week FE							✓	✓
Day-of-week FE		✓		✓		✓		✓
Tropical-night effect (%)	15.2	14.5	14.3	13.7	15.8	14.9	14.9	14.1
Mean dep. var.	0.007	0.007	0.008	0.008	0.024	0.024	0.062	0.062
Mean accidents/day	10.67	10.67	10.67	10.67	10.67	10.67	10.67	10.67
Daily Δ accidents	1.63	1.54	1.53	1.45	1.69	1.60	1.59	1.51
Pseudo-R^2	0.341	0.354	0.345	0.358	0.242	0.257	0.178	0.198
Observations	3,253,330	3,253,330	3,092,721	3,092,721	974,884	974,884	378,787	378,787

Notes: The dependent variable is the number of commuting drivers involved in traffic accidents. All columns are estimated by PPML. Temperature bins are defined using daily minimum temperature; the omitted category is 15°C–20°C. Weather controls include precipitation, maximum temperature, and maximum wind speed. Standard errors clustered by municipality are reported in parentheses. The tropical-night effect is computed as $100 \times [\exp(\hat{\alpha}) - 1]$, where $\hat{\alpha}$ is the coefficient on the $>$ 20°C bin. Mean dep. var. is the column-specific mean of the municipality-day outcome. Mean accidents/day is the mean number of commuting drivers involved in accidents per calendar day in the column-specific estimation sample. Daily Δ accidents is computed as $[\exp(\hat{\alpha}) - 1] \times$ mean accidents/day and refers to commuting drivers involved in accidents. Significance levels: * $p < 0.10$, ** $p < 0.05$, *** $p < 0.01$.

and a social cost of 4.6€ million over the sample period, according to the DGT-approved valuations reported by Pérez et al. (2015)—a figure that excludes broader economic costs associated with sick leave, reduced productivity, worker substitution, and administrative burden.[13] While tropical nights were relatively uncommon in the sample municipalities, the burden could substantially escalate as exposure rises. If these municipalities each experience eight additional tropical nights per year—roughly the midpoint between the average increases projected under the medium- and high-emissions scenarios for the medium-term horizon—my estimates would imply approximately 18 additional casualties and 0.8€ million in additional social costs per year—an increment roughly equal to the historical annual burden.

Section 5 provides a detailed projection analysis using granular climate-model projections.

3.2 Additional results and robustness checks

I next examine whether the main result in Table 1 is robust to alternative outcome definitions, sample restrictions that more closely align measured nighttime temperature with drivers' likely exposure, and alternative classifications of tropical-night exposure. Table 2 reports the coefficient on the tropical-night indicator under two representative specifications: the preferred baseline specification, which includes province-by-month and day-of-the-week fixed effects, and the most demanding specification, which includes municipality-by-week and day-of-the-week fixed effects. The full set of estimates across the eight specifications in Table 1 is reported in Table B.3 (Appendix B.2).

The first three rows in Table 2 address accident classification and exposure assignment. The first row restricts the outcome to accidents in which all drivers involved are classified as commuting. Since the baseline sample includes all commuting drivers involved in traffic accidents, this restriction removes (multi-vehicle) cases in which the crash may have been caused by a non-commuting driver. The estimated effect is larger than in Table 1, implying roughly a 21% increase, consistent with attenuation in the broader sample. The second row addresses potential mismatch between the municipality of residence and the location where the driver spent the preceding night. To reduce this source of measurement error, I restrict the sample to accidents occurring within the same province as the driver's municipality of residence. Given the relatively small geographic size of Spanish provinces, this restriction limits the scope for large discrepancies between recorded residential exposure and actual nighttime exposure. The estimates remain close to the baseline. The third row shows that the results are not driven by the assignment of weather from nearby stations: excluding municipalities without their own weather station yields estimates that are, if anything, slightly larger.

The remaining checks examine timing and threshold sensitivity. The fourth row excludes observations for which the daily minimum temperature is recorded after 11:00 p.m. On such days, the 24-hour minimum may partly reflect cooling during the following night rather than conditions during the pre-

[13]The calculation is based on the attributable share implied by the preferred coefficient, $[1 - \exp(-0.135)] = 0.126$. During the sample period, 30,322 commuting-driver involvements in the baseline municipalities are associated with 35,848 casualties—1.182 casualties per involvement. Applying this attributable share and rate to the commuting-driver involvements recorded on tropical-night days (690) yields approximately 103 casualties. Finally, I assume that these casualties follow the severity distribution in the same sample—90.89% minor injuries, 7.52% serious injuries, and 1.59% fatalities—and value them at 6,100€ per minor injury, 219,000€ per serious injury, and 1.4€ million per fatality, as reported by Pérez et al. (2015).

Table 2. Robustness of the tropical-night effect

	Preferred baseline Table 1, col. (2)			Most demanding Table 1, col. (8)		
Robustness check	Coef.	Effect (%)	Observations	Coef.	Effect (%)	Observations
All involved drivers are commuting	0.194*** (0.0741)	21.4	2,616,803	0.189** (0.0750)	20.8	247,847
Accident in same province as residence	0.124** (0.0503)	13.2	2,900,782	0.126** (0.0529)	13.4	336,304
Municipalities with weather station	0.151*** (0.0560)	16.3	517,439	0.155*** (0.0554)	16.8	131,453
Drop late-evening minimum temperatures	0.131*** (0.0433)	14.0	2,773,645	0.132*** (0.0458)	14.1	310,581
Early-day accidents only	0.148** (0.0709)	15.9	2,506,229	0.146** (0.0732)	15.7	242,894
Alternative omitted temperature bin	0.119** (0.0501)	12.6	3,104,805	0.127** (0.0517)	13.5	354,942

Notes: Each row reports the coefficient on the tropical-night indicator (minimum temperature above 20°C). All specifications are estimated by PPML and include weather controls, municipality fixed effects, week-by-year fixed effects, and day-of-week fixed effects. The preferred baseline specification additionally includes province-by-month fixed effects, while the most demanding specification instead includes municipality-by-week fixed effects. The omitted temperature category is 15°C–20°C, except in the final row, where the omitted category is 15°C–18°C. Percentage effects are computed as $100 \times [\exp(\hat{\alpha}) - 1]$, where $\hat{\alpha}$ is the coefficient on the $>$ 20°C bin. Standard errors clustered by municipality are reported in parentheses. Significance levels: * $p < 0.10$, ** $p < 0.05$, *** $p < 0.01$.

ceding night. The estimates are nearly unchanged. The fifth row restricts the outcome to early-day commuting accidents (7:00 a.m. to 2:59 p.m.), when drivers are most likely to be affected by heat-related sleep disruption. The estimated effects are somewhat larger than in Table 1, consistent with the sleep-disruption interpretation. The last row uses a narrower omitted temperature bin, 15°C-18°C, excluding the 18°C-20°C range from the reference category. This specification compares tropical-night days to a cleaner benchmark of physiologically favorable nighttime temperatures (Wang et al., 2015), while removing borderline nights just below the tropical-night threshold. The estimates remain similar, indicating that the main result is not driven by the precise classification of nights near 20°C.

A related concern is that the tropical-night coefficient may partly capture correlated daytime heat or shocks that coincide with hot nights, rather than conditions during the preceding night. I examine this possibility with three complementary checks in Appendix B.2. First, Table B.4 replaces the baseline linear control for same-day maximum temperature with temperature bins (Panel A), then adds bins for previous-day maximum temperature (Panel B). Second, Table B.5 adds calendar-date fixed effects to absorb shocks common to municipalities on the same date (Panel A), and also combines these fixed

effects with binned same-day maximum temperature (Panel B).[14] Third, Table B.6 restricts the outcome to accidents before 11:00 a.m. (Panel A) and, more stringently, before 9:00 a.m. (Panel B), making same-day daytime heat an implausible explanation for the Panel B estimates. Across these tests, the tropical-night coefficients remain positive and comparable in magnitude to those in Table 1, and are statistically significant in nearly all columns—with two exceptions confined to the most demanding specifications.

Next, I examine the estimated relationship using other traffic-accident categories recorded by the DGT. This exercise sheds light on the scope of the mechanism by comparing trips that differ in how easily they can be postponed and in how accustomed drivers are to operating under adverse conditions. If nighttime heat affects accident risk primarily through sleep disruption, the effect should be most pronounced for routine trips that are difficult to postpone, and weaker for discretionary travel or for professional drivers. Appendix B.2 reports estimates for three supplementary samples.

First, Table B.7 expands the baseline outcome to include other work- and school-related trips—drivers traveling on work assignments, students traveling to educational institutions, and parents transporting children to or from school—which, like commuting trips, are relatively difficult to postpone. Consistent with this interpretation, the estimated effect for this broader routine-travel sample remains positive and is similar in magnitude to (if anything slightly larger than) the baseline estimate. By contrast, estimates for holiday-related trips, shown in Table B.8 (Panel A), are small and statistically indistinguishable from zero. The same is true for accidents involving professional drivers, who are likely more accustomed to driving under adverse conditions (e.g., police, firefighters, freight-transport drivers, etc.)—see Table B.8 (Panel B). These patterns suggest that the relevant margin is routine, time-constrained travel by non-professional drivers, rather than traffic accident risk more broadly.

Finally, I examine whether recent exposure to elevated nighttime temperatures further increases accident risk, consistent with the possibility that repeated heat-induced sleep disruption compounds over time. Following Somanathan et al. (2021), Bigler and Janzen (2024), and Drescher and Janzen (2025), I estimate an augmented version of equation (2.1) that includes an indicator for at least one tropical night in the days preceding each observation. Table B.9, Panel A, uses a five-day window (corresponding to a typical workweek), while Panel B uses a seven-day window. In both specifications, the contemporaneous tropical-night coefficient remains close to the baseline estimate. The coefficient on recent exposure

[14] These specifications cannot include the week-by-year and day-of-the-week fixed effects used in the baseline models, because calendar-date fixed effects absorb them.

is positive across specifications (although statistically significant in only some), providing suggestive evidence that repeated nighttime heat may compound accident risk.

4 Heterogeneous effects

I next examine whether the average effect of tropical nights differs across places and population groups that may be differentially vulnerable to nighttime heat. I focus on three margins: adaptation, gender, and income. These dimensions are central to the interpretation of the estimates and to the policy relevance of the paper, as they help identify where and among whom the costs of rising nighttime temperatures are likely to be most concentrated.

4.1 Adaptation

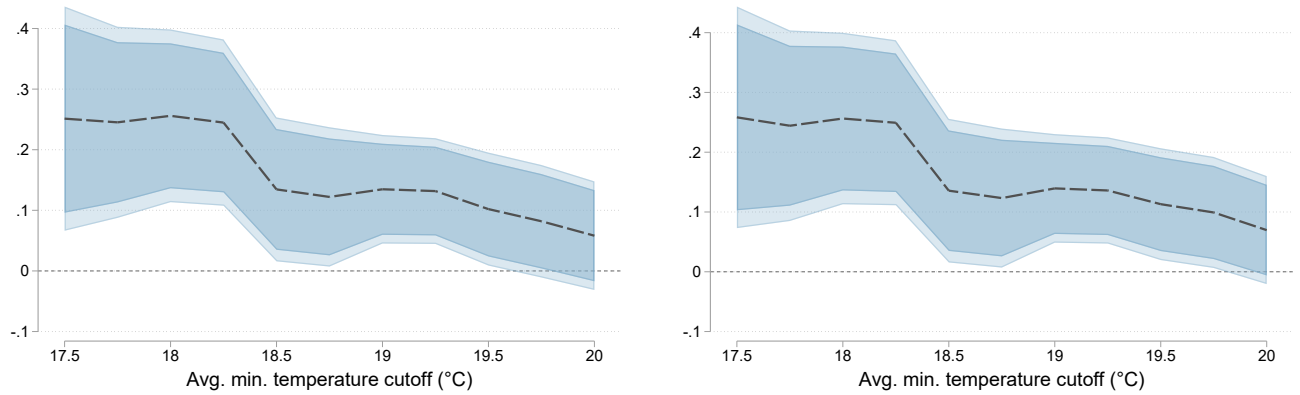
A distinctive feature of my empirical setting is Spain's pronounced spatial variation in temperatures: Spain is among the most climatically diverse countries in Europe (Comín et al., 2019)—Figure A.5 (Appendix A) documents substantial cross-municipality differences in average minimum temperatures. This variation creates scope for differences in exposure and adaptation: in municipalities where tropical nights are common, residents may be more acclimatized or better equipped to cope with nighttime heat; in cooler municipalities, such adaptation is likely more limited—see Figure A.7 (Appendix A). For this reason, the baseline sample focuses on municipalities where tropical nights are relatively uncommon, defined as those with average monthly minimum temperatures below 19°C.[15]

I then examine this adaptation hypothesis by estimating equation (2.1) across samples defined by alternative thresholds for average monthly minimum temperature. If adaptation attenuates the effect of tropical nights, the estimated coefficient should decline as the threshold becomes more permissive and municipalities with warmer nighttime climates enter the sample. Conversely, the estimated effect should become more pronounced as the threshold is lowered and the sample is restricted to municipalities where tropical nights are less common.

Figure 1 presents the results of this adaptation-hypothesis test. The figure reports estimates of equation (2.1) across subsamples defined by progressively higher thresholds of average monthly minimum

[15] More than 76% of Spanish municipalities satisfy this criterion, including Madrid and many other major urban areas. Figure A.6 (Appendix A) maps the municipalities included in this baseline sample.

Figure 1. The effect of tropical nights by local nighttime climate



(A) Province × month FE + day-of-week FE

(B) Municipality × month FE + day-of-week FE

Notes: The figure reports the estimated coefficient on the tropical-night indicator (minimum temperature above 20°C) from equation (2.1) across subsamples of municipalities defined by alternative average minimum temperature cutoffs. Each estimate uses municipalities whose highest monthly average minimum temperature does not exceed the cutoff shown on the horizontal axis, which ranges from 17.5°C to 20°C in increments of 0.25°C. The dashed line connects the point estimates. All specifications include weather controls, municipality fixed effects, week-by-year fixed effects, and day-of-the-week fixed effects. Panel A reports estimates from the preferred baseline specification, which additionally includes province-by-month fixed effects; Panel B reports estimates from a more demanding specification with municipality-by-month fixed effects. Shaded areas denote 90% (darker blue) and 95% (lighter blue) confidence intervals based on standard errors clustered at the municipality level.

temperature, comparing the effect of tropical nights across municipalities with different historical exposure to nighttime heat. Panel A reports estimates from the preferred baseline specification—including province-by-month and day-of-the-week fixed effects; Panel B reports estimates from a more demanding specification with municipality-by-month and day-of-the-week fixed effects.[16]

In both panels, the estimates display a clear downward pattern: the effect of tropical nights declines as the sample expands to include municipalities with higher average monthly minimum temperatures. Among municipalities below the 17.5°C threshold, the coefficient is approximately 0.27 and significant at the 1% level, implying a roughly 31% increase in commuting accident incidence on tropical-night days. The effect then declines steadily as the threshold rises and becomes statistically indistinguishable from zero when municipalities below the 19.75°C threshold are included. A nearly identical pattern is observed using alternative specifications—see Figure B.1 (Appendix B.3).

These patterns have important implications for the projection exercise in Section 5. The smaller effect in historically warmer municipalities is consistent with adaptation reducing the adverse effects of

[16]Figure B.1 (Appendix B.3) reports the corresponding estimates across the remaining specifications.

nighttime heat (Kahn, 2016). At the same time, the larger effects in cooler municipalities suggest that populations in those areas may be more vulnerable. As tropical nights spread into areas where they have traditionally been uncommon, short- and medium-run damages may therefore exceed those implied by estimates from already warm locations. This pattern highlights the importance of accounting for the geography and speed of adaptation when projecting climate damages.

4.2 Gender

I next examine whether the effect of tropical nights differs by gender. I first document the gender gradient in the estimates and then present suggestive evidence on potential mechanisms.

Gender heterogeneity. I begin by estimating equation (2.1) separately by gender, using the number of female and male commuting drivers involved in traffic accidents as the outcome variable.[17] Panels A and B of Table 3 report the results for female and male drivers, respectively. The estimates point to pronounced gender heterogeneity. For female drivers, the tropical-night coefficient is positive, significant at the 1% level in every specification, and stable across columns (ranging from 0.261 to 0.283). These estimates imply a 29.8%-32.7% increase in the number of female commuting drivers involved in traffic accidents on tropical-night days—roughly twice the effect reported in Table 1. By contrast, the corresponding coefficients for male drivers are smaller (around 0.07) and statistically indistinguishable from zero. Thus, the estimated response is small and imprecise for men but large and precise for women, suggesting that the average effect is driven primarily by female commuting drivers.

A back-of-the-envelope calculation based on the point estimates in Table 3 highlights the gender disparity. Comparing the "Daily Δ accidents" row in Table 3 with the corresponding row in Table 1 suggests that female drivers account for roughly three-quarters of the implied excess commuting accidents associated with tropical nights. This disproportionate burden emerges despite lower baseline accident involvement among women: mean commuting accidents per day are 3.73 for women, compared with 6.94 for men—a pattern consistent with a large literature documenting that women tend to commute less, or display a stronger aversion to commuting, than men (Black et al., 2014; Petrongolo and Ronchi,

[17] As a robustness check, Table B.10 (Appendix B.4) replicates the analysis using only accidents in which the sole driver (in single-vehicle accidents) or all involved drivers (in multi-vehicle accidents) belong to the corresponding gender. Analogous to the restriction used in the first row of Table 2, this removes cases in which a crash involving a driver of one gender may also reflect the behavior of drivers of the other gender.

Table 3. The impact of tropical nights on commuting accidents by gender

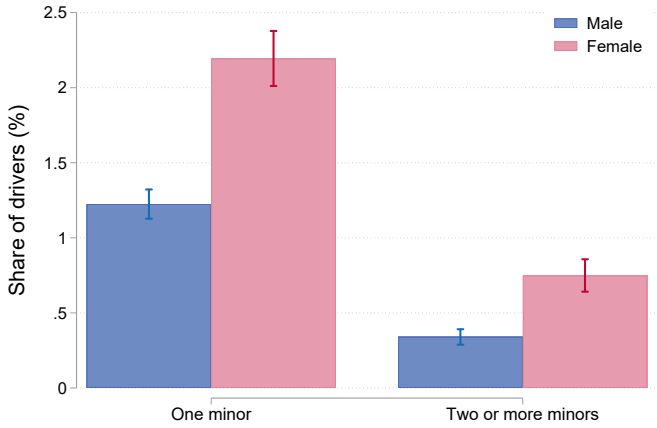
	(1)	(2)	(3)	(4)	(5)	(6)	(7)	(8)
				Panel A. Female drivers				
> 20°C (tropical night)	0.271***	0.261***	0.269***	0.261***	0.283***	0.271***	0.272***	0.261***
	(0.0748)	(0.0766)	(0.0754)	(0.0767)	(0.0767)	(0.0784)	(0.0774)	(0.0788)
Tropical-night effect (%)	31.1	29.8	30.9	29.8	32.7	31.1	31.3	29.8
Mean dep. var.	0.004	0.004	0.005	0.005	0.016	0.016	0.045	0.045
Mean accidents/day	3.73	3.73	3.73	3.73	3.73	3.73	3.73	3.73
Daily Δ accidents	1.16	1.11	1.15	1.11	1.22	1.16	1.16	1.12
Pseudo-R^2	0.256	0.268	0.254	0.267	0.157	0.173	0.105	0.124
Observations	2,008,897	2,008,897	1,663,601	1,663,601	520,478	520,478	180,862	180,862
				Panel B. Male drivers				
> 20°C (tropical night)	0.0782	0.0720	0.0680	0.0625	0.0808	0.0748	0.0729	0.0676
	(0.0636)	(0.0589)	(0.0640)	(0.0591)	(0.0647)	(0.0599)	(0.0644)	(0.0598)
Tropical-night effect (%)	8.1	7.5	7.0	6.4	8.4	7.8	7.6	7.0
Mean dep. var.	0.006	0.006	0.006	0.006	0.020	0.020	0.055	0.055
Mean accidents/day	6.94	6.94	6.94	6.94	6.94	6.94	6.94	6.94
Daily Δ accidents	0.56	0.52	0.49	0.45	0.58	0.54	0.52	0.49
Pseudo-R^2	0.313	0.325	0.316	0.329	0.210	0.225	0.149	0.167
Observations	2,735,413	2,735,413	2,521,046	2,521,046	748,291	748,291	278,061	278,061
				Controls and fixed effects (both panels)				
Weather controls	✓	✓	✓	✓	✓	✓	✓	✓
Mun. & week-year FE	✓	✓	✓	✓	✓	✓	✓	✓
Prov. × month FE	✓	✓						
Prov. × week FE			✓	✓				
Mun. × month FE					✓	✓		
Mun. × week FE							✓	✓
Day-of-week FE		✓		✓		✓		✓

Notes: The dependent variable is the number of commuting drivers of the corresponding gender involved in traffic accidents. Panel A reports estimates for female drivers; Panel B reports estimates for male drivers. All columns are estimated by PPML. Temperature bins are defined using daily minimum temperature; the omitted category is 15°C–20°C. Weather controls include precipitation, maximum temperature, and maximum wind speed. Standard errors clustered by municipality are reported in parentheses. The tropical-night effect is computed as $100 \times [\exp(\hat{\alpha}) - 1]$, where $\hat{\alpha}$ is the coefficient on the > 20°C bin. Mean dep. var. is the column-specific mean of the municipality-day outcome. Mean accidents/day is the mean number of commuting drivers involved in accidents per calendar day in the column-specific estimation sample. Daily Δ accidents is computed as $[\exp(\hat{\alpha}) - 1] \times$ mean accidents/day and refers to commuting drivers involved in accidents. Significance levels: * $p < 0.10$, ** $p < 0.05$, *** $p < 0.01$.

2020; Le Barbanchon et al., 2021; Farré et al., 2023; Borghorst et al., 2024; Bütikofer et al., 2025).[18] I therefore next examine potential mechanisms behind this gender disparity.

Potential mechanisms. One potential explanation for women's greater response, particularly among working mothers, operates through gendered time use and caregiving norms. A well-established literature documents that domestic and caregiving responsibilities fall disproportionately on women (Cubas et al., 2021, 2023; Buzard et al., 2025). In my setting, these responsibilities may translate into greater involvement in school drop-off and pick-up trips on the way to or from work. Figure 2 provides descriptive evidence consistent with this mechanism: among commuting drivers involved in accidents, the share traveling with at least one minor was about 80% higher among female drivers than among male drivers (2.9% versus 1.6%).[19] This pattern therefore suggests a gender imbalance in child-related transportation responsibilities during commuting trips; additional descriptive evidence is reported in Appendix A.[20]

Figure 2. Number of minor passengers among drivers involved in commuting accidents by gender



Notes: The figure displays the share of commuting drivers involved in accidents who were traveling with exactly one passenger under age 18 or with two or more passengers under age 18 in the vehicle they were driving by gender. Shares are calculated relative to all drivers of the corresponding gender involved in commuting accidents. The data was obtained from the DGT and covers January 2014 to December 2019. Bars denote sample shares, and whiskers indicate 95% confidence intervals.

Caregiving responsibilities likely extend beyond school drop-off and pick-up: prior research doc-

[18]To put the larger estimated response among female drivers in context, the 2018 Madrid Household Mobility Survey shows that, among residents of the municipalities in my sample, women's car commutes were similar in duration to men's or, if anything, slightly shorter: car trips between home and work averaged 27.6 minutes for women and 29.5 minutes for men.

[19]Under Spanish labor regulations, accidents occurring while transporting children to or from school qualify as *in itinere* accidents, provided the trip follows the habitual commuting route (Márquez Pérez et al., 2016).

[20]Outside the commuting context, Figure A.9 shows that the monthly number of female drivers involved in accidents while transporting children to or from school averages 8.54, compared with 5.21 for male drivers (approximately 64% higher).

uments that women disproportionately shoulder many other child-related tasks (Guryan et al., 2008; Buzard et al., 2025). Such responsibilities may intensify women's time pressure and compress daily schedules, increasing the urgency with which routine activities are undertaken relative to men. This, in turn, may increase women's vulnerability to commuting accident risk, especially following adverse nighttime conditions (such as tropical nights). I next present two empirical exercises that provide suggestive support for this mechanism.

First, if the mechanism above is partly driven by child-related responsibilities, the gender gap should be attenuated among drivers for whom such responsibilities are likely less prevalent. The dataset does not report parental status, but it records age. I therefore estimate the baseline specification separately for women and men under age 30—a cutoff motivated by data from INE showing that the median age at first birth during my sample period was 30.8 years.[21] Under the assumption that most working women below this age have not yet had children, child- and caregiving-related time constraints should be less relevant for this group. The results, reported in Table B.11 (Appendix B.4), are in line with this prediction. Among drivers under 30, the estimated effects are positive and similar in magnitude for women (Panel A) and men (Panel B): the coefficients range from 0.264 to 0.282 for women and from 0.228 to 0.256 for men.[22] Thus, in contrast to the full-sample gender pattern, there is little evidence of a pronounced differential female response among younger commuting drivers.

Second, I examine whether the gender gap documented in Table 3 is especially pronounced for commuting accidents in which excessive speed was recorded as a contributing factor. I do so by estimating equation (2.1) separately for women and men, using as the outcome the number of commuting accidents involving drivers of each gender for which excessive speed was identified as a contributing factor. This empirical exercise is motivated by the time-pressure mechanism: if child- and caregiving-related constraints compress women's schedules and increase the urgency of commuting trips, this presumably increases their likelihood of speeding during commuting. Consequently, the effect of tropical nights should be especially pronounced for accidents linked to speeding among women. Consistent with this prediction, Table B.12 (Appendix B.4) shows that the gender gap is substantially larger within the subset of speed-related commuting accidents. For women (Panel A), the estimated effect is large, positive, and

[21] The median age at first birth is likely to be even higher among working mothers (Casad et al., 2012).

[22] The implied percentage effects are comparable (31% for women and 28% for men). The slightly larger value in the "Daily Δ accidents" row for men reflects their higher mean number of accidents per day (rather than a larger proportional response).

statistically significant across all columns. By contrast, the corresponding estimates for men (Panel B) are substantially smaller in magnitude and generally not statistically significant at conventional levels.[23]

A complementary channel that may further contribute to the larger estimated effect among women is physiological sensitivity to heat. Several studies show that women are, on average, more susceptible to heat exposure than men (Yu et al., 2010; Follos et al., 2020; Navas-Martin et al., 2022).[24] This vulnerability may be particularly acute during perimenopause and menopause, when hormonal changes can affect thermoregulation (Monteleone et al., 2018; Conti et al., 2025), potentially heightening sensitivity to nighttime heat and, in turn, elevating the commuting-accident risk among women at these stages. Table B.14 (Appendix B.4) provides suggestive evidence consistent with this channel. The estimated effect of tropical nights among women is largest for the age cohort associated with the transition into perimenopause and the onset of menopause, that is, women aged 48-51. By contrast, the estimated effects are smaller and generally statistically indistinguishable from zero among both younger women, who are less likely to have entered perimenopause, and older women in later stages of menopause.[25]

In summary, the results in this section show that the safety costs of tropical nights are not evenly distributed by gender, with the average effect documented in Table 1 driven primarily by female commuting drivers. The evidence points to two complementary channels behind this gradient: gendered time constraints and caregiving responsibilities, and physiological vulnerability. These findings highlight a previously overlooked climate-related channel through which gendered constraints can translate into unequal labor-market costs, linking the literature on climate damages to the literature on gender gaps and motherhood penalties. From a policy perspective, the results point to the value of measures that reduce commuting exposure during heat wave episodes, such as flexible start times or temporary WFH arrangements, especially for workers with caregiving responsibilities. This policy implication complements evidence that flexible work arrangements can disproportionately benefit women and help narrow gender disparities in labor-market outcomes (Arntz et al., 2022; Le Barbanchon et al., 2021).

[23] As an additional test, Table B.13 (Appendix B.4) replicates the speeding analysis for women under 30 (i.e., women who are less likely to have child-related responsibilities). The estimates of interest are much smaller than the corresponding estimates in Table B.12 (Panel A) and statistically indistinguishable from zero, consistent with the interpretation that caregiving-related time constraints contribute to the gender differences documented above.

[24] For example, women tend to exhibit higher thresholds for the onset of sweating and distinct thermoregulatory responses to heat stress, which affect blood-flow and pressure regulation (Kaciuba-Uscilko and Grucza, 2001; Charkoudian et al., 2017).

[25] One possible interpretation is that heightened physiological vulnerability associated with this transition attenuates over time as women adapt to post-menopausal conditions.

4.3 Income

Finally, I examine whether the effect of tropical nights on commuting accident risk varies across local income groups. This analysis is motivated by a large literature showing that lower-income households are more vulnerable to extreme weather conditions than higher-income households. In the context of nighttime heat, such heterogeneity may arise from differences in housing quality, insulation, AC ownership and use, and other investments that improve indoor thermal comfort (Memmott et al., 2021; Cong et al., 2022; Zhang and Xu, 2025).[26] These constraints are especially relevant for hot nights, since they limit households' ability to maintain thermally comfortable sleeping conditions. I therefore expect the adverse effects of tropical nights to be more pronounced among lower-income population groups.

To examine this hypothesis, I use municipality-level data on household net income from INE to classify municipalities into above- and below-median-income groups. I then estimate a modified version of equation (2.1) that interacts the tropical-night indicator with indicators for the two income groups—which I refer to, for brevity, as high- and low-income municipalities.[27] Table 4 reports the results. Consistent with my hypothesis, the tropical-night point estimates are systematically larger in low-income municipalities: across specifications, the coefficient ranges from 0.22 to 0.26 in low-income municipalities, compared with 0.11 to 0.14 in high-income municipalities. Translating these estimates into accident counts yields a similar pattern: the number of excess commuting accidents attributable to tropical nights over the sample period is approximately 2.9 times larger among residents of low-income municipalities than among residents of high-income municipalities.

These estimates should be interpreted as suggestive: although the point estimates are systematically larger in low-income municipalities, they are also less precisely estimated than those for high-income municipalities.[28] This imprecision is consistent with the fact that commuting accidents are less frequent in low-income municipalities, which reduces statistical power—likely reflecting lower car commuting among lower-income residents (Barwick et al., 2024). For this reason, I also report a more conservative calculation of the implied distributional burden that anchors the aggregate number of excess accidents

[26] Although the diffusion of AC has substantially improved households' ability to cope with heat (Barreca et al., 2016), important disparities in use remain. For example, Doremus et al. (2022) show that low-income households exhibit smaller increases in energy consumption during heat waves, consistent with evidence that they are more sensitive to energy prices and more likely to experience utility disconnections (Barreca et al., 2022; Rubin and Auffhammer, 2024).

[27] The results are similar when municipalities are classified using gross household income (Table B.15, Appendix B.5).

[28] In fact, formal tests do not reject equality between the low- and high-income coefficients at conventional levels.

Table 4. The impact of tropical nights on commuting accidents by income

	(1)	(2)	(3)	(4)	(5)	(6)	(7)	(8)
$>$ 20°C (low income)	0.237*	0.261*	0.227*	0.260*	0.222	0.245*	0.222	0.253*
	(0.143)	(0.144)	(0.138)	(0.139)	(0.146)	(0.146)	(0.142)	(0.144)
$>$ 20°C (high income)	0.128**	0.115**	0.121**	0.107**	0.136***	0.122**	0.126**	0.112**
	(0.0518)	(0.0481)	(0.0538)	(0.0495)	(0.0519)	(0.0480)	(0.0548)	(0.0506)
Weather controls	✓	✓	✓	✓	✓	✓	✓	✓
Mun. & week-year FE	✓	✓	✓	✓	✓	✓	✓	✓
Prov. × month FE	✓	✓						
Prov. × week FE			✓	✓				
Mun. × month FE					✓	✓		
Mun. × week FE							✓	✓
Day-of-week FE		✓		✓		✓		✓
Mean dep. var.	0.007	0.007	0.008	0.008	0.024	0.024	0.062	0.062
Mean accidents/day	10.61	10.61	10.61	10.61	10.61	10.61	10.61	10.61
				Low-income				
Tropical-night effect (%)	26.7	29.8	25.5	29.7	24.9	27.8	24.9	28.8
Total Δ accidents	51.88	57.96	50.10	58.32	51.65	57.48	52.69	61.10
Total Δ accidents (conservative)	33.85	33.09	30.94	30.69	42.58	41.35	42.72	42.13
				High-income				
Tropical-night effect (%)	13.7	12.2	12.9	11.3	14.6	13.0	13.4	11.9
Total Δ accidents	21.64	19.30	20.94	18.48	24.95	22.34	23.99	21.14
				Comparison across income groups				
Low/high ratio	2.40	3.00	2.39	3.16	2.07	2.57	2.20	2.89
Low/high ratio (conservative)	1.56	1.71	1.48	1.66	1.71	1.85	1.78	1.99
Pseudo-R^2	0.343	0.355	0.347	0.359	0.243	0.258	0.179	0.199
Observations	3,233,997	3,233,997	3,072,155	3,072,155	967,121	967,121	375,833	375,833

Notes: The dependent variable is the number of commuting drivers involved in traffic accidents. All columns are estimated by PPML. The table reports coefficients on the tropical-night indicator interacted with indicators for municipalities at or below (low income) and above (high income) the median of municipality-level household net income from INE. Temperature bins are defined using daily minimum temperature; the omitted category is 15°C–20°C. Weather controls include precipitation, maximum temperature, and maximum wind speed. Standard errors clustered by municipality are reported in parentheses. Tropical-night effects are computed as $100 \times [\exp(\hat{\alpha}_g) - 1]$, where $\hat{\alpha}_g$ is the income-group-specific coefficient on the $>$ 20°C indicator. Mean dep. var. is the column-specific mean of the municipality-day outcome. Mean accidents/day is the mean number of commuting drivers involved in accidents per calendar day in the column-specific estimation sample. Total Δ accidents for group g is computed as $[\exp(\hat{\alpha}_g) - 1] \times$ mean accidents/day $\times f_g \times (365 \times 6)$, where f_g is the mean across municipality-years in the estimation sample of the within-year mean of the indicator for a tropical night in income group g. The conservative low-income total equals the pooled aggregate estimate underlying the corresponding column of Table 1 minus the high-income total reported here. Low/high ratios divide the respective low-income total by the high-income total. All accident statistics refer to commuting drivers involved in accidents. Formal tests do not reject equality between the low- and high-income coefficients at conventional levels. Significance levels: * $p < 0.10$, ** $p < 0.05$, *** $p < 0.01$.

to the pooled estimates in Table 1. Specifically, I infer the number of excess accidents in low-income municipalities as the difference between the pooled aggregate effect and the number of excess accidents in high-income municipalities reported in Table 4 (both of which are estimated more precisely). This calculation implies about 31-43 excess accidents attributable to tropical nights among residents of low-income municipalities, which is still roughly 1.5-2 times the corresponding estimate for high-income municipalities. Overall, the pattern is consistent with the broader climate-adaptation literature showing that economically disadvantaged populations are less able to shield themselves from extreme heat.

5 Projected costs of rising nighttime temperatures

The estimates above imply that tropical nights already impose a meaningful toll through commuting accidents, casualties, and social costs. I now ask how this burden is likely to evolve as climate change further raises nighttime temperatures. To do so, I combine my estimates from equation (2.1) with municipality-level projections of future tropical-night exposure from state-of-the-art global climate models under alternative emissions scenarios. This exercise allows me to quantify the resulting implied increase in commuting accident risk and associated casualties and social costs.

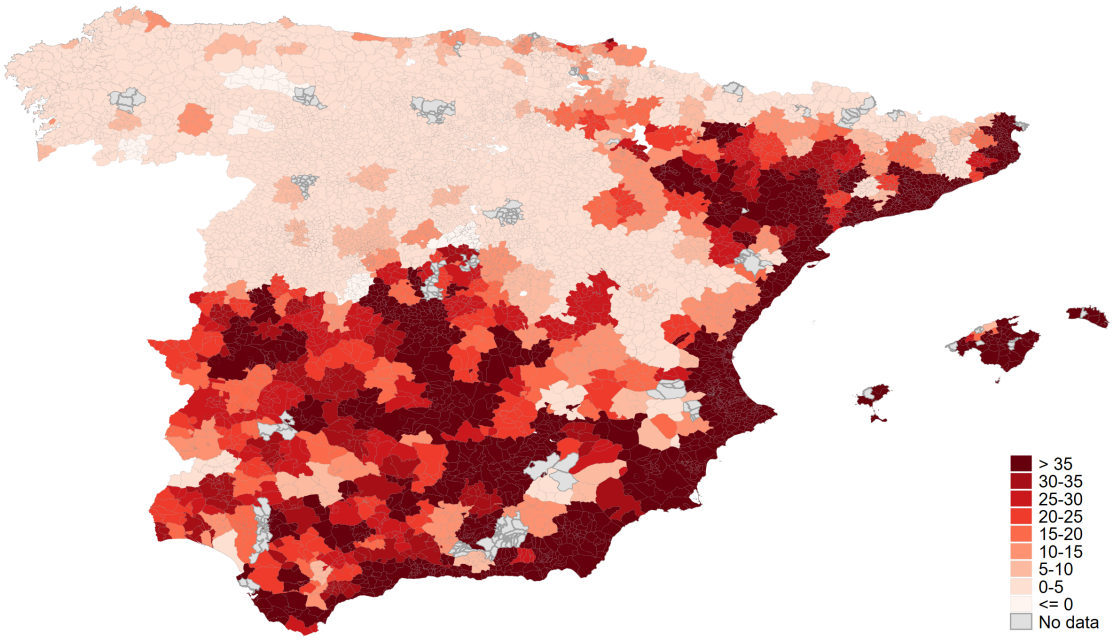
Specifically, I leverage climate projections from 11 global climate models included in Phase 6 of the Coupled Model Intercomparison Project (CMIP6)—the international model-comparison exercise underlying the Intergovernmental Panel on Climate Change (IPCC) Sixth Assessment Report. The projections cover four emissions scenarios, which I refer to as low, medium, high, and very high emissions,[29] and three 30-year horizons: near term (2011-2040), medium term (2041-2070), and long term (2071-2100). These projections are statistically downscaled to the weather-station level in Spain by AEMET and the Spanish National Research Council (CSIC).[30] For each climate model, emissions scenario, and horizon, the data provides the projected annual number of days with minimum temperatures above 20°C (that is, tropical nights) at each weather station. I then compute projected increases in tropical nights relative to the 1971-2000 historical baseline period, and aggregate these station-level projections to the municipality level using the same procedure as in the construction of the weather variables in Section 2.1.

Figure 3 maps the projected increase in tropical nights across Spanish municipalities under the

[29] These correspond to the Shared Socioeconomic Pathways SSP1-2.6 (low), SSP2-4.5 (medium), SSP3-7.0 (high), and SSP5-8.5 (very high), which are standard emissions scenarios used in the IPCC Sixth Assessment Report.

[30] The downscaled projections are distributed through the *AdapteCCa* data server (https://escenarios.adaptecca.es/).

Figure 3. Projected increase in annual tropical nights across municipalities, medium-term horizon (2041-2070) and medium-emissions scenario (SSP2-4.5)

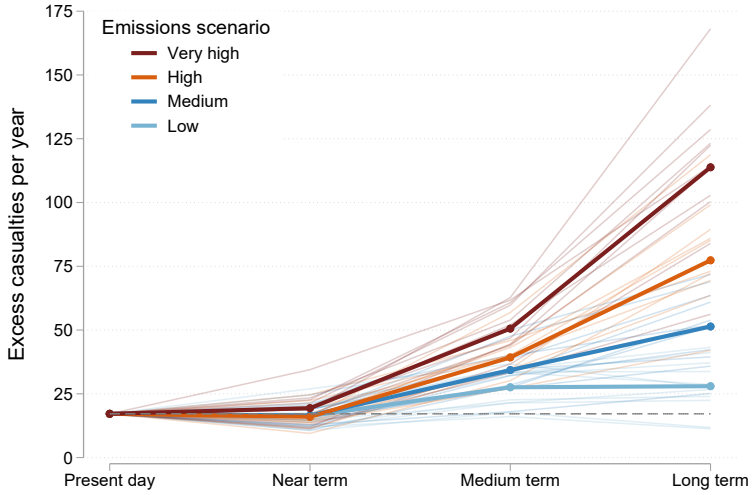


Notes: The figure maps the projected increase in the annual number of tropical nights across Spanish municipalities for the medium-term horizon (2041-2070) under the intermediate-emissions scenario (SSP2-4.5), relative to the 1971-2000 historical baseline. A tropical night is defined by a daily minimum temperature above 20°C. Changes are expressed in nights per year. Projections are averaged across 11 CMIP6 global climate models: ACCESS-CM2, CMCC-CM2-SR5, CNRM-ESM2-1, EC-Earth3-Veg, IITM-ESM, KACE-1-0-G, MIROC6, MPI-ESM1-2-HR, MRI-ESM2-0, NorESM2-MM, and UKESM1-0-LL. For visual clarity, municipalities in the Canary Islands and the overseas cities of Ceuta and Melilla are not displayed.

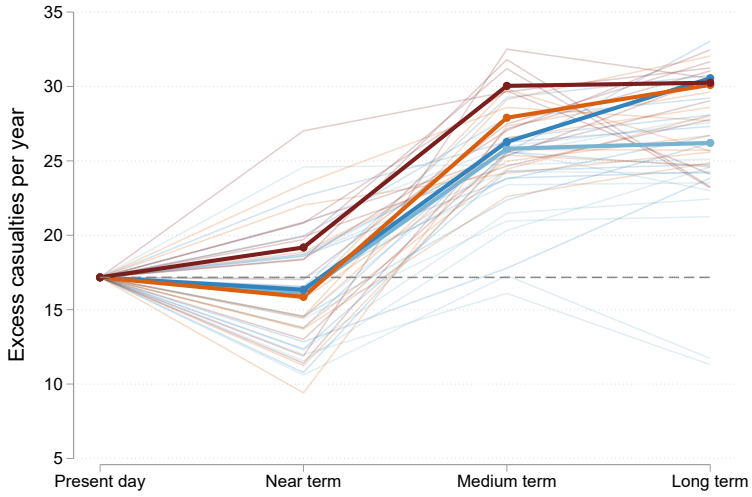
medium-emissions scenario (SSP2-4.5). It reports the average projection across the 11 climate models for the medium-term horizon (2041-2070)—corresponding maps for the near- and long-term horizons are reported in Figure A.10 (Appendix A). Although projected increases vary substantially across municipalities, the rise in tropical-night exposure is widespread across the country, including in areas where such events have historically been relatively uncommon.

I translate these municipality-level climate projections into excess casualties, using the present-day calculation in Section 3.1 as the benchmark. That calculation applies the attributable share, $[1-\exp(-\hat{\alpha})]$, to commuting-driver involvements observed on tropical-night days in the sample municipalities and converts the resulting implied excess involvements into casualties using the observed casualty-per-involvement rate (see footnote 13). I then project the additional excess casualties implied by increases in tropical-night exposure relative to the 2014-2019 sample period, using the preferred baseline estimate—column (2) of Table 1. For each municipality in the sample, emissions scenario, and climate model, I

Figure 4. Projected excess casualties under alternative adaptation assumptions



(A) No additional adaptation



(B) Adaptation-adjusted projection

Notes: The figure shows projected excess casualties per year associated with accidents involving commuting drivers in the sample municipalities, allowing future tropical-night exposure to evolve across emissions scenarios, horizons, and climate models. Panel A presents the no-additional-adaptation projection. Panel B presents an adaptation-adjusted projection, in which, for each emissions scenario, horizon, and climate model, municipalities whose projected maximum across months of mean monthly minimum temperature reaches or exceeds 19.75°C are excluded from the future incremental burden. The present-day benchmark is obtained by applying the attributable-share transformation $[1 - \exp(-\hat{\alpha})]$ to commuting-driver involvements observed on tropical-night days during 2014-2019 and converting the resulting excess involvements into casualties using the observed casualty-per-involvement rate. Future increments use the preferred baseline estimate from column (2) of Table 1, and are calculated by multiplying the cumulative increase in the annual number of tropical nights relative to the 2014-2019 sample period by each municipality's average daily number of commuting drivers involved in accidents and by the implied proportional effect $[\exp(\hat{\alpha}) - 1]$. They are then converted into casualties using the same casualty-per-involvement rate. Near term, medium term, and long term refer to 2011-2040, 2041-2070, and 2071-2100, respectively. Thin lines report projections from the 11 individual climate models, while thick lines report projections based on climate measures averaged across the 11 models.

multiply the cumulative increase in the annual number of tropical nights by the municipality's average daily number of commuting drivers involved in accidents and by the estimated proportional effect, $[\exp(\hat{\alpha}) - 1]$.[31] Finally, I convert the resulting excess commuting-driver involvements into casualties using the same casualty-per-involvement rate as in the present-day calculation.

The resulting projections, displayed in Figure 4, show how excess casualties are expected to evolve under the climate projections. Panel A shows that, in the absence of additional adaptation, projected excess casualties increase under all emissions scenarios. The trajectories remain close to the present-day benchmark in the near term but rise substantially under every scenario by the medium term, with trajectories diverging thereafter. By the long term, projected excess casualties exceed six times the present-day benchmark under the very-high-emissions scenario and four times that benchmark under the high-emissions scenario. Under the medium-emissions scenario, they reach about 51 per year—roughly three times the present-day burden—whereas the low-emissions trajectory stabilizes after the medium term at about 28 excess casualties per year. Even in the latter case, this represents an increase of roughly 60% relative to the present day.

Then, building on the evidence in Section 4.1, I provide an adaptation-adjusted projection in which the effect of tropical nights is attenuated for municipalities whose projected nighttime climate resembles that of historically warmer locations. Specifically, for each emissions scenario, horizon, and climate model, municipalities whose projected maximum across months of mean monthly minimum temperature is at or above 19.75°C are excluded from the future incremental burden calculation.[32] This cutoff is motivated by the adaptation exercise in Section 4.1, where the estimated effect becomes statistically indistinguishable from zero once municipalities at or below this threshold are included. I apply this cutoff separately at each horizon, in such a way that municipalities may contribute to the projected excess casualties in the near term but drop out in later horizons if projected nighttime temperatures reach or exceed the 19.75°C threshold.

The result of this analysis is provided in Figure 4, Panel B, which shows that allowing for adaptation

[31] For the present-day benchmark, I use the attributable-share transformation $[1 - \exp(-\hat{\alpha})]$ because the calculation starts from observed commuting-driver involvements on tropical-night days. For future increments, I use the proportional effect $[\exp(\hat{\alpha}) - 1]$ because these increments are calculated from municipality-level average daily involvement rates and projected additional tropical nights.

[32] This adaptation threshold is applied to projected temperature measures from the climate models, whereas the adaptation exercise in Section 4.1 uses actual observed weather data. These measures are therefore conceptually analogous, though not numerically identical: both are defined as the maximum across months of mean monthly minimum temperature. As a sanity check, Figure A.11 (Appendix A) documents their empirical relationship.

dampens the projected increase in excess casualties relative to the no-additional-adaptation benchmark (Panel A). As in Panel A, the near-term trajectories remain close to the present-day level, with some scenarios implying even a slight decline in the casualty burden. By the medium term, however, the projected burden rises, with averages across the 11 climate models that are fairly similar in magnitude across scenarios. These averages largely stabilize in the long term, reaching roughly 26-31 excess casualties per year. Thus, even under this conservative adaptation-adjusted projection, the implied casualty burden remains approximately 50-80% above the present-day level in the medium and long term.

I monetize these projected casualty burdens using the same empirical injury-severity distribution and DGT-approved valuations used in Section 3.1 (Pérez et al., 2015). As reported there, the present-day benchmark of over 17 excess casualties per year corresponds to an annual social cost of about 0.76€ million. In the no-additional-adaptation benchmark (Figure 4, Panel A), the implied annual social cost reaches about 2.3€ million by the long term under medium emissions—roughly three times its present-day level—and about 5.0€ million under very high emissions, more than six times that level. Under the adaptation-adjusted projection (Figure 4, Panel B), annual social costs stabilize at approximately 1.2€-1.4€ million across emissions scenarios.[33] This result illustrates that, while adaptation can substantially reduce projected climate-related damages in my setting, it does not eliminate them.

These projected social costs also have an important distributional dimension, as demonstrated by Figure B.2 (Appendix B.4), which reports analogous projections by gender (assuming no additional adaptation), using the estimates in Table 3. Consistent with the heterogeneity documented in that table, the implied excess-casualty burden is concentrated among female workers.[34] This pattern points to an additional climate-related channel through which gendered constraints may contribute to unequal labor-market costs, with implications for gender gaps in the labor market.

Overall, these results highlight policy implications along two margins. First, the gap between Panels A and B in Figure 4 illustrates the value of adaptation policies that improve households' ability to maintain adequate sleeping conditions during episodes of elevated nighttime heat, such as heatwaves—e.g., better housing quality, passive cooling, and access to affordable cooling technologies (Barreca et al.,

[33] As in Section 3.1, these figures exclude additional firm-side costs associated with sick leave and workplace disruptions, as well as broader costs associated with worker substitution, lost productivity, and administrative burden.

[34] The estimates for male drivers in Table 3 (Panel B) are less precise than the corresponding estimates for female drivers (Panel A). Accordingly, the male projections should be interpreted with care and viewed as illustrating the distributional implications of the gender-specific point estimates.

2016; Santamouris and Vasilakopoulou, 2026).[35] Given the income heterogeneity documented in Section 4.3, these interventions may be especially valuable for lower-income households, which are likely less able to shield themselves from nighttime heat (Pavanello et al., 2021; Doremus et al., 2022). At the same time, consistent with earlier evidence that adaptation can buffer climate damages (Carleton et al., 2022), Panel B suggests that adaptation of the magnitude implied by responses in historically warmer municipalities is unlikely to fully offset the projected increase in accident risk.

The projected burden that persists even after allowing for adaptation points to a second, labor-market policy margin. Because these projections use data from 2014-2019—a period before the pandemic-era diffusion of WFH, when remote work remained limited in Spain (Jerbashian and Vilalta-Bufí, 2024; Rubino et al., 2024)—my results suggest that flexible start times or temporary WFH during heat waves could weaken the link between heat-disrupted sleep and work-related risks, of which commuting accidents are one measurable example.[36] This labor-market response is particularly relevant in Spain, where remote work remains below the EU average.[37] More broadly, these findings extend the usual workplace-heat policy debate: labor-market adaptation can reduce climate-related risks not only inside the workplace, but also by changing whether and when workers commute during extreme heat.

The gender-specific projections further suggest that such policies may be especially valuable for female workers, particularly those with caregiving responsibilities. This points to a novel climate-related channel through which flexible work arrangements can mitigate gender disparities, complementing existing evidence on workplace flexibility and gender gaps in labor-market outcomes (Wiswall and Zafar, 2018; Le Barbanchon et al., 2021; Basso et al., 2026).

[35] AC penetration remains comparatively limited in Europe: according to IEA (2026) and EIA (2022), about 20% of European households were equipped with AC in 2025, compared with nearly 90% of US households in 2020. In Spain, installing AC can also face legal constraints, including rules governing building façades, exterior configuration, licensing, and noise—see, e.g., *Ley de Propiedad Horizontal* (article 7) and Madrid's municipal guidance on AC units on façades.

[36] This policy margin is increasingly salient in heat-adaptation debates. For example, in the UK, official guidance and parliamentary briefings emphasize employers' responsibility to manage heat-related workplace risks and identify flexible working arrangements, including WFH or off-peak travel, as potential mitigation measures (Health and Safety Executive, 2026; Balogun, 2026). Prior research also shows that workers make use of flexible work arrangements in response to adverse and extreme weather conditions (Behrer and Park, 2017; Li, 2023).

[37] According to Eurostat, in 2023, 7.1% of employees in Spain sometimes worked from home, compared with the EU average of 13.3%.

6 Conclusions

This paper shows that nighttime heat creates meaningful labor-market costs. Combining nationwide administrative records of commuting traffic accidents in Spain with granular station-level weather data, I find that tropical nights—days on which minimum temperatures exceed 20°C—increase the number of commuting drivers involved in accidents by about 14-16%. Several patterns are consistent with impaired rest as a mechanism: the effect is larger for early-day accidents and extends to other routine work- and school-related trips, but disappears for more discretionary travel or professional drivers. The burden is also unevenly distributed, with larger effects in historically cooler municipalities, among female commuting drivers, and in lower-income places. My results imply sizable present-day social costs and suggest that, as tropical nights become more frequent due to climate change, nighttime heat will generate growing damages unless further adaptation attenuates the effect.

These findings broaden the scope of climate-damages research beyond direct (onsite) exposure to adverse conditions at work to conditions outside work that may compromise next-day safety. They also point to adaptation margins beyond the usual focus on workplace conditions, consistent with recent calls to treat sleep as a policy-relevant margin (Rao et al., 2021): improving households' ability to maintain safe sleeping conditions during hot nights and allowing flexibility in whether and when workers commute may both reduce climate-related accident risk. Future research could combine administrative outcomes with direct measures of indoor temperature, housing quality, and cooling access to better identify the mechanisms behind these effects and to assess which adaptation policies most effectively protect vulnerable workers.

References

Alexander, L. V., X. Zhang, T. C. Peterson, J. Caesar, B. Gleason, A. Klein Tank, M. Haylock, D. Collins, B. Trewin, F. Rahimzadeh, et al. (2006). Global observed changes in daily climate extremes of temperature and precipitation. *Journal of Geophysical Research: Atmospheres 111*(D5).

Arntz, M., S. B. Yahmed, and F. Berlingieri (2022). Working from home, hours worked and wages:

Heterogeneity by gender and parenthood. *Labour Economics 76*, 102169.

Balogun, B. (2026). Working in Hot Weather: What Does the Law Say? House of Commons Library Research Briefing CBP-10925. Accessed July 23, 2026.

Barreca, A., K. Clay, O. Deschenes, M. Greenstone, and J. S. Shapiro (2016). Adapting to climate change: The remarkable decline in the US temperature-mortality relationship over the twentieth century. *Journal of Political Economy 124*(1), 105–159.

Barreca, A., R. J. Park, and P. Stainier (2022). High temperatures and electricity disconnections for low-income homes in California. *Nature Energy 7*(11), 1052–1064.

Barwick, P. J., S. Li, A. Waxman, J. Wu, and T. Xia (2024). Efficiency and equity impacts of urban transportation policies with equilibrium sorting. *American Economic Review 114*(10), 3161–3205.

Basso, G., M. De Paola, S. Lattanzio, and M. Paradisi (2026). Workplace flexibility and the motherhood penalty: Evidence from the diffusion of remote work. Technical report, Centre for Economic Policy Research.

Behrer, A. P. and J. Park (2017). Will we adapt? Temperature, labor and adaptation to climate change. *Harvard Project on Climate Agreements Working Paper*, 16–81.

Bessone, P., G. Rao, F. Schilbach, H. Schofield, and M. Toma (2021). The economic consequences of increasing sleep among the urban poor. *The Quarterly Journal of Economics 136*(3), 1887–1941.

Bigler, P. and B. Janzen (2024). Too hot to sleep. *Journal of Environmental Economics and Management 128*, 103063.

Black, D. A., N. Kolesnikova, and L. J. Taylor (2014). Why do so few women work in New York (and so many in Minneapolis)? Labor supply of married women across US cities. *Journal of Urban Economics 79*, 59–71.

Borghorst, M., I. Mulalic, and J. Van Ommeren (2024). Commuting, gender and children. *Journal of Urban Economics 144*, 103709.

Bütikofer, A., R. Karadakic, and A. Willén (2025). Parenthood and the gender gap in commuting. *Journal of Public Economics 248*, 105371.

Buzard, K., L. K. Gee, and O. Stoddard (2025). Who you gonna call? Gender inequality in external demands for parental involvement. *The Quarterly Journal of Economics*, qjaf027.

Cabral, M. and M. Dillender (2024). Air pollution, wildfire smoke, and worker health. Technical report, National Bureau of Economic Research.

Cappuccio, F. P., L. D'Elia, P. Strazzullo, and M. A. Miller (2010). Sleep duration and all-cause mortality: a systematic review and meta-analysis of prospective studies. *Sleep 33*(5), 585–592.

Carleton, T., A. Jina, M. Delgado, M. Greenstone, T. Houser, S. Hsiang, A. Hultgren, R. E. Kopp, K. E. McCusker, I. Nath, J. Rising, A. Rode, H. K. Seo, A. Viaene, J. Yuan, and A. T. Zhang (2022). Valuing the Global Mortality Consequences of Climate Change Accounting for Adaptation Costs and Benefits. *The Quarterly Journal of Economics 137*(4), 2037–2105.

Carrell, S. E., T. Maghakian, and J. E. West (2011). A's from Zzzz's? The causal effect of school start time on the academic achievement of adolescents. *American Economic Journal: Economic Policy 3*(3), 62–81.

Casad, B. J., A. Marcus-Newhall, B. Nakawaki, A. S. Kasabian, and J. LeMaster (2012). Younger age at first childbirth predicts mothers' lower economic and psychological well-being later in life. *Journal of Family and Economic Issues 33*(4), 421–435.

Charkoudian, N., E. C. Hart, J. N. Barnes, and M. J. Joyner (2017). Autonomic control of body temperature and blood pressure: influences of female sex hormones. *Clinical Autonomic Research 27*, 149–155.

Chevance, G., K. Minor, C. Vielma, E. Campi, C. O'Callaghan-Gordo, X. Basagaña, J. Ballester, and P. Bernard (2024). A systematic review of ambient heat and sleep in a warming climate. *Sleep Medicine Reviews*, 101915.

CIPD (2024). Flexible working arrangements can help employees keep cool in hot weather, says the Chartered Institute of Personnel and Development. Chartered Institute of Personnel and Development. Accessed: August 18, 2026.

Comín, J. S., N. P. Mayoral, A. A. Cortijo, P. S.-O. Rodríguez, and A. del Campo García (2019). España en mapas: una síntesis geográfica. El primer producto del Atlas Nacional de España del siglo XXI. *Observatorio Medioambiental 22*, 337.

Cong, S., D. Nock, Y. L. Qiu, and B. Xing (2022). Unveiling hidden energy poverty using the energy equity gap. *Nature Communications 13*(1), 2456.

Conti, G., R. Ginja, P. Persson, and B. Willage (2025). The menopause penalty. Technical report, National Bureau of Economic Research.

Correa, J., P. Dorta, A. López-Díez, and J. Díaz-Pacheco (2024). Analysis of tropical nights in Spain (1970–2023): Minimum temperatures as an indicator of climate change. *International Journal of Climatology 44*(9), 3006–3027.

Correia, S. (2015). Singletons, cluster-robust standard errors and fixed effects: A bad mix. *Technical Note, Duke University 7*.

Correia, S., P. Guimarães, and T. Zylkin (2020). Fast Poisson estimation with high-dimensional fixed effects. *The Stata Journal 20*(1), 95–115.

Crespi, A., S. Terzi, S. Cocuccioni, M. Zebisch, J. Berckmans, and H.-M. Füssel (2020). Climate-related hazard indices for europe. ETC/CCA Technical Paper 2020/1, European Topic Centre on Climate Change Impacts, Vulnerability and Adaptation (ETC/CCA), Bologna, Italy.

Cubas, G., C. Juhn, and P. Silos (2021). Work-care balance over the day and the gender wage gap. In *AEA Papers and Proceedings*, Volume 111, pp. 149–153.

Cubas, G., C. Juhn, and P. Silos (2023). Coordinated work schedules and the gender wage gap. *The Economic Journal 133*(651), 1036–1066.

Dell, M., B. F. Jones, and B. A. Olken (2014). What do we learn from the weather? The new climate-economy literature. *Journal of Economic Literature 52*(3), 740–798.

Dillender, M. (2021). Climate change and occupational health: Are there limits to our ability to adapt? *Journal of Human Resources 56*(1), 184–224.

Donat, M., L. V. Alexander, H. Yang, I. Durre, R. Vose, R. J. Dunn, K. M. Willett, E. Aguilar, M. Brunet, J. Caesar, et al. (2013). Updated analyses of temperature and precipitation extreme indices since the beginning of the twentieth century: The HadEX2 dataset. *Journal of Geophysical Research: Atmospheres 118*(5), 2098–2118.

Doremus, J. M., I. Jacqz, and S. Johnston (2022). Sweating the energy bill: Extreme weather, poor households, and the energy spending gap. *Journal of Environmental Economics and Management 112*, 102609.

Drescher, K. and B. Janzen (2025). When weather wounds workers: The impact of temperature on workplace accidents. *Journal of Public Economics 241*, 105258.

EEA (2020). Climate-related hazard indices for Europe. https://climate-adapt.eea.europa.eu/en/metadata/publications/climate-related-hazard-indices-for-europe-etc-cca-technical-paper-1-2020/etc-cca_technical_paper_1_2020_final.pdf/@@download/file. Accessed July 23, 2026.

EIA (2022, May). Nearly 90% of U.S. households used air conditioning in 2020. Today in Energy. Accessed July 24, 2026.

Escobar Carias, M., D. W. Johnston, R. Knott, and R. Sweeney (2024). Temperature's toll on decision-making. *The Economic Journal 134*(663), 2746–2771.

European Environment Agency (2021). Heat and cold – extreme heat. In *Europe's changing climate hazards: An index-based interactive EEA report*. EEA Report No. 15/2021.

Farré, L., J. Jofre-Monseny, and J. Torrecillas (2023). Commuting time and the gender gap in labor market participation. *Journal of Economic Geography 23*(4), 847–870.

Follos, F., C. Linares, J. Vellón, J. A. Lopez-Bueno, M. Luna, G. Sánchez-Martínez, and J. Díaz (2020). The evolution of minimum mortality temperatures as an indicator of heat adaptation: the cases of Madrid and Seville (Spain). *Science of The Total Environment 747*, 141259.

Gibson, M. and J. Shrader (2018). Time use and labor productivity: The returns to sleep. *Review of Economics and Statistics 100*(5), 783–798.

Giuntella, O., S. Saccardo, and S. Sadoff (2026). Sleep: Educational impact and habit formation. *Journal of Political Economy 134*(8).

Graff Zivin, J. and M. Neidell (2014). Temperature and the allocation of time: Implications for climate change. *Journal of Labor Economics 32*(1), 1–26.

Guryan, J., E. Hurst, and M. Kearney (2008). Parental education and parental time with children. *Journal of Economic perspectives 22*(3), 23–46.

Health and Safety Executive (2026). Temperature in the workplace: Managing workplace temperatures. Accessed: August 18, 2026.

Hsiang, S. (2016). Climate econometrics. *Annual Review of Resource Economics 8*, 43–75.

IEA (2026, July). Share of households equipped with air conditioner by region, 2015–2025. IEA Data and Statistics. Accessed July 24, 2026.

Jagnani, M. (2024). Children's sleep and human capital production. *Review of Economics and Statistics 106*(4), 983–996.

Jerbashian, V. and M. Vilalta-Bufí (2024). On working from home in European countries. *International Journal of Manpower 45*(5), 908–925.

Kaciuba-Uscilko, H. and R. Grucza (2001). Gender differences in thermoregulation. *Current Opinion in Clinical Nutrition & Metabolic Care 4*(6), 533–536.

Kahn, M. E. (2016). The climate change adaptation literature. *Review of Environmental Economics and Policy*.

Kuruc, K., M. LoPalo, and S. O'Connor (2025). The Willingness to Pay for a Cooler Day: Evidence from 50 Years of Major League Baseball Games. *American Economic Journal: Applied Economics 17*(1), 126–159.

Lavy, V., G. Rachkovski, and O. Yoresh (2025). Heads up: Does air pollution cause workplace accidents? *Journal of Public Economics 251*, 105472.

Le Barbanchon, T., R. Rathelot, and A. Roulet (2021). Gender differences in job search: Trading off commute against wage. *The Quarterly Journal of Economics 136*(1), 381–426.

Li, W. (2023). Is Working from Home a Way of Adaptation to Climate Change? *Available at SSRN 5154992*.

Márquez Pérez, S. et al. (2016). Metodología para la integración de la seguridad vial en la empresa, para reducir el índice de accidentes laborales de tráfico.

Memmott, T., S. Carley, M. Graff, and D. M. Konisky (2021). Sociodemographic disparities in energy insecurity among low-income households before and during the COVID-19 pandemic. *Nature energy 6*(2), 186–193.

Met Office (2025). Understanding tropical nights and their impact. https://www.metoffice.gov.uk/blog/2025/understand-tropical-nights-and-their-impact. Accessed July 23, 2026.

Minor, K., A. Bjerre-Nielsen, S. S. Jonasdottir, S. Lehmann, and N. Obradovich (2022). Rising temperatures erode human sleep globally. *One Earth 5*(5), 534–549.

Monteleone, P., G. Mascagni, A. Giannini, A. R. Genazzani, and T. Simoncini (2018). Symptoms of menopause—global prevalence, physiology and implications. *Nature Reviews Endocrinology 14*(4), 199–215.

Navas-Martin, M. A., J. A. Lopez-Bueno, M. S. Ascaso-Sánchez, R. Sarmiento-Suárez, F. Follos, J. M. Vellón, I. Mirón, M. Y. Luna, G. Sánchez-Martínez, D. Culqui, et al. (2022). Gender differences in adaptation to heat in Spain (1983–2018). *Environmental Research 215*, 113986.

Obradovich, N., R. Migliorini, S. C. Mednick, and J. H. Fowler (2017). Nighttime temperature and human sleep loss in a changing climate. *Science advances 3*(5), e1601555.

Okamoto-Mizuno, K. and K. Mizuno (2012). Effects of thermal environment on sleep and circadian rhythm. *Journal of Physiological Anthropology 31*(1), 14.

Okamoto-Mizuno, K., K. Mizuno, S. Michie, A. Maeda, and S. Iizuka (1999). Effects of humid heat exposure on human sleep stages and body temperature. *Sleep 22*(6), 767–773.

Pavanello, F., E. De Cian, M. Davide, M. Mistry, T. Cruz, P. Bezerra, D. Jagu, S. Renner, R. Schaeffer, and A. F. P. Lucena (2021). Air-conditioning and the adaptation cooling deficit in emerging economies. *Nature Communications 12*(1), 6460.

Pecillo, M. (2012). International comparison of occupational accident insurance system. https://oshwiki.osha.europa.eu/en/themes/international-comparison-occupational-accident-insurance-system. Accessed May 28, 2025.

Pérez, J. E. M., F. I. S. Martínez, J. M. A. Perpinán, and J. L. P. Prades (2015). La valoración monetaria de los costes humanos de la siniestralidad vial en España. *Gaceta Sanitaria 29*, 76–78.

Petrongolo, B. and M. Ronchi (2020). Gender gaps and the structure of local labor markets. *Labour Economics 64*, 101819.

Rao, G., S. Redline, F. Schilbach, H. Schofield, and M. Toma (2021). Informing sleep policy through field experiments. *Science 374*(6567), 530–533.

Rippstein, V., E. de Schrijver, S. Eckert, and A. M. Vicedo-Cabrera (2023). Trends in tropical nights and their effects on mortality in Switzerland across 50 years. *PLoS climate 2*(4), e0000162.

Royé, D., F. Sera, A. Tobías, R. Lowe, A. Gasparrini, M. Pascal, F. de'Donato, B. Nunes, and J. P. Teixeira (2021). Effects of hot nights on mortality in Southern Europe. *Epidemiology 32*(4), 487–498.

Rubin, E. and M. Auffhammer (2024). Quantifying heterogeneity in the price elasticity of residential natural gas. *Journal of the Association of Environmental and Resource Economists 11*(2), 319–357.

Rubino, N., J. G. Clemente, and O. Quesada (2024). Teleworking Dynamics in Spain: Pre and Post-Pandemic Insights. *SAGE Open 14*(3), 21582440241260565.

Sager, L. (2019). Estimating the effect of air pollution on road safety using atmospheric temperature inversions. *Journal of Environmental Economics and Management 98*, 102250.

Salminen, S. (2012). Commuting accidents. https://oshwiki.osha.europa.eu/en/themes/commuting-accidents. Accessed July 23, 2026.

Santamouris, M. and K. Vasilakopoulou (2026). Passive cooling for the built environment. *Nature Reviews Clean Technology*.

Smith, A. C. (2016). Spring forward at your own risk: daylight saving time and fatal vehicle crashes. *American Economic Journal: Applied Economics 8*(2), 65–91.

Somanathan, E., R. Somanathan, A. Sudarshan, and M. Tewari (2021). The impact of temperature on productivity and labor supply: Evidence from Indian manufacturing. *Journal of Political Economy 129*(6), 1797–1827.

Teyton, A., M. Tremblay, I. Tardif, M.-A. Lemieux, K. Nour, and T. Benmarhnia (2022). A longitudinal study on the impact of indoor temperature on heat-related symptoms in older adults living in non–air-conditioned households. *Environmental Health Perspectives 130*(7), 077003.

The Guardian (2022, July). Unions call for maximum UK workplace temperature as heatwave descends. *The Guardian*. Accessed: August 18, 2026.

Vargas-Garrido, H., E. Moyano-Díaz, and K. Andrades (2021). Sleep problems are related to commuting accidents rather than to workplace accidents. *BMC public health 21*, 1–7.

Wang, C., K. Liu, and H. Wang (2023). The effects of temperature on sleep experience: evidence from China. *Applied Economics 55*(40), 4678–4694.

Wang, Y., Y. Liu, C. Song, and J. Liu (2015). Appropriate indoor operative temperature and bedding micro climate temperature that satisfies the requirements of sleep thermal comfort. *Building and Environment 92*, 20–29.

Wiswall, M. and B. Zafar (2018). Preference for the workplace, investment in human capital, and gender. *The Quarterly Journal of Economics 133*(1), 457–507.

WMO (2009). Guidelines on analysis of extremes in a changing climate in support of informed decisions for adaptation. https://www.wcrp-climate.org/documents/WCDMP_TD_1500.pdf. Accessed July 23, 2026.

Yu, W., P. Vaneckova, K. Mengersen, X. Pan, and S. Tong (2010). Is the association between temperature and mortality modified by age, gender and socio-economic status? *Science of the total environment 408*(17), 3513–3518.

Zhang, H. and S. Xu (2025). Climate Change, Air Conditioning Adoption, and Household Electricity Use: Evidence from the Northwestern United States. *Environmental and Resource Economics 88*(9), 2469–2501.

Zhang, P., O. Deschenes, K. Meng, and J. Zhang (2018). Temperature effects on productivity and factor reallocation: Evidence from a half million Chinese manufacturing plants. *Journal of Environmental Economics and Management 88*, 1–17.

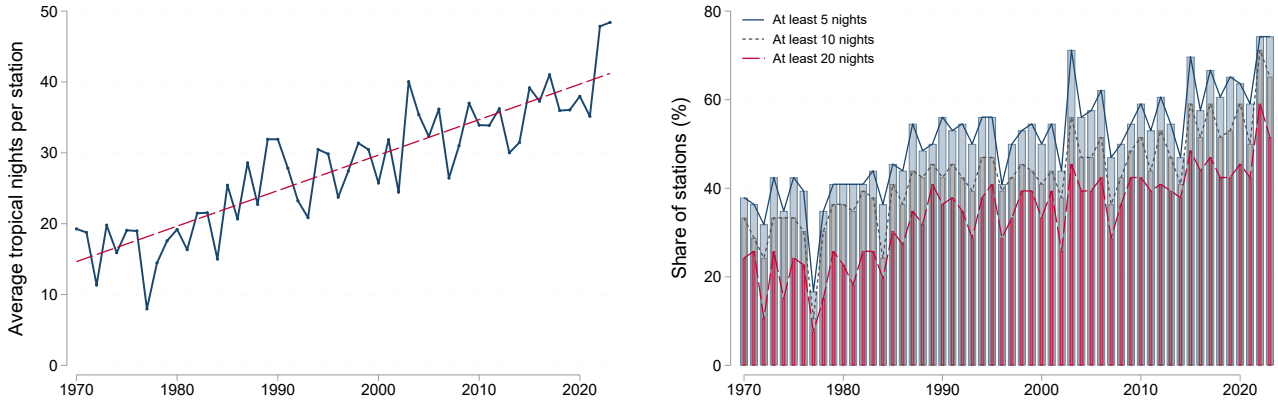
Zhang, S., M. Zhang, Y. Yuan, Z. Li, X. Li, and X. Li (2025). Health risks and genetic architecture of objectively measured multidimensional sleep health. *Nature Communications 16*(1), 7026.

Zheng, N. S., J. Annis, H. Master, L. Han, K. Gleichauf, J. H. Ching, M. Nasser, P. Coleman, S. Desine, D. M. Ruderfer, J. Hernandez, L. D. Schneider, and E. L. Brittain (2024). Sleep patterns and risk of chronic disease as measured by long-term monitoring with commercial wearable devices in the All of Us Research Program. *Nature Medicine 30*(9), 2648–2656.

Appendix A. Additional background information

In this appendix, I provide additional background tables and figures. I begin by presenting evidence on the growing prevalence of tropical nights in Spain, the setting of my empirical analysis. To this end, I use daily station-level minimum-temperature records spanning more than half a century (1970-2023) from the public repository accompanying Correa et al. (2024)—the authors obtained the underlying data from AEMET.[38] Figure A.1 summarizes the resulting trends. Panel A first plots, for every year, the average number of tropical nights across the weather stations included in the sample, together with its fitted linear trend. Panel B then plots the annual share of stations recording at least 5, 10, or 20 tropical nights over the same period.[39]

Figure A.1. Tropical nights across Spanish weather stations (1970-2023)



(A) Average annual number of tropical nights

(B) Share of stations with frequent tropical nights

Notes: The figure illustrates the evolution of the frequency of tropical nights in Spain from 1970 to 2023. Panel A plots the average annual number of tropical nights across weather stations. The solid line shows the annual station average, and the dashed line reports the corresponding fitted linear trend. Panel B plots the annual share of stations recording at least 5, 10, or 20 tropical nights—the analysis excludes weather stations in the Canary Islands. The data come from the public repository accompanying Correa et al. (2024). The underlying daily minimum-temperature records were collected by the AEMET and quality-controlled and homogenized by the authors, who retained 75 stations across 44 provinces with sufficiently long and continuous records for the 1970-2023 period.

The figure shows that tropical nights have become more frequent both on average and across stations. Specifically, the average annual number of tropical nights per station more than doubled, increasing from approximately 16 in the 1970s to 39 during 2014-2023 (Panel A). Over the same periods, the

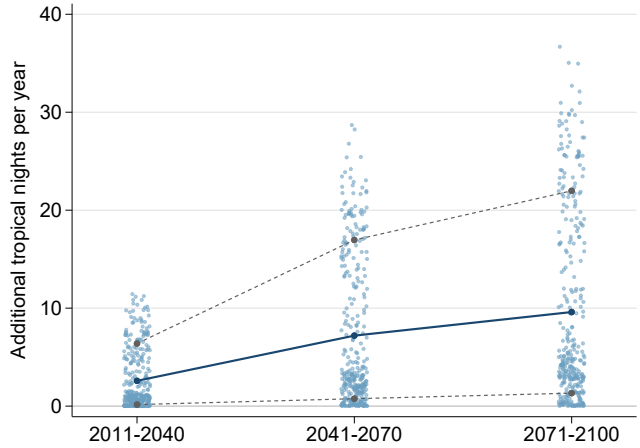
[38] Correa et al. (2024) screened and homogenized the original AEMET records, retaining 75 stations (across 44 provinces) with sufficiently long and continuous time series over 1970-2023. See their paper for further details.

[39] Weather stations in the Canary Islands are excluded from this analysis because their subtropical location and distinct climatic conditions result in a substantially higher baseline frequency of tropical nights than in the rest of Spain.

average annual share of stations recording at least 10 tropical nights rose from 35.2% to 59.2% (Panel B).

Next, I place the evidence for Spain in a broader European context. Figure A.2 shows the projected changes in the average annual number of tropical nights across European NUTS-2 regions relative to the 1991-2020 baseline, obtained from the European Climate Data Explorer.[40] The projections are reported under an intermediate scenario for future greenhouse-gas concentrations—Representative Concentration Pathway 4.5 (RCP4.5)—across three horizons: 2011-2040, 2041-2070, and 2071-2100. Each dot represents the projected change for one NUTS-2 region in a given horizon, while the black line reports the mean across regions.

Figure A.2. Projected increases in tropical nights across European regions



Notes: The figure shows projected increases in the average annual number of tropical nights across European NUTS-2 regions under the RCP4.5 (intermediate) emissions scenario, relative to each region's 1991-2020 baseline. Each gray dot corresponds to one NUTS-2 region in a given future horizon. The black line reports the average change across NUTS-2 regions, while the thinner gray lines report the mean change among the top and bottom terciles of regions in each horizon—terciles are defined separately within each future horizon according to the projected increase in tropical nights. For visual clarity, the figure excludes two NUTS-2 regions (ES63 and ES70), whose projected increases exceed 40 additional tropical nights per year. Data come from the European Climate Data Explorer, available through the Climate-ADAPT tropical-nights indicator.

The figure shows that projected increases in tropical nights become substantially larger across successive horizons. The cross-regional mean rises from about 3 additional tropical nights per year in the near-term horizon to more than 9 by the end of the century (2071-2100). In the upper tercile of projected regional changes within each horizon, the corresponding mean rises from approximately 7 to about 22 additional tropical nights per year.

Table A.1 then reports summary statistics for key variables in the empirical analysis at four obser-

[40]The projections are available through *Climate-ADAPT* (https://climate-adapt.eea.europa.eu/en/metadata/indicators/tropical-nights).

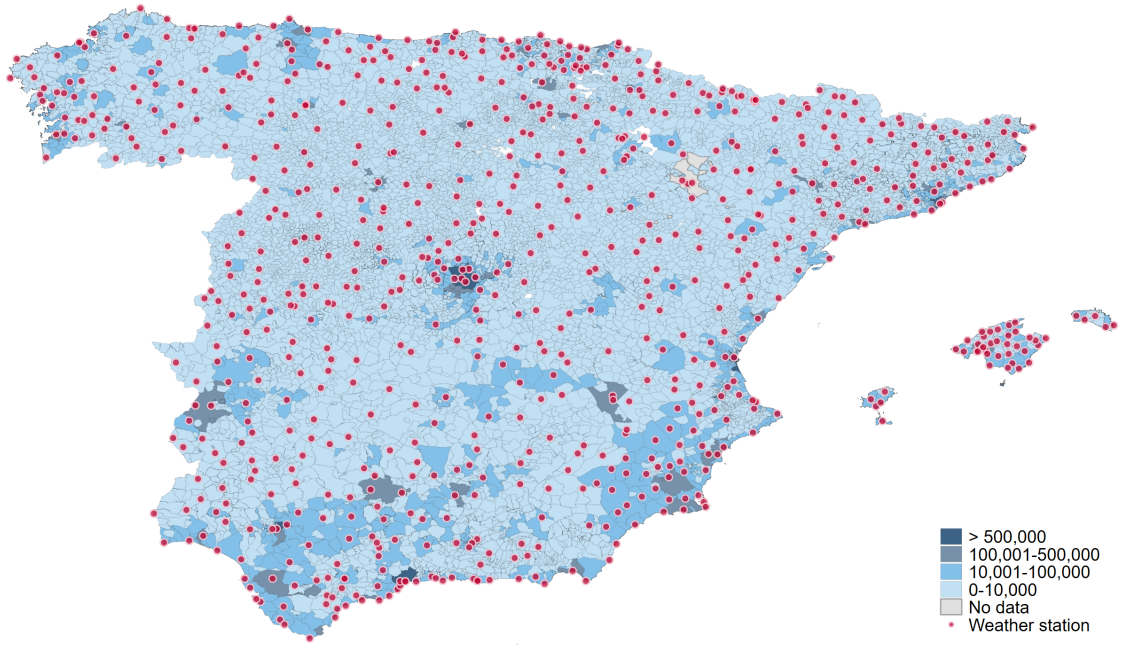
Table A.1. Driver, accident, weather, and municipality summary statistics

	Mean	Std. dev.	Min.	Max.	Observations
	Panel A. Commuting-driver characteristics (driver-involvement level)				
Female	0.333	0.471	0	1	73,710
Driver license issue year	1999	12.060	1952	2019	68,802
Age	39.846	12.478	7	97	73,531
Minor injury (within 24 h)	0.528	0.499	0	1	73,735
Serious injury (within 24 h)	0.042	0.201	0	1	73,735
Fatality (within 24 h)	0.006	0.078	0	1	73,735
Minor injury (within 30 days)	0.528	0.499	0	1	73,735
Serious injury (within 30 days)	0.041	0.199	0	1	73,735
Fatality (within 30 days)	0.007	0.082	0	1	73,735
	Panel B. Commuting accident characteristics (accident level)				
Time (24-h format)	12.984	5.141	0	23	57,505
Highway accident	0.214	0.410	0	1	57,505
# commuting drivers involved	1.282	0.558	1	14	57,505
# vehicles involved	1.946	0.858	1	39	57,505
# pedestrians involved	0.093	0.321	0	9	57,505
# minor injuries (within 24 h)	1.309	0.978	0	34	57,505
# serious injuries (within 24 h)	0.107	0.355	0	9	57,505
# fatalities (within 24 h)	0.019	0.151	0	5	57,505
# minor injuries (within 30 days)	1.309	0.978	0	34	57,505
# serious injuries (within 30 days)	0.104	0.351	0	9	57,505
# fatalities (within 30 days)	0.022	0.161	0	5	57,505
	Panel C. Weather variables (weather station-day level)				
Minimum temperature (°C)	9.91	6.69	-20.5	32.9	1,568,672
Average temperature (°C)	15.4	6.95	-10.7	37.3	1,568,672
Maximum temperature (°C)	20.89	7.98	-8.1	47.3	1,568,672
Rainfall (mm)	1.68	5.99	0	352.2	1,525,457
Maximum wind speed (km/h)	35.07	14.69	0	180	1,312,134
	Panel D. Income data (municipality level)				
Household net income (1,000 €/year)	25.962	6.591	13.534	83.852	6,897
Household gross income (1,000 €/year)	29.797	8.715	14.267	116.628	6,617

Notes: Summary statistics for driver, accident, weather, and income variables used in the empirical analysis: mean, standard deviation, minimum, and maximum. Panel A reports characteristics of commuting drivers involved in traffic accidents. Panel B reports characteristics of accidents involving at least one commuting driver. Panel C reports weather variables at the weather station-day level, while Panel D reports income variables at the municipality level. Observations reports the number of non-missing observations for each variable.

vational levels. Panel A describes the characteristics of commuting drivers involved in accidents in the DGT records over the full period (January 2014-December 2019), with each driver constituting one observation.[41] Panel B reports characteristics of the (unique) accidents involving at least one commuting driver. Panel C provides station-day summary statistics for weather variables (including the weather controls used in the empirical analysis) from AEMET over the same period. Finally, Panel D reports municipality-level household income measures used in the heterogeneity analysis.

Figure A.3. AEMET weather-station network and municipal population



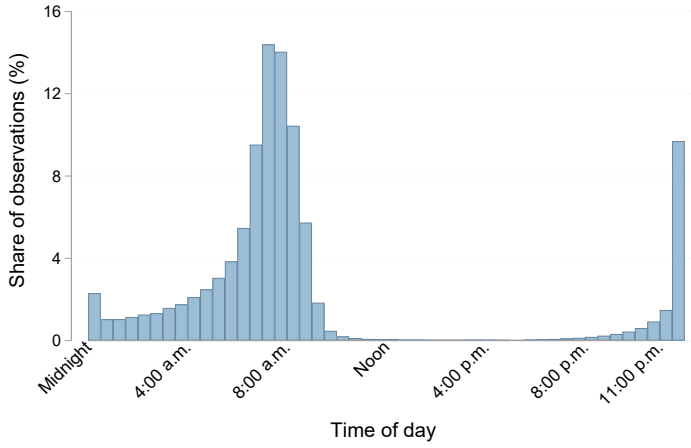
Notes: The figure maps the AEMET weather stations located in mainland Spain and the Balearic Islands—each small red circle denotes one weather station. Municipal population in 2019 is represented by the blue color scale. Thin gray lines indicate municipal boundaries. For visual clarity, the Canary Islands and the overseas cities of Ceuta and Melilla are not displayed.

Next, Figure A.3 maps the 782-station AEMET weather network located in mainland Spain and the Balearic Islands I use in my analysis (the AEMET dataset contains 858 weather stations overall), as well as municipality population across Spain. As explained in the main text, the full AEMET dataset contains 858 stations located in 784 municipalities across Spain, including 23 with populations exceeding 200,000. When multiple stations are available within a municipality, I average weather conditions across those stations.

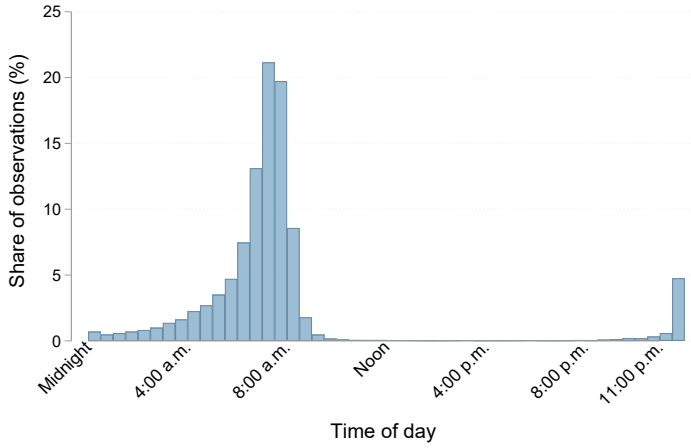
Then, in Figure A.4 I display the timing of the recorded daily minimum temperature. Panel A uses all

[41] The data include 91 records (0.12%) of drivers aged 15 or younger coded as commuting. These ages are difficult to reconcile with travel to or from work, suggesting an error in the recorded age.

Figure A.4. Timing of daily minimum temperatures across municipalities (January 2014-December 2019)



(A) All days

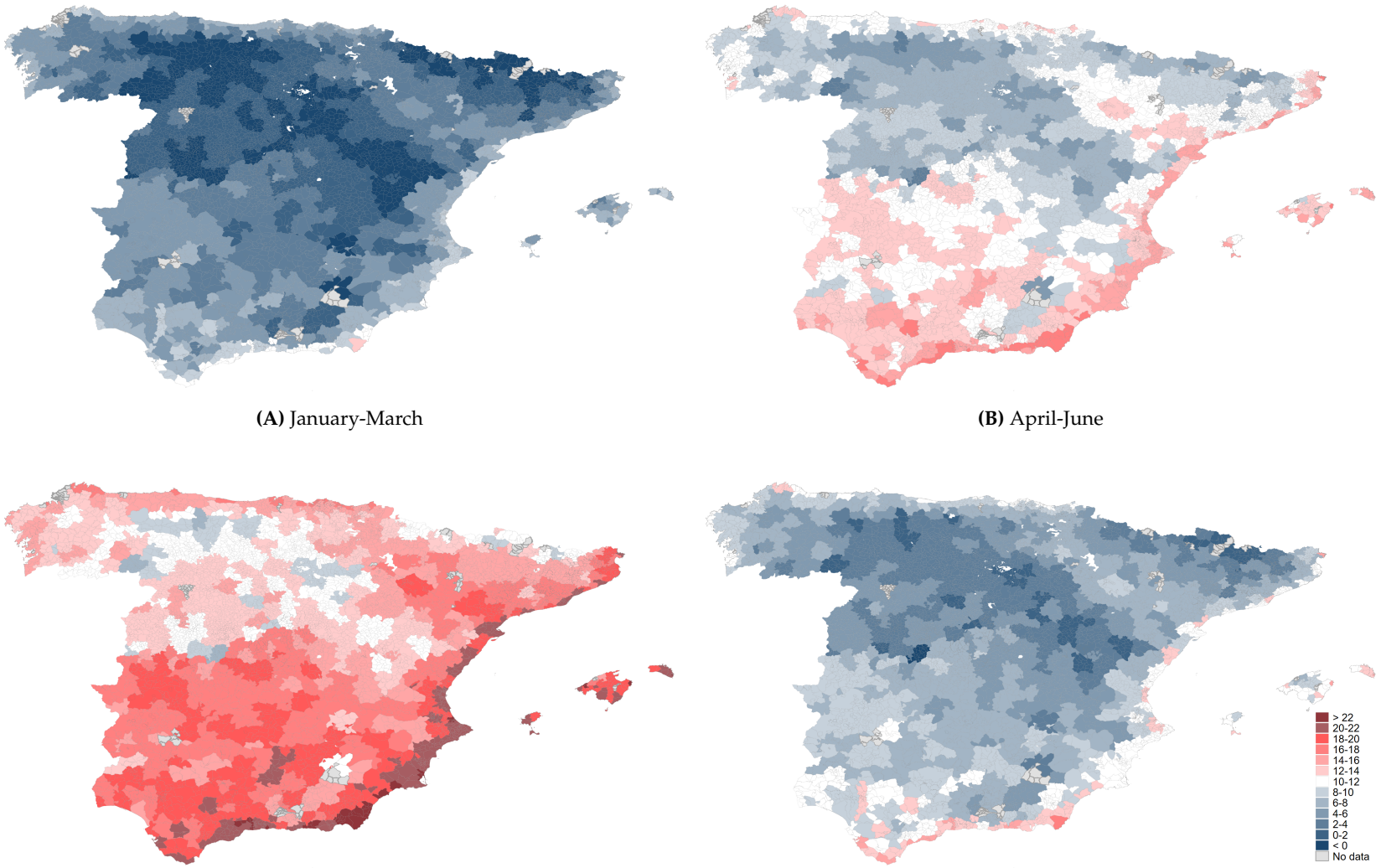


(B) Tropical-night days

Notes: The figure plots the distribution of the time of day of daily minimum temperatures. Temperature measures are constructed from AEMET weather-station data using the municipality-level weather assignment described in Section 2.1. Panel A includes all municipality-day observations between January 2014 and December 2019, while Panel B restricts the sample to tropical-night municipality-days (defined as days with a minimum temperature above 20°C). Bars report the percentage of observations falling within each 30-minute interval. Time is displayed using a 12-hour clock.

observations, whereas in Panel B I restrict the sample to tropical-night days. In about 85% of full-sample observations, the minimum is recorded during late-night or early-morning hours and therefore closely reflects nighttime conditions. In about 12% of observations, it is recorded after 11:00 p.m., when it may instead reflect cooling during the subsequent night. Note that this concern is much smaller on tropical-night days: fewer than 5% of such observations are recorded after 11:00 p.m., while approximately 93% occur during late-night or early-morning hours.

Figure A.5. Average monthly minimum temperature across municipalities by calendar quarter (May 2013-May 2023)



(A) January-March

(B) April-June

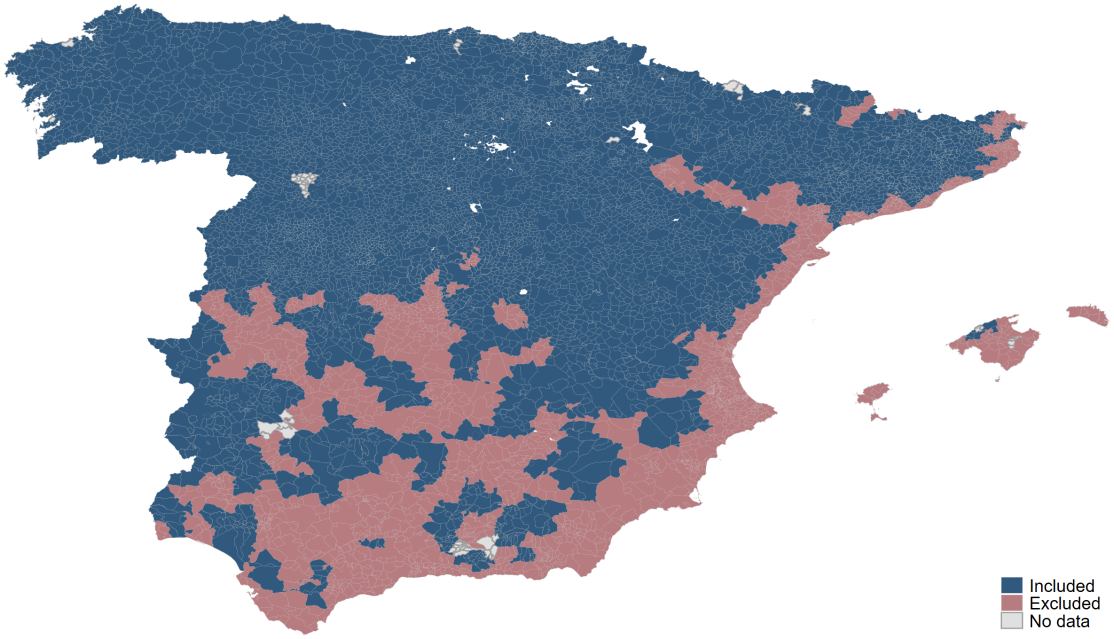
(C) July-September

(D) October-December

Notes: The figure maps average monthly minimum temperatures across Spanish municipalities by calendar quarter. Each panel reports the municipality-level average for the three calendar months indicated. Temperature measures are constructed from AEMET weather-station data using the municipality-level weather assignment described in Section 2.1. The map uses the full available weather record (May 2013-May 2023), which extends beyond the period covered by the accident data used in the main analysis. For visual clarity, municipalities in the Canary Islands and the overseas cities of Ceuta and Melilla are not displayed.

Figure A.5 illustrates the pronounced climatic diversity of Spain discussed in the main text by mapping average monthly minimum temperatures across municipalities for each calendar quarter. Average minimum temperatures vary sharply across space (reflecting differences in coastal proximity and elevation): some municipalities record average minimum temperatures above 15°C even in spring and fall, whereas others remain below 10°C even during the summer months.

Figure A.6. Municipalities included in and excluded from the baseline sample

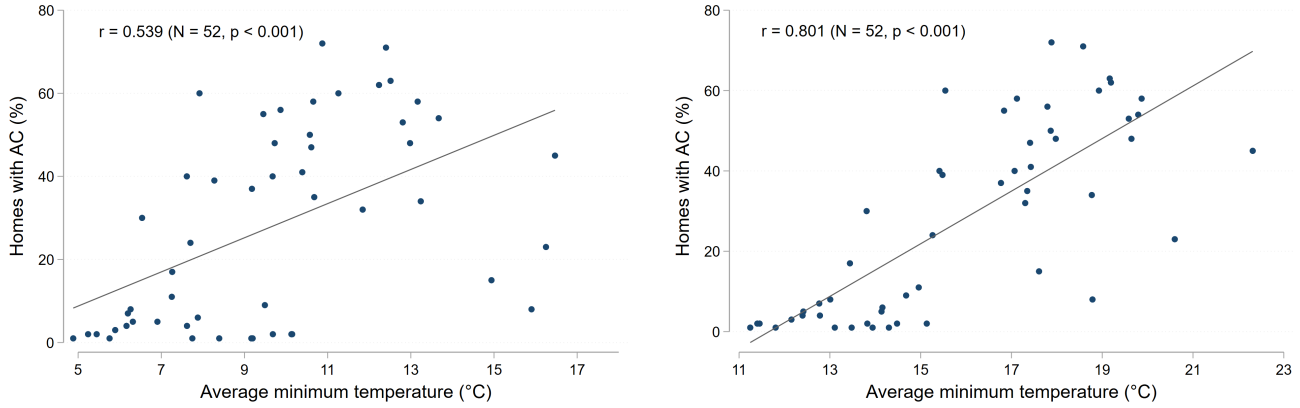


Notes: The figure maps municipalities included in and excluded from the baseline sample used in Section 3.1. Municipalities included in the baseline sample (shown in dark blue) have a monthly average minimum temperature below 19°C; excluded municipalities (shown in muted red) have a monthly average minimum temperature at or above 19°C. Temperature measures are constructed from AEMET weather-station data using the municipality-level weather assignment described in Section 2.1. The map uses the full available weather record (May 2013-May 2023), which extends beyond the period covered by the accident data used in the main analysis. For visual clarity, municipalities in the Canary Islands and the overseas cities of Ceuta and Melilla are not displayed.

The spatial heterogeneity in climate documented above creates scope for differences in adaptation: residents of municipalities where tropical nights are common may be more acclimatized or better equipped to cope with nighttime heat, whereas adaptation may be more limited in historically cooler municipalities. For this reason, the baseline sample focuses on municipalities where tropical nights are relatively uncommon, defined as those with average monthly minimum temperatures below 19°C—I then explicitly examine how the estimates change under alternative temperature thresholds. Figure A.6 maps the municipalities included in this baseline sample. More than 76% of Spanish municipalities sat-

isfy this criterion, including Madrid and municipalities in its metropolitan area, as well as several major metropolitan areas in northern and inland Spain.

Figure A.7. AC penetration in provincial capitals and province-level minimum temperatures



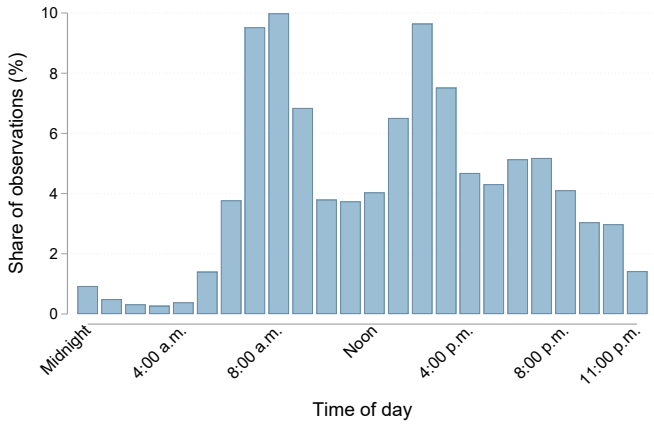
(A) Annual **(B)** Summer (June-August)

Notes: The figure plots the share of homes listed for sale or rent with AC in each Spanish provincial capital (as of July 2023) against the corresponding province's average minimum temperature. Panel A uses the annual average minimum temperature, whereas Panel B uses the average minimum temperature during the summer months (June–August). Data on AC penetration was obtained from Idealista. Temperature measures are constructed from AEMET data using the full available weather record (May 2013-May 2023), which extends beyond the period covered by the accident data used in the main analysis. Each panel includes a fitted regression line estimated via OLS (dark gray line). Panel annotations report the correlation coefficient, the number of observations, and the corresponding p-value.

Next, in Figure A.7 I provide descriptive evidence consistent with greater adaptation to nighttime heat in warmer locations. Panel A plots province-level annual average minimum temperatures against the share of homes listed for sale or rent with AC across Spain's provincial capitals, using data from Idealista (the leading online real estate platform in Spain). Panel B repeats the exercise using average minimum temperatures during the summer months (June-August). Both panels show a positive and statistically significant cross-sectional relationship: provincial capitals located in warmer provinces tend to be better equipped to cope with nighttime heat, as shown by a higher share of listed homes advertising AC.

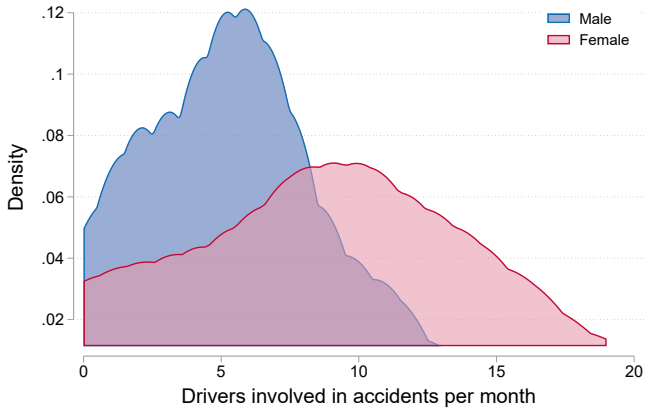
Figure A.8 then displays the distribution of commuting drivers involved in accidents in the sample by time of day. Commuting-driver observations are concentrated in the 7:00 a.m.-2:59 p.m. window, consistent with routine morning and early-afternoon commuting patterns. This pattern motivates the robustness check in which I restrict the analysis to accidents occurring during this window, when the consequences of sleep disruption following nighttime heat are likely to be most salient.

Figure A.8. Commuting drivers involved in accidents by time of day (January 2014-December 2019)



Notes: The figure plots the distribution of drivers involved in accidents while traveling to or from work by time of day. Bars report the percentage of commuting-driver observations falling within each hourly interval. The data was obtained from the DGT and cover January 2014 to December 2019. Time is displayed using a 12-hour clock.

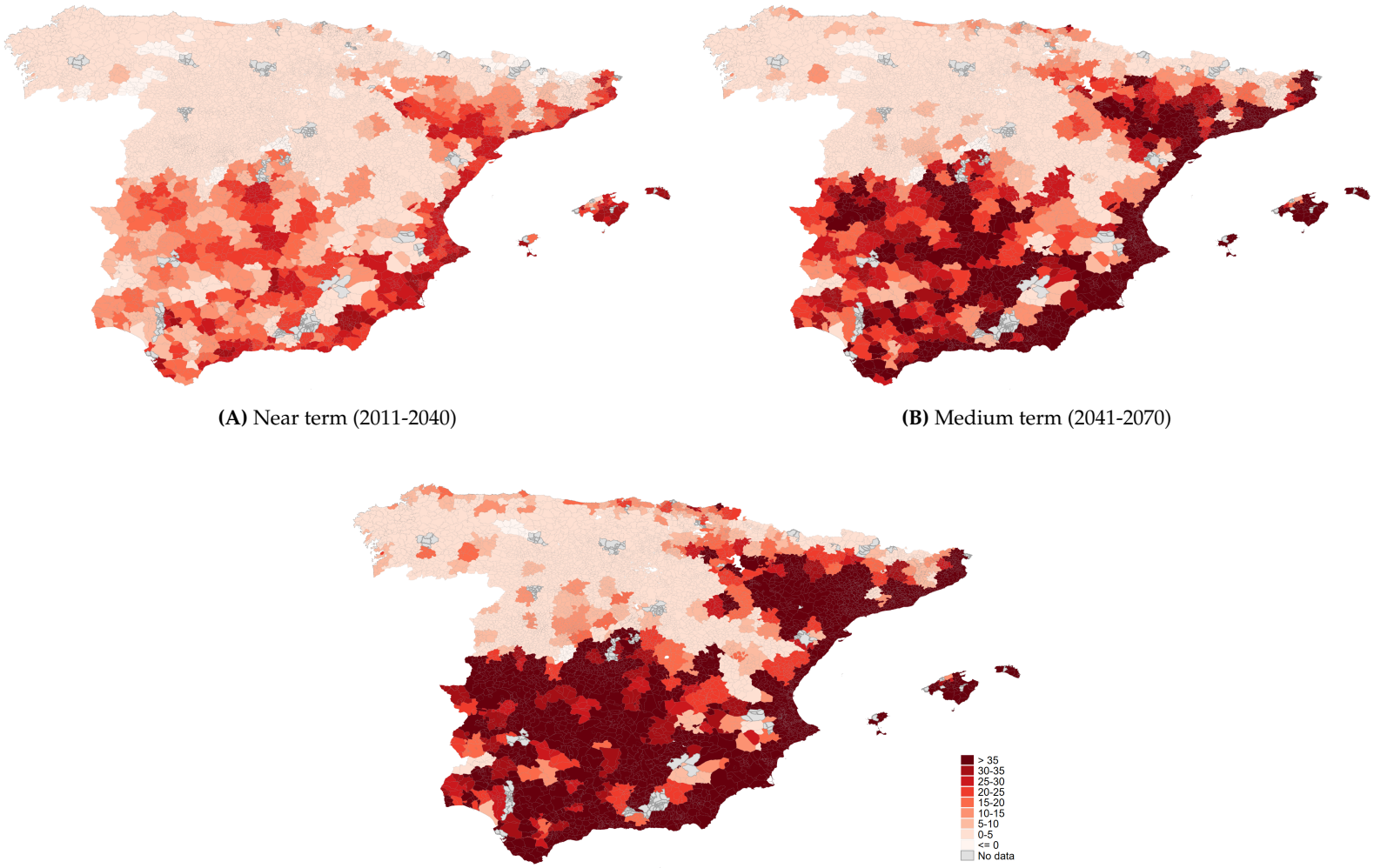
Figure A.9. Monthly number of drivers involved in accidents while transporting children to or from school by gender



Notes: The figure plots kernel density estimates of the monthly number of drivers involved in traffic accidents while transporting children to or from school by gender. The data was obtained from the DGT and cover January 2014 to December 2019. The mean (median) monthly count is 5.21 (5.5) for male drivers and 8.54 (8.5) for female drivers.

Next, Figure 2 in the main text shows that, among commuting drivers involved in accidents, the share traveling with at least one minor passenger is higher among women than among men. This pattern is consistent with gender differences in child-related travel during commuting trips. Figure A.9 complements this evidence by showing that the monthly number of drivers involved in accidents while transporting children to or from school (outside the commuting context) is also substantially higher for women than for men.

Figure A.10. Projected increase in annual tropical nights across municipalities, medium-emissions scenario (SSP2-4.5)



(A) Near term (2011-2040)

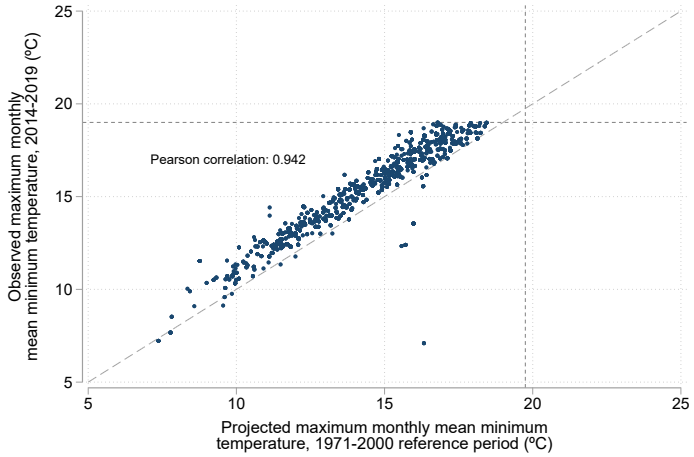
(B) Medium term (2041-2070)

(C) Long term (2071-2100)

Notes: The figure maps the projected increase in the annual number of tropical nights across Spanish municipalities under the intermediate-emissions scenario (SSP2-4.5), relative to the 1971-2000 historical baseline. Panels A, B, and C report projections for the near-term (2011-2040), medium-term (2041-2070), and long-term (2071-2100) horizons, respectively. A tropical night is defined by a daily minimum temperature above 20°C. Changes are expressed in nights per year. Projections are averaged across 11 CMIP6 global climate models: ACCESS-CM2, CMCC-CM2-SR5, CNRM-ESM2-1, EC-Earth3-Veg, IITM-ESM, KACE-1-0-G, MIROC6, MPI-ESM1-2-HR, MRI-ESM2-0, NorESM2-MM, and UKESM1-0-LL. For visual clarity, municipalities in the Canary Islands and the overseas cities of Ceuta and Melilla are not displayed.

In the main text, Figure 3 provides a map of projected increases in tropical nights across Spanish municipalities under the medium-emissions scenario (SSP2-4.5) for the medium-term horizon (2041-2070)—the projections are averaged across the 11 climate models. To facilitate comparison across horizons, Figure A.10 reports the corresponding maps for the near- and long-term horizons. The maps show that projected increases in tropical nights are widespread across Spain and become larger across successive horizons.

Figure A.11. Observed and projected nighttime climate measures



Notes: The figure compares observed and projected measures of nighttime climate at the municipality level. The vertical axis reports the observed maximum across months of mean monthly minimum temperature during 2014-2019, while the horizontal axis reports the corresponding projected measure for the 1971-2000 historical reference period from the climate-model data. Each point represents a municipality. The gray dashed line is the 45-degree reference line. The gray dashed lines indicate the 19°C observed threshold used to define the baseline sample and the 19.75°C projected threshold used in the adaptation-adjusted projection.

Finally, Figure 4 (Panel B) in the main text presents an adaptation-adjusted projection of the future excess accident burden. Following the adaptation evidence in Section 4.1, the calculation excludes municipalities whose model-based maximum monthly mean minimum temperature exceeds 19.75°C. This threshold is applied to climate-model measures, whereas the adaptation exercise in Section 4.1 uses observed weather data. Although the two measures are not numerically identical, both are defined as the maximum across months of mean monthly minimum temperature (and are therefore expected to be closely related). Hence, as a sanity check, Figure A.11 compares the observed and model-based measures at the municipality level. As expected, they are strongly correlated, with a correlation coefficient above 0.94.

Appendix B. Additional empirical results

In this appendix, I report additional estimates and robustness checks that complement the analysis in the main text.

Appendix B.1. Main results using Conley standard errors

I begin by assessing the robustness of the main results to spatial and temporal correlation in the regression errors. The estimates in the main text cluster standard errors at the municipality level—thus allowing for arbitrary serial correlation and heteroskedasticity within municipalities—but assume that regression errors are independent across municipalities. This assumption may be restrictive if nearby municipalities share unobserved shocks affecting commuting accidents or exhibit spatially correlated errors. I therefore estimate again the main specifications using Conley standard errors, which allow regression errors to be correlated across nearby municipality-day observations (with allowable spatial correlation declining with distance and reaching zero beyond a chosen cutoff) as well as over a specified temporal window.

First, Table B.1 reports the specifications in Table 1 in the main text using Conley standard errors. Specifically, I allow regression errors to be correlated across observations from municipalities within 100 kilometers of one another and over a seven-day temporal window. Because this adjustment changes only the estimated covariance matrix, the point estimates are identical to those in Table 1; only the standard errors (and resulting inference) differ. The results remain closely aligned with the baseline inference in Table 1: across columns, the coefficient on the tropical-night indicator remains statistically significant at the 5% level. By contrast, the coefficients on the colder temperature bins remain small and statistically indistinguishable from zero.

Next, Table B.2 assesses the sensitivity of the Conley-based inference to alternative spatial cutoffs and temporal windows. Specifically, Panels A, B, and C of this table report the coefficient of interest using spatial cutoffs of 50, 100, and 150 kilometers, respectively, while holding the temporal window fixed at seven days. Panel D then retains the 100-kilometer spatial cutoff and instead uses a 14-day temporal window. Across panels and columns, the coefficient on the tropical-night indicator remains statistically distinguishable from zero at conventional levels.

Table B.1. The impact of minimum nighttime temperature on commuting accidents using Conley standard errors

	(1)	(2)	(3)	(4)	(5)	(6)	(7)	(8)
$\leq 0°$C	0.0516	0.0758	0.0606	0.0889	0.0459	0.0712	0.0433	0.0729
	(0.0651)	(0.0619)	(0.0653)	(0.0620)	(0.0655)	(0.0623)	(0.0659)	(0.0624)
0–5°C	0.0054	0.0307	0.0115	0.0399	0.0014	0.0275	-0.0013	0.0280
	(0.0519)	(0.0497)	(0.0522)	(0.0498)	(0.0526)	(0.0502)	(0.0530)	(0.0505)
5–10°C	0.0282	0.0548	0.0359	0.0651	0.0229	0.0508	0.0266	0.0572
	(0.0425)	(0.0405)	(0.0423)	(0.0403)	(0.0434)	(0.0413)	(0.0433)	(0.0411)
10–15°C	0.0255	0.0432	0.0276	0.0459	0.0154	0.0341	0.0146	0.0329
	(0.0317)	(0.0303)	(0.0314)	(0.0301)	(0.0325)	(0.0310)	(0.0325)	(0.0309)
$> 20°$C (tropical night)	0.142**	0.135**	0.134**	0.128**	0.147**	0.139**	0.139**	0.132**
	(0.0609)	(0.0588)	(0.0627)	(0.0601)	(0.0614)	(0.0594)	(0.0623)	(0.0597)
Weather controls	✓	✓	✓	✓	✓	✓	✓	✓
Mun. & week-year FE	✓	✓	✓	✓	✓	✓	✓	✓
Prov. × month FE	✓	✓						
Prov. × week FE			✓	✓				
Mun. × month FE					✓	✓		
Mun. × week FE							✓	✓
Day-of-week FE		✓		✓		✓		✓
Tropical-night effect (%)	15.2	14.5	14.3	13.7	15.8	14.9	14.9	14.1
Mean dep. var.	0.007	0.007	0.008	0.008	0.024	0.024	0.062	0.062
Mean accidents/day	10.67	10.67	10.67	10.67	10.67	10.67	10.67	10.67
Daily Δ accidents	1.63	1.54	1.53	1.45	1.69	1.60	1.59	1.51
Pseudo-R^2	0.341	0.354	0.345	0.358	0.242	0.257	0.178	0.198
Observations	3,253,330	3,253,330	3,092,721	3,092,721	974,884	974,884	378,787	378,787

Notes: The dependent variable is the number of commuting drivers involved in traffic accidents. All columns are estimated by PPML. Temperature bins are defined using daily minimum temperature; the omitted category is 15°C–20°C. Weather controls include precipitation, maximum temperature, and maximum wind speed. Conley standard errors allowing for spatial correlation within 100 km and serial correlation up to 7 days, using Bartlett spatial and temporal kernels, are reported in parentheses. The tropical-night effect is computed as $100 \times [\exp(\hat{\alpha}) - 1]$, where $\hat{\alpha}$ is the coefficient on the $> 20°$C bin. Mean dep. var. is the column-specific mean of the municipality-day outcome. Mean accidents/day is the mean number of commuting drivers involved in accidents per calendar day in the column-specific estimation sample. Daily Δ accidents is computed as $[\exp(\hat{\alpha}) - 1] \times$ mean accidents/day and refers to commuting drivers involved in accidents. Significance levels: * $p < 0.10$, ** $p < 0.05$, *** $p < 0.01$.

Table B.2. The impact of tropical nights on commuting accidents using alternative Conley standard errors

	(1)	(2)	(3)	(4)	(5)	(6)	(7)	(8)
				Panel A. 50 km spatial cutoff, 7-day serial lag				
$>$ 20°C (tropical night)	0.142**	0.135**	0.134**	0.128**	0.147**	0.139**	0.139**	0.132**
	(0.0602)	(0.0591)	(0.0614)	(0.0598)	(0.0605)	(0.0595)	(0.0610)	(0.0593)
Mean dep. var.	0.007	0.007	0.008	0.008	0.024	0.024	0.062	0.062
Observations	3,253,330	3,253,330	3,092,721	3,092,721	974,884	974,884	378,787	378,787
				Panel B. 100 km spatial cutoff, 7-day serial lag				
$>$ 20°C (tropical night)	0.142**	0.135**	0.134**	0.128**	0.147**	0.139**	0.139**	0.132**
	(0.0609)	(0.0588)	(0.0627)	(0.0601)	(0.0614)	(0.0594)	(0.0623)	(0.0597)
Mean dep. var.	0.007	0.007	0.008	0.008	0.024	0.024	0.062	0.062
Observations	3,253,330	3,253,330	3,092,721	3,092,721	974,884	974,884	378,787	378,787
				Panel C. 150 km spatial cutoff, 7-day serial lag				
$>$ 20°C (tropical night)	0.142**	0.135**	0.134**	0.128**	0.147**	0.139**	0.139**	0.132**
	(0.0605)	(0.0580)	(0.0628)	(0.0597)	(0.0611)	(0.0587)	(0.0624)	(0.0593)
Mean dep. var.	0.007	0.007	0.008	0.008	0.024	0.024	0.062	0.062
Observations	3,253,330	3,253,330	3,092,721	3,092,721	974,884	974,884	378,787	378,787
				Panel D. 100 km spatial cutoff, 14-day serial lag				
$>$ 20°C (tropical night)	0.142**	0.135**	0.134**	0.128**	0.147**	0.139**	0.139**	0.132**
	(0.0612)	(0.0599)	(0.0629)	(0.0612)	(0.0615)	(0.0602)	(0.0618)	(0.0600)
Mean dep. var.	0.007	0.007	0.008	0.008	0.024	0.024	0.062	0.062
Observations	3,253,330	3,253,330	3,092,721	3,092,721	974,884	974,884	378,787	378,787
				Controls and fixed effects (all panels)				
Weather controls	✓	✓	✓	✓	✓	✓	✓	✓
Mun. & week-year FE	✓	✓	✓	✓	✓	✓	✓	✓
Prov. $\times$ month FE	✓	✓						
Prov. $\times$ week FE			✓	✓				
Mun. $\times$ month FE					✓	✓		
Mun. $\times$ week FE							✓	✓
Day-of-week FE		✓		✓		✓		✓

Notes: The dependent variable is the number of commuting drivers involved in traffic accidents. All columns are estimated by PPML. The table reports the coefficient on the tropical-night indicator (daily minimum temperature above 20°C). Temperature bins are defined using daily minimum temperature; the omitted category is 15°C–20°C. Weather controls include precipitation, maximum temperature, and maximum wind speed. Conley standard errors, using Bartlett spatial and temporal kernels with the spatial cutoffs and serial lags indicated in the panel headings, are reported in parentheses. Mean dep. var. is the column-specific mean of the municipality-day outcome. Significance levels: * $p < 0.10$, ** $p < 0.05$, *** $p < 0.01$.

Appendix B.2. Main results: additional analyses and robustness checks

This appendix provides additional analyses and robustness checks for the main results. First, Table 2 in the main text provides a summary of six robustness checks addressing accident definition, exposure measurement, and timing and temperature-bin specifications. In particular, the six rows of this table show that the estimates are robust to *(i)* restricting the analysis to accidents in which all involved drivers are commuting; *(ii)* restricting the sample to accidents occurring in the same province as the commuting driver's municipality of residence; *(iii)* restricting the sample to municipalities with their own weather station; *(iv)* excluding observations for which the daily minimum temperature is recorded after 11:00 p.m.; *(v)* restricting the analysis to accidents occurring early in the day; and *(vi)* using an alternative omitted temperature bin. To keep the presentation concise, Table 2 reports the coefficient on the tropical-night indicator for both the preferred and the most demanding specifications—Columns (2) and (8), respectively, of Table 1. For completeness, Table B.3 reports the corresponding estimates for all eight specifications, with Panels A-F corresponding, in order, to the six rows in Table 2.

As discussed in the main text, Table B.4 examines whether the results are sensitive to more flexible controls for daytime heat. Panel A replaces the baseline linear control for same-day maximum temperature with temperature bins; Panel B also includes bins for previous-day maximum temperature. In both panels, each maximum-temperature measure enters in 5°C bins from 10°C to 35°C, with separate bins for temperatures at or below 10°C and above 35°C (the 20-25°C bin is omitted). Across both panels, the tropical-night coefficients remain positive, range from 0.137 to 0.164, and are statistically significant either at the 1% or the 5% level in every specification. The estimates are broadly comparable to those in Table 1.

Next, Table B.5 adds calendar-date fixed effects to account for shocks common to municipalities on the same day. These fixed effects absorb the week-by-year and day-of-the-week fixed effects used in the baseline specifications. Panel A retains a linear control for same-day maximum temperature, while Panel B instead uses maximum-temperature bins. Comparing municipalities on the same date still yields an estimated increase of about 13-15% in the count of commuting drivers involved in accidents on tropical-night days, with statistically significant coefficients in every specification.

Turning to accident timing, Table B.6 repeats the baseline specifications using outcomes restricted to accidents before 11:00 a.m. (Panel A) and before 9:00 a.m. (Panel B). The tropical-night coefficients are

Table B.3. Robustness of the tropical-night effect: full specifications

	(1)	(2)	(3)	(4)	(5)	(6)	(7)	(8)
				Panel A. All involved drivers are commuting				
>20°C (tropical night)	0.205***	0.194***	0.187***	0.179**	0.209***	0.198***	0.198***	0.189**
	(0.0738)	(0.0741)	(0.0716)	(0.0718)	(0.0767)	(0.0768)	(0.0749)	(0.0750)
Mean dep. var.	0.005	0.005	0.006	0.006	0.019	0.019	0.053	0.053
Observations	2,616,803	2,616,803	2,360,426	2,360,426	688,596	688,596	247,847	247,847
				Panel B. Accident in same province as residence				
>20°C (tropical night)	0.132**	0.124**	0.125**	0.117**	0.140***	0.132***	0.133**	0.126**
	(0.0533)	(0.0503)	(0.0542)	(0.0511)	(0.0542)	(0.0510)	(0.0560)	(0.0529)
Mean dep. var.	0.007	0.007	0.008	0.008	0.024	0.024	0.062	0.062
Observations	2,900,782	2,900,782	2,748,912	2,748,912	862,781	862,781	336,304	336,304
				Panel C. Municipalities with weather station				
>20°C (tropical night)	0.161**	0.151***	0.157**	0.145***	0.160**	0.150***	0.165***	0.155***
	(0.0634)	(0.0560)	(0.0630)	(0.0557)	(0.0640)	(0.0564)	(0.0619)	(0.0554)
Mean dep. var.	0.026	0.026	0.031	0.031	0.053	0.053	0.104	0.104
Observations	517,439	517,439	435,047	435,047	259,147	259,147	131,453	131,453
				Panel D. Drop late-evening minimum temperatures				
>20°C (tropical night)	0.142***	0.131***	0.137***	0.128***	0.142***	0.131***	0.139***	0.132***
	(0.0464)	(0.0433)	(0.0480)	(0.0445)	(0.0476)	(0.0442)	(0.0494)	(0.0458)
Mean dep. var.	0.008	0.008	0.008	0.008	0.026	0.026	0.068	0.068
Observations	2,773,645	2,773,645	2,608,684	2,608,684	808,819	808,819	310,581	310,581
				Panel E. Early-day accidents only				
>20°C (tropical night)	0.158**	0.148**	0.149**	0.141**	0.159**	0.147**	0.156**	0.146**
	(0.0719)	(0.0709)	(0.0722)	(0.0715)	(0.0729)	(0.0722)	(0.0724)	(0.0732)
Mean dep. var.	0.005	0.005	0.006	0.006	0.019	0.019	0.052	0.052
Observations	2,506,229	2,506,229	2,232,504	2,232,504	668,712	668,712	242,894	242,894
				Panel F. Alternative omitted temperature bin				
>20°C (tropical night)	0.129**	0.119**	0.126**	0.117**	0.134**	0.123**	0.133**	0.127**
	(0.0523)	(0.0501)	(0.0528)	(0.0498)	(0.0534)	(0.0509)	(0.0547)	(0.0517)
Mean dep. var.	0.007	0.007	0.008	0.008	0.024	0.024	0.063	0.063
Observations	3,104,805	3,104,805	2,941,723	2,941,723	920,118	920,118	354,942	354,942
				Controls and fixed effects (all panels)				
Weather controls	✓	✓	✓	✓	✓	✓	✓	✓
Mun. & week-year FE	✓	✓	✓	✓	✓	✓	✓	✓
Prov. × month FE	✓	✓						
Prov. × week FE			✓	✓				
Mun. × month FE					✓	✓		
Mun. × week FE							✓	✓
Day-of-week FE		✓		✓		✓		✓

Notes: The dependent variable is the number of commuting drivers involved in traffic accidents. Each panel reports the full set of specifications for the correspondingly labeled robustness check in Table 2. All columns are estimated by PPML and report the coefficient on the tropical-night indicator (daily minimum temperature above 20°C). Temperature bins are defined using daily minimum temperature; the omitted category is 15°C–20°C, except in Panel F, where the omitted category is 15°C–18°C. Weather controls include precipitation, maximum temperature, and maximum wind speed. Standard errors clustered by municipality are reported in parentheses. Mean dep. var. is the column-specific mean of the municipality-day outcome. Significance levels: * $p < 0.10$, ** $p < 0.05$, *** $p < 0.01$.

Table B.4. The impact of tropical nights on commuting accidents with flexible controls for maximum temperature

	(1)	(2)	(3)	(4)	(5)	(6)	(7)	(8)
	Panel A. Flexible same-day maximum temperature							
> 20°C (tropical night)	0.160***	0.145***	0.151***	0.137***	0.164***	0.149***	0.156***	0.143***
	(0.0544)	(0.0483)	(0.0563)	(0.0495)	(0.0557)	(0.0493)	(0.0583)	(0.0514)
Tropical-night effect (%)	17.4	15.6	16.3	14.7	17.8	16.1	16.9	15.4
Mean dep. var.	0.007	0.007	0.008	0.008	0.024	0.024	0.062	0.062
Mean accidents/day	10.67	10.67	10.67	10.67	10.67	10.67	10.67	10.67
Daily Δ accidents	1.85	1.67	1.74	1.57	1.90	1.71	1.81	1.64
Pseudo-R^2	0.341	0.354	0.345	0.358	0.242	0.257	0.178	0.198
Observations	3,253,330	3,253,330	3,092,721	3,092,721	974,884	974,884	378,787	378,787
	Panel B. Flexible same-day and previous-day maximum temperatures							
> 20°C (tropical night)	0.151***	0.146***	0.142**	0.137**	0.155***	0.150***	0.149**	0.146***
	(0.0552)	(0.0515)	(0.0576)	(0.0531)	(0.0568)	(0.0528)	(0.0598)	(0.0555)
Tropical-night effect (%)	16.3	15.7	15.3	14.7	16.8	16.2	16.1	15.7
Mean dep. var.	0.007	0.007	0.008	0.008	0.024	0.024	0.063	0.063
Mean accidents/day	10.49	10.49	10.49	10.49	10.49	10.49	10.49	10.49
Daily Δ accidents	1.71	1.65	1.60	1.53	1.75	1.69	1.68	1.64
Pseudo-R^2	0.342	0.354	0.345	0.358	0.242	0.258	0.179	0.198
Observations	3,104,320	3,104,320	2,946,180	2,946,180	932,821	932,821	362,306	362,306
	Controls and fixed effects (both panels)							
Precipitation & wind speed	✓	✓	✓	✓	✓	✓	✓	✓
Mun. & week-year FE	✓	✓	✓	✓	✓	✓	✓	✓
Prov. $\times$ month FE	✓	✓						
Prov. $\times$ week FE			✓	✓				
Mun. $\times$ month FE					✓	✓		
Mun. $\times$ week FE							✓	✓
Day-of-week FE		✓		✓		✓		✓

Notes: The dependent variable is the number of commuting drivers involved in traffic accidents. All columns are estimated by PPML. Panel A controls flexibly for same-day maximum temperature. Panel B includes flexible controls for both same-day and previous-day maximum temperatures in the same regression. Each maximum temperature is entered in bins of at most 10°C, 10–15°C, 15–20°C, 20–25°C, 25–30°C, 30–35°C, and above 35°C; the 20–25°C bin is omitted. Both panels include minimum-temperature bins, with 15–20°C omitted, as well as precipitation and maximum wind speed. Standard errors clustered by municipality are reported in parentheses. The tropical-night effect is computed as $100 \times [\exp(\hat{\alpha}) - 1]$, where $\hat{\alpha}$ is the coefficient on the > 20°C minimum-temperature bin. Mean dep. var. is the column-specific mean of the municipality-day outcome. Mean accidents/day is the mean number of commuting drivers involved in accidents per calendar day in the column-specific estimation sample. Daily Δ accidents is computed as $[\exp(\hat{\alpha}) - 1] \times$ mean accidents/day and refers to commuting drivers involved in accidents. Panel B requires previous-day maximum temperature and therefore uses its own estimation sample. Significance levels: * $p < 0.10$, ** $p < 0.05$, *** $p < 0.01$.

Table B.5. The impact of tropical nights on commuting accidents with calendar-date fixed effects

	(1)	(2)	(3)	(4)
	Panel A. Calendar-date FE			
$> 20°$C (tropical night)	0.132***	0.121**	0.137***	0.128**
	(0.0477)	(0.0493)	(0.0485)	(0.0505)
Tropical-night effect (%)	14.1	12.9	14.7	13.7
Mean dep. var.	0.007	0.008	0.024	0.062
Mean accidents/day	10.79	10.79	10.79	10.79
Daily Δ accidents	1.52	1.39	1.59	1.48
Pseudo-R^2	0.364	0.369	0.270	0.213
Observations	3,224,581	3,065,052	966,317	375,452
	Panel B. Calendar-date FE and max. temp.			
$> 20°$C (tropical night)	0.139***	0.125**	0.143***	0.133**
	(0.0496)	(0.0508)	(0.0506)	(0.0522)
Tropical-night effect (%)	14.9	13.3	15.4	14.2
Mean dep. var.	0.007	0.008	0.024	0.062
Mean accidents/day	10.79	10.79	10.79	10.79
Daily Δ accidents	1.60	1.44	1.66	1.54
Pseudo-R^2	0.364	0.369	0.270	0.213
Observations	3,224,581	3,065,052	966,317	375,452
	Controls and fixed effects (both panels)			
Precipitation & wind speed	✓	✓	✓	✓
Mun. & calendar-date FE	✓	✓	✓	✓
Prov. × month FE	✓			
Prov. × week FE		✓		
Mun. × month FE			✓	
Mun. × week FE				✓

Notes: The dependent variable is the number of commuting drivers involved in traffic accidents. All columns are estimated by PPML and include calendar-date fixed effects, which absorb shocks common to municipalities on the same date. Panel A controls linearly for same-day maximum temperature. Panel B instead controls for same-day maximum temperature in bins of at most 10°C, 10–15°C, 15–20°C, 20–25°C, 25–30°C, 30–35°C, and above 35°C; the 20–25°C bin is omitted. Both panels include minimum-temperature bins, with 15–20°C omitted, as well as precipitation and maximum wind speed. Standard errors clustered by municipality are reported in parentheses. The tropical-night effect is computed as $100 \times [\exp(\hat{\alpha}) - 1]$, where $\hat{\alpha}$ is the coefficient on the $> 20°$C minimum-temperature bin. Mean dep. var. is the column-specific mean of the municipality-day outcome. Mean accidents/day is the mean number of commuting drivers involved in accidents per calendar day in the column-specific estimation sample. Daily Δ accidents is computed as $[\exp(\hat{\alpha}) - 1] \times$ mean accidents/day and refers to commuting drivers involved in accidents. Significance levels: * $p < 0.10$, ** $p < 0.05$, *** $p < 0.01$.

positive throughout and larger in the earlier window in every corresponding column. In each panel, they are statistically significant in columns (1)-(6), but not in the last two columns, which use the most demanding municipality-by-week fixed effects. These additional results make the explanation based solely on daytime heat experienced further less plausible.

Table B.6. The impact of tropical nights on early-morning commuting accidents

	(1)	(2)	(3)	(4)	(5)	(6)	(7)	(8)
				Panel A. Accidents before 11:00 a.m.				
$> 20°$C (tropical night)	0.165**	0.147**	0.145*	0.127*	0.154**	0.133*	0.125	0.102
	(0.0735)	(0.0731)	(0.0764)	(0.0752)	(0.0745)	(0.0735)	(0.0800)	(0.0785)
Tropical-night effect (%)	17.9	15.8	15.6	13.5	16.6	14.2	13.3	10.7
Mean dep. var.	0.004	0.004	0.005	0.005	0.017	0.017	0.048	0.048
Mean accidents/day	4.08	4.08	4.08	4.08	4.08	4.08	4.08	4.08
Daily Δ accidents	0.73	0.65	0.64	0.55	0.68	0.58	0.54	0.44
Pseudo-R^2	0.275	0.290	0.275	0.291	0.178	0.196	0.127	0.150
Observations	2,101,877	2,101,877	1,757,503	1,757,503	538,353	538,353	184,296	184,296
				Panel B. Accidents before 9:00 a.m.				
$> 20°$C (tropical night)	0.188**	0.175**	0.165*	0.157*	0.174**	0.160*	0.142	0.128
	(0.0852)	(0.0841)	(0.0871)	(0.0848)	(0.0883)	(0.0866)	(0.0937)	(0.0909)
Tropical-night effect (%)	20.7	19.1	17.9	17.0	19.0	17.4	15.3	13.7
Mean dep. var.	0.004	0.004	0.005	0.005	0.015	0.015	0.045	0.045
Mean accidents/day	2.93	2.93	2.93	2.93	2.93	2.93	2.93	2.93
Daily Δ accidents	0.61	0.56	0.53	0.50	0.56	0.51	0.45	0.40
Pseudo-R^2	0.247	0.260	0.244	0.259	0.151	0.169	0.104	0.126
Observations	1,767,750	1,767,750	1,365,045	1,365,045	435,125	435,125	142,853	142,853
				Controls and fixed effects (both panels)				
Weather controls	✓	✓	✓	✓	✓	✓	✓	✓
Mun. & week-year FE	✓	✓	✓	✓	✓	✓	✓	✓
Prov. × month FE	✓	✓						
Prov. × week FE			✓	✓				
Mun. × month FE					✓	✓		
Mun. × week FE							✓	✓
Day-of-week FE		✓		✓		✓		✓

Notes: The dependent variable is the number of commuting drivers involved in traffic accidents occurring before 11:00 a.m. in Panel A and before 9:00 a.m. in Panel B. All columns are estimated by PPML. Temperature bins are defined using daily minimum temperature; the omitted category is 15°C–20°C. Weather controls include precipitation, same-day maximum temperature, and maximum wind speed. Standard errors clustered by municipality are reported in parentheses. The tropical-night effect is computed as $100 \times [\exp(\hat{\alpha}) - 1]$, where $\hat{\alpha}$ is the coefficient on the $> 20°$C bin. Mean dep. var. is the column-specific mean of the municipality-day outcome. Mean accidents/day is the mean number of commuting drivers involved in accidents per calendar day in the column-specific estimation sample. Daily Δ accidents is computed as $[\exp(\hat{\alpha}) - 1] \times$ mean accidents/day and refers to commuting drivers involved in accidents. Significance levels: * $p < 0.10$, ** $p < 0.05$, *** $p < 0.01$.

Next, as explained in the main text, I examine whether the main result persists under a broader measure of routine work- and school-related travel that is also largely non-discretionary. Specifically,

the DGT also records accidents involving drivers traveling on work-related assignments, students traveling to educational institutions, and parents driving children to or from school. Although these trip categories do not fall within the strict definition of commuting,[42] such trips are typically routine and may be difficult to postpone. I therefore re-estimate equation (2.1) using an outcome that includes these additional accident categories alongside baseline commuting accidents.

Table B.7. The impact of tropical nights on commuting and other routine work- and school-related travel accidents

	(1)	(2)	(3)	(4)	(5)	(6)	(7)	(8)
$>$ 20°C (tropical night)	0.148***	0.141***	0.141***	0.133***	0.150***	0.143***	0.144***	0.136***
	(0.0462)	(0.0431)	(0.0467)	(0.0434)	(0.0466)	(0.0436)	(0.0470)	(0.0439)
Weather controls	✓	✓	✓	✓	✓	✓	✓	✓
Mun. & week-year FE	✓	✓	✓	✓	✓	✓	✓	✓
Prov. × month FE	✓	✓						
Prov. × week FE			✓	✓				
Mun. × month FE					✓	✓		
Mun. × week FE							✓	✓
Day-of-week FE		✓		✓		✓		✓
Tropical-night effect (%)	16.0	15.1	15.1	14.2	16.2	15.4	15.5	14.6
Mean dep. var.	0.008	0.008	0.008	0.008	0.026	0.026	0.066	0.066
Mean accidents/day	12.54	12.54	12.54	12.54	12.54	12.54	12.54	12.54
Daily Δ accidents	2.00	1.90	1.89	1.79	2.04	1.93	1.95	1.83
Pseudo-R^2	0.358	0.370	0.361	0.374	0.258	0.274	0.192	0.211
Observations	3,398,090	3,398,090	3,254,751	3,254,751	1,050,166	1,050,166	416,851	416,851

Notes: The dependent variable is the number of drivers involved in traffic accidents while commuting, traveling on work-related assignments, traveling to educational institutions, or driving children to or from school. All columns are estimated by PPML and report the coefficient on the tropical-night indicator (daily minimum temperature above 20°C). Temperature bins are defined using daily minimum temperature; the omitted category is 15°C–20°C. Weather controls include precipitation, maximum temperature, and maximum wind speed. Standard errors clustered by municipality are reported in parentheses. The tropical-night effect is computed as $100 \times [\exp(\hat{\alpha}) - 1]$, where $\hat{\alpha}$ is the coefficient on the $>$ 20°C bin. Mean dep. var. is the column-specific mean of the municipality-day outcome. Mean accidents/day is the mean number of drivers in these travel categories involved in accidents per calendar day in the column-specific estimation sample. Daily Δ accidents is computed as $[\exp(\hat{\alpha}) - 1] \times$ mean accidents/day. All accident statistics refer to drivers involved in accidents. Significance levels: * $p < 0.10$, ** $p < 0.05$, *** $p < 0.01$.

The empirical results are presented in Table B.7, which mirrors the structure of Table 1. The estimated coefficient on the tropical-night indicator remains positive and statistically significant at the 1% level in every specification, ranging from 0.133 to 0.150. These estimates are comparable to (and generally slightly larger than) those in Table 1. Thus, the main pattern persists when the outcome is broadened to include other routine work- and school-related trips, a result consistent with the relevance of nighttime heat for time-constrained and unavoidable travel.

[42] Unlike *in itinere* (commuting) accidents, these categories are not subject to the labor-insurance provisions that require commuting status to be explicitly verified. I therefore treat them as supplementary evidence and focus the baseline analysis on the commuting-accident sample.

Table B.8. The impact of tropical nights on accidents involving holiday travelers and professional drivers

	(1)	(2)	(3)	(4)	(5)	(6)	(7)	(8)
	Panel A. Drivers traveling for holidays or long weekends							
$>$ 20°C (tropical night)	-0.0335	-0.0126	-0.0488	-0.0301	-0.0570	-0.0318	-0.0779	-0.0582
	(0.136)	(0.136)	(0.144)	(0.143)	(0.135)	(0.136)	(0.137)	(0.138)
Mean dep. var.	0.003	0.003	0.007	0.007	0.013	0.013	0.044	0.044
Observations	230,368	230,368	120,726	120,726	59,154	59,154	17,972	17,972
	Panel B. Professional drivers							
$>$ 20°C (tropical night)	-0.0206	-0.0331	-0.0193	-0.0319	-0.0044	-0.0190	-0.0031	-0.0173
	(0.0740)	(0.0784)	(0.0774)	(0.0809)	(0.0753)	(0.0793)	(0.0795)	(0.0824)
Mean dep. var.	0.004	0.004	0.004	0.004	0.016	0.016	0.046	0.046
Observations	2,452,197	2,452,197	2,159,809	2,159,809	592,516	592,516	205,395	205,395
	Controls and fixed effects (both panels)							
Weather controls	✓	✓	✓	✓	✓	✓	✓	✓
Mun. & week-year FE	✓	✓	✓	✓	✓	✓	✓	✓
Prov. $\times$ month FE	✓	✓						
Prov. $\times$ week FE			✓	✓				
Mun. $\times$ month FE					✓	✓		
Mun. $\times$ week FE							✓	✓
Day-of-week FE		✓		✓		✓		✓

Notes: The dependent variable is the number of drivers of the corresponding type involved in traffic accidents. Panel A reports estimates for drivers traveling for holidays or long weekends; Panel B reports estimates for professional drivers. All columns are estimated by PPML and report the coefficient on the tropical-night indicator (daily minimum temperature above 20°C). Temperature bins are defined using daily minimum temperature; the omitted category is 15°C–20°C. Weather controls include precipitation, maximum temperature, and maximum wind speed. Standard errors clustered by municipality are reported in parentheses. Mean dep. var. is the column-specific mean of the municipality-day outcome. Significance levels: * $p < 0.10$, ** $p < 0.05$, *** $p < 0.01$.

To further evaluate the sleep-disruption interpretation, I next focus on accidents involving holiday-related travel. The DGT records whether a driver involved in an accident was traveling for a holiday or long weekend. Unlike commuting and other work- or school-related travel, these trips are generally discretionary and can more easily be postponed, delayed, or canceled. Thus, if the main effect estimated in this paper reflects the combination of heat-disrupted sleep and workers' limited ability to avoid routine travel, the effect should be weaker or absent for holiday-related trips—a reduction in discretionary travel following tropical nights could even lead to fewer accidents involving such travelers. The coefficients for the tropical-night indicator using the subsample of drivers involved in holiday-related accidents are shown in Table B.8, Panel A. The point estimates are negative in all eight specifications but statistically indistinguishable from zero. In line with my prediction, this pattern is consistent with the possibility that discretionary trips are deferred or avoided following tropical nights.

A related possibility is that driving experience and specialized training help mitigate the consequences of impaired attention following disrupted sleep. To explore this possibility, I next examine whether the effect of tropical nights differs between professional drivers and typical commuters. Specifically, the DGT records accidents occurring during the performance of occupations such as freight transport, taxi and bus services, cleaning and waste collection, road maintenance, firefighting, police patrol, and ambulance operations. Unlike typical commuters, driving forms part of these workers' occupational duties, and they may have greater driving experience or more specialized training. Consequently, if these characteristics mitigate the consequences of impaired attention, the estimated effect of tropical nights may be smaller among this group.[43] Estimates for this subsample are presented in Table B.8, Panel B. The coefficient of interest is close to zero and statistically indistinguishable from zero across all columns, consistent with the possibility of a weaker response during professional driving.

Finally, I examine the effects of both contemporaneous and lagged exposure to elevated nighttime temperatures on accident risk by augmenting equation (2.1) with an indicator for whether at least one tropical night occurred in the preceding days (excluding the current day). Table B.9 reports these estimates using a five-day window in Panel A and the corresponding estimates using a seven-day window in Panel B. In both panels, the contemporaneous tropical-night coefficient remains close to the baseline estimate in Table 1. Moreover, the coefficient on recent exposure is positive across specifications but

[43] To the extent that some professional drivers (e.g., freight transport drivers) can adjust their schedules or postpone non-urgent tasks, such flexibility could also attenuate the effect of tropical nights on accident risk.

Table B.9. The impact of current and lagged tropical nights on commuting accidents

	(1)	(2)	(3)	(4)	(5)	(6)	(7)	(8)
				Panel A. Five-day lag window				
$>20°$C (tropical night)	0.127***	0.120***	0.124**	0.117**	0.131***	0.124***	0.130**	0.123**
	(0.0481)	(0.0456)	(0.0502)	(0.0471)	(0.0490)	(0.0463)	(0.0514)	(0.0484)
$>20°$C (previous 5 days)	0.0579	0.0593	0.0440	0.0471	0.0710*	0.0712*	0.0472	0.0469
	(0.0378)	(0.0388)	(0.0383)	(0.0396)	(0.0377)	(0.0387)	(0.0394)	(0.0411)
Mean dep. var.	0.007	0.007	0.008	0.008	0.024	0.024	0.062	0.062
Observations	3,253,330	3,253,330	3,092,721	3,092,721	973,230	973,230	378,248	378,248
				Panel B. Seven-day lag window				
$>20°$C (tropical night)	0.128***	0.122***	0.125**	0.119***	0.132***	0.126***	0.130**	0.124***
	(0.0469)	(0.0445)	(0.0490)	(0.0461)	(0.0479)	(0.0454)	(0.0506)	(0.0477)
$>20°$C (previous 7 days)	0.0617	0.0571	0.0465	0.0428	0.0759**	0.0707*	0.0536	0.0477
	(0.0388)	(0.0370)	(0.0377)	(0.0364)	(0.0380)	(0.0362)	(0.0381)	(0.0369)
Mean dep. var.	0.007	0.007	0.008	0.008	0.024	0.024	0.062	0.062
Observations	3,253,330	3,253,330	3,092,721	3,092,721	974,884	974,884	378,787	378,787
				Controls and fixed effects (both panels)				
Weather controls	✓	✓	✓	✓	✓	✓	✓	✓
Mun. & week-year FE	✓	✓	✓	✓	✓	✓	✓	✓
Prov. × month FE	✓	✓						
Prov. × week FE			✓	✓				
Mun. × month FE					✓	✓		
Mun. × week FE							✓	✓
Day-of-week FE		✓		✓		✓		✓

Notes: The dependent variable is the number of commuting drivers involved in traffic accidents. All columns are estimated by PPML. The tropical-night indicator equals one when daily minimum temperature exceeds 20°C. The lagged indicator equals one if at least one tropical night occurred during the previous five days in Panel A or during the previous seven days in Panel B. Temperature bins for the current night are defined using daily minimum temperature; the omitted category is 15°C–20°C. Weather controls include precipitation, maximum temperature, and maximum wind speed. Standard errors clustered by municipality are reported in parentheses. Mean dep. var. is the column-specific mean of the municipality-day outcome. Significance levels: * $p < 0.10$, ** $p < 0.05$, *** $p < 0.01$.

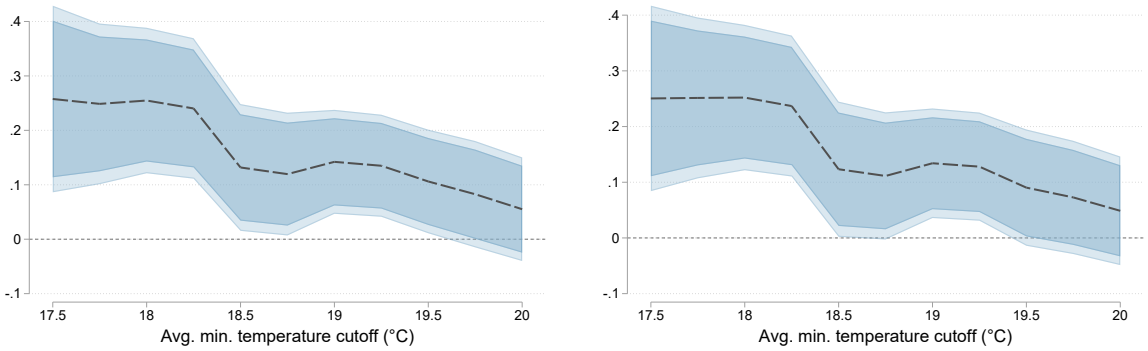
less precisely estimated, reaching conventional significance levels in only some columns. These results provide suggestive evidence that recent nighttime heat exposure contributes to accident risk beyond the contemporaneous effect.

Appendix B.3. Adaptation: additional results and robustness checks

Section 4.1 in the main text examines how the estimated effect of tropical nights changes as the sample expands to include municipalities with warmer nighttime climates. Specifically, I re-estimate equation (2.1) across samples defined by progressively higher thresholds for the maximum monthly mean minimum temperature. Figure 1 in the main text presents these estimates for the preferred baseline specification (Panel A) and a more demanding specification that includes municipality-by-month and day-of-the-week fixed effects (Panel B)—corresponding to Columns (2) and (6) of Table 1, respectively.

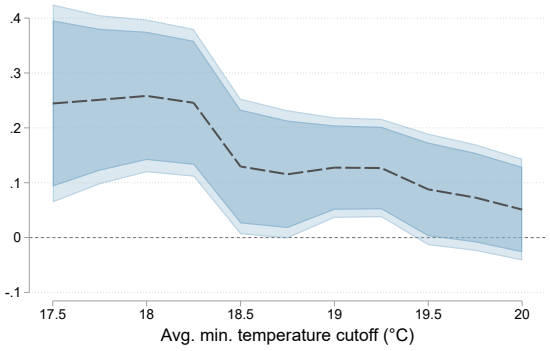
For the sake of completeness, Figure B.1 extends this exercise to the six remaining model specifications in Table 1, with Panels A-F corresponding to Columns (1), (3)-(5), and (7)-(8), respectively. All these figures display a nearly identical pattern: the estimated effect of tropical nights is larger in samples restricted to historically cooler municipalities and declines as municipalities with warmer nighttime climates enter the sample. As discussed in the main text, this pattern is consistent with adaptation attenuating the adverse effects of nighttime heat in historically warmer locations.

Figure B.1. The effect of tropical nights by local nighttime climate (alternative model specifications)

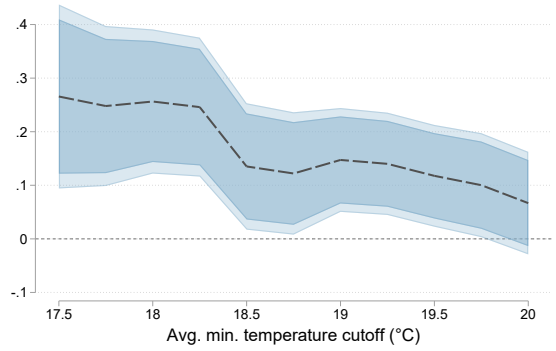


(A) Province × month FE

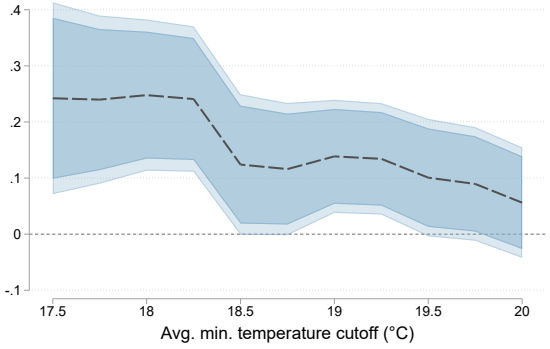
(B) Province × week FE



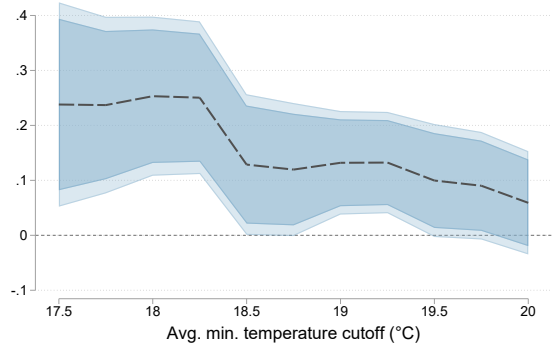
(C) Province × week FE + day-of-the-week FE



(D) Municipality × month FE



(E) Municipality × week FE



(F) Municipality × week FE + day-of-the-week FE

Notes: The figure reports the estimated coefficient on the tropical-night indicator (minimum temperature above 20°C) from equation (2.1) across subsamples of municipalities defined by alternative average minimum temperature cutoffs. Each estimate uses municipalities whose highest monthly average minimum temperature does not exceed the cutoff shown on the horizontal axis, which ranges from 17.5°C to 20°C in increments of 0.25°C. The dashed line connects the point estimates. All specifications include weather controls, municipality fixed effects, and week-by-year fixed effects. The panels additionally include province-by-month fixed effects (Panel A); province-by-week fixed effects (Panel B); province-by-week and day-of-the-week fixed effects (Panel C); municipality-by-month fixed effects (Panel D); municipality-by-week fixed effects (Panel E); and municipality-by-week and day-of-the-week fixed effects (Panel F). Shaded areas denote 90% (darker blue) and 95% (lighter blue) confidence intervals based on standard errors clustered at the municipality level.

Appendix B.4. Gender: additional results and robustness checks

This appendix presents additional evidence on the gender heterogeneity discussed in Section 4.2. I begin that section by estimating equation (2.1) separately by gender, using the number of female and male commuting drivers involved in traffic accidents as the respective outcomes. However, involvement does not necessarily imply responsibility for the accident: in a collision involving both female and male drivers, for example, a female commuter may be involved even if a male driver caused the crash (and vice versa). To address this concern, I repeat the analysis using commuting-driver counts from accidents in which the sole driver involved (in single-driver accidents) or all involved drivers (in multi-driver accidents) are of the corresponding gender. This restriction excludes mixed-gender collisions.

Table B.10 reports the results, which display a similar gender pattern to those in Table 3 in the main text. For female commuting drivers (Panel A), the tropical-night coefficient remains positive and statistically significant across all columns. These coefficients are somewhat larger than their counterparts in Table 3, although the implied daily increase is smaller—reflecting the lower baseline daily count in the restricted sample. For male commuting drivers (Panel B), the estimated coefficients remain considerably smaller than those for women and statistically indistinguishable from zero across all specifications.

Next, I also estimate the effect separately for female and male commuting drivers under 30. As discussed in the main text, this cutoff is motivated by data from INE showing that the median age at first birth during the sample period was 30.8 years. The exercise therefore focuses on an age group for whom child-related responsibilities are likely less prevalent. Table B.11 reports the results of this empirical exercise. Across specifications, the estimated coefficient ranges from 0.264 to 0.282 for women (statistically significant at the 10% level in seven specifications) and from 0.228 to 0.256 for men (significant at the 5% level throughout). Thus, although the estimates remain somewhat larger for women, the gender difference is considerably smaller than in Table 3. Moreover, because the mean daily number of male commuting drivers under 30 involved in accidents is higher, the implied daily increase is larger for men: approximately 0.43-0.49 additional male drivers, compared with 0.30-0.33 additional female drivers. This pattern differs from the results in Table 3, where the estimated effect is statistically significant for women but not for men.

I next examine the gender-specific response for commuting accidents in which excessive speed was recorded as a contributing factor. As explained in Section 4.2, this exercise speaks to the proposed

Table B.10. The impact of tropical nights on commuting accidents by gender (all involved drivers of the same gender)

	(1)	(2)	(3)	(4)	(5)	(6)	(7)	(8)
				Panel A. Female drivers				
$> 20°$C (tropical night)	0.357***	0.346***	0.383***	0.373***	0.359***	0.344***	0.368***	0.349***
	(0.127)	(0.133)	(0.125)	(0.129)	(0.128)	(0.134)	(0.126)	(0.131)
Tropical-night effect (%)	42.9	41.3	46.7	45.2	43.2	41.1	44.5	41.8
Mean dep. var.	0.003	0.003	0.004	0.004	0.012	0.012	0.037	0.037
Mean accidents/day	1.69	1.69	1.69	1.69	1.69	1.69	1.69	1.69
Daily Δ accidents	0.73	0.70	0.79	0.76	0.73	0.70	0.75	0.71
Pseudo-R^2	0.195	0.205	0.194	0.204	0.106	0.118	0.071	0.087
Observations	1,451,981	1,451,981	1,040,097	1,040,097	318,626	318,626	98,622	98,622
				Panel B. Male drivers				
$> 20°$C (tropical night)	0.0886	0.0839	0.0830	0.0777	0.0918	0.0863	0.0882	0.0837
	(0.0732)	(0.0687)	(0.0740)	(0.0693)	(0.0744)	(0.0701)	(0.0749)	(0.0706)
Tropical-night effect (%)	9.3	8.8	8.7	8.1	9.6	9.0	9.2	8.7
Mean dep. var.	0.004	0.004	0.005	0.005	0.017	0.017	0.049	0.049
Mean accidents/day	5.00	5.00	5.00	5.00	5.00	5.00	5.00	5.00
Daily Δ accidents	0.46	0.44	0.43	0.40	0.48	0.45	0.46	0.44
Pseudo-R^2	0.280	0.289	0.284	0.294	0.177	0.189	0.120	0.134
Observations	2,451,410	2,451,410	2,203,406	2,203,406	625,660	625,660	223,323	223,323
				Controls and fixed effects (both panels)				
Weather controls	✓	✓	✓	✓	✓	✓	✓	✓
Mun. & week-year FE	✓	✓	✓	✓	✓	✓	✓	✓
Prov. × month FE	✓	✓						
Prov. × week FE			✓	✓				
Mun. × month FE					✓	✓		
Mun. × week FE							✓	✓
Day-of-week FE		✓		✓		✓		✓

Notes: The dependent variable is the number of commuting drivers of the corresponding gender involved in accidents in which the sole driver (in single-driver accidents) or all involved drivers (in multi-driver accidents) are of that gender. Panel A reports estimates for accidents involving only female drivers; Panel B reports estimates for accidents involving only male drivers. All columns are estimated by PPML. Temperature bins are defined using daily minimum temperature; the omitted category is 15°C–20°C. Weather controls include precipitation, maximum temperature, and maximum wind speed. Standard errors clustered by municipality are reported in parentheses. The tropical-night effect is computed as $100 \times [\exp(\hat{\alpha}) - 1]$, where $\hat{\alpha}$ is the coefficient on the $> 20°$C bin. Mean dep. var. is the column-specific mean of the municipality-day outcome. Mean accidents/day is the mean number of commuting drivers involved in accidents per calendar day in the column-specific estimation sample. Daily Δ accidents is computed as $[\exp(\hat{\alpha}) - 1] \times$ mean accidents/day and refers to commuting drivers involved in accidents. Significance levels: * $p < 0.10$, ** $p < 0.05$, *** $p < 0.01$.

Table B.11. The impact of tropical nights on commuting accidents by gender (drivers under 30)

	(1)	(2)	(3)	(4)	(5)	(6)	(7)	(8)
				Panel A. Female drivers under 30				
$>$ 20°C (tropical night)	0.268*	0.266	0.264*	0.266*	0.282*	0.278*	0.279*	0.271*
	(0.162)	(0.164)	(0.152)	(0.154)	(0.165)	(0.166)	(0.154)	(0.156)
Tropical-night effect (%)	30.7	30.5	30.2	30.5	32.6	32.0	32.2	31.1
Mean dep. var.	0.002	0.002	0.003	0.003	0.011	0.011	0.035	0.035
Mean accidents/day	1.01	1.01	1.01	1.01	1.01	1.01	1.01	1.01
Daily Δ accidents	0.31	0.31	0.30	0.31	0.33	0.32	0.32	0.31
Pseudo-R^2	0.173	0.181	0.174	0.182	0.090	0.100	0.057	0.070
Observations	993,669	993,669	663,237	663,237	206,443	206,443	61,831	61,831
				Panel B. Male drivers under 30				
$>$ 20°C (tropical night)	0.255**	0.256**	0.229**	0.228**	0.246**	0.247**	0.236**	0.233**
	(0.107)	(0.107)	(0.105)	(0.105)	(0.110)	(0.109)	(0.106)	(0.106)
Tropical-night effect (%)	29.0	29.2	25.7	25.6	27.9	28.0	26.6	26.2
Mean dep. var.	0.003	0.003	0.004	0.004	0.013	0.013	0.038	0.038
Mean accidents/day	1.67	1.67	1.67	1.67	1.67	1.67	1.68	1.68
Daily Δ accidents	0.49	0.49	0.43	0.43	0.47	0.47	0.45	0.44
Pseudo-R^2	0.214	0.220	0.215	0.221	0.117	0.125	0.075	0.085
Observations	1,319,297	1,319,297	956,529	956,529	292,283	292,283	95,530	95,530
				Controls and fixed effects (both panels)				
Weather controls	✓	✓	✓	✓	✓	✓	✓	✓
Mun. & week-year FE	✓	✓	✓	✓	✓	✓	✓	✓
Prov. $\times$ month FE	✓	✓						
Prov. $\times$ week FE			✓	✓				
Mun. $\times$ month FE					✓	✓		
Mun. $\times$ week FE							✓	✓
Day-of-week FE		✓		✓		✓		✓

Notes: The dependent variable is the number of commuting drivers under 30 of the corresponding gender involved in traffic accidents. Panel A reports estimates for female drivers under 30; Panel B reports estimates for male drivers under 30. All columns are estimated by PPML. Temperature bins are defined using daily minimum temperature; the omitted category is 15°C–20°C. Weather controls include precipitation, maximum temperature, and maximum wind speed. Standard errors clustered by municipality are reported in parentheses. The tropical-night effect is computed as $100 \times [\exp(\hat{\alpha}) - 1]$, where $\hat{\alpha}$ is the coefficient on the $>$ 20°C bin. Mean dep. var. is the column-specific mean of the municipality-day outcome. Mean accidents/day is the mean number of commuting drivers under 30 of the corresponding gender involved in accidents per calendar day in the column-specific estimation sample. Daily Δ accidents is computed as $[\exp(\hat{\alpha}) - 1] \times$ mean accidents/day and refers to commuting drivers under 30 of the corresponding gender involved in accidents. Significance levels: * $p < 0.10$, ** $p < 0.05$, *** $p < 0.01$.

Table B.12. The impact of tropical nights on commuting accidents involving excessive speed by gender

	(1)	(2)	(3)	(4)	(5)	(6)	(7)	(8)
				Panel A. Female drivers				
$>20°$C (tropical night)	0.984***	0.984***	0.935**	0.937**	1.067***	1.052***	1.012***	1.014**
	(0.338)	(0.341)	(0.368)	(0.374)	(0.360)	(0.365)	(0.385)	(0.394)
Tropical-night effect (%)	167.5	167.5	154.7	155.2	190.7	186.3	175.1	175.7
Mean dep. var.	0.002	0.002	0.003	0.003	0.009	0.009	0.032	0.032
Mean accidents/day	0.43	0.43	0.43	0.43	0.43	0.43	0.43	0.43
Daily Δ accidents	0.73	0.73	0.67	0.67	0.83	0.81	0.76	0.76
Pseudo-R^2	0.138	0.144	0.153	0.159	0.090	0.098	0.083	0.093
Observations	422,923	422,923	263,387	263,387	91,849	91,849	26,162	26,162
				Panel B. Male drivers				
$>20°$C (tropical night)	0.331	0.332	0.292	0.298	0.337*	0.338	0.310	0.309
	(0.205)	(0.206)	(0.212)	(0.214)	(0.205)	(0.206)	(0.217)	(0.220)
Tropical-night effect (%)	39.2	39.4	33.9	34.7	40.1	40.2	36.3	36.2
Mean dep. var.	0.002	0.002	0.003	0.003	0.009	0.009	0.033	0.033
Mean accidents/day	0.67	0.67	0.67	0.67	0.67	0.67	0.67	0.67
Daily Δ accidents	0.26	0.26	0.23	0.23	0.27	0.27	0.24	0.24
Pseudo-R^2	0.153	0.159	0.153	0.161	0.080	0.089	0.052	0.063
Observations	736,270	736,270	429,232	429,232	151,359	151,359	43,100	43,100
				Controls and fixed effects (both panels)				
Weather controls	✓	✓	✓	✓	✓	✓	✓	✓
Mun. & week-year FE	✓	✓	✓	✓	✓	✓	✓	✓
Prov. $\times$ month FE	✓	✓						
Prov. $\times$ week FE			✓	✓				
Mun. $\times$ month FE					✓	✓		
Mun. $\times$ week FE							✓	✓
Day-of-week FE		✓		✓		✓		✓

Notes: The dependent variable is the number of commuting drivers of the corresponding gender involved in traffic accidents in which excessive speed was recorded as a contributing factor. Panel A reports estimates for female drivers; Panel B reports estimates for male drivers. All columns are estimated by PPML. Temperature bins are defined using daily minimum temperature; the omitted category is 15°C–20°C. Weather controls include precipitation, maximum temperature, and maximum wind speed. Standard errors clustered by municipality are reported in parentheses. The tropical-night effect is computed as $100 \times [\exp(\hat{\alpha}) - 1]$, where $\hat{\alpha}$ is the coefficient on the $>20°$C bin. Mean dep. var. is the column-specific mean of the municipality-day outcome. Mean accidents/day is the mean number of commuting drivers of the corresponding gender involved in accidents in which excessive speed was recorded as a contributing factor per calendar day in the column-specific estimation sample. Daily Δ accidents is computed as $[\exp(\hat{\alpha}) - 1] \times$ mean accidents/day and refers to commuting drivers of the corresponding gender involved in such accidents. Significance levels: * $p < 0.10$, ** $p < 0.05$, *** $p < 0.01$.

time-pressure mechanism: if caregiving responsibilities compress women's daily schedules and make it harder to adjust departure times following disrupted sleep, pressure to maintain those schedules may make speeding-related accident involvement particularly responsive to tropical nights among women.

Table B.12 reports the full set of estimates. The coefficient on the tropical-night indicator is approximately 1 for women and statistically significant at least at the 5% level across all specifications. However, the corresponding estimates for men are considerably smaller (approximately 0.3), and generally statistically indistinguishable from zero. The implied daily increase is also larger for women despite the higher baseline incidence among male drivers. These point estimates reveal a substantially stronger speeding-related response among women and are consistent with the hypothesis that time constraints constitute one channel through which disrupted sleep affects commuting behavior.

Table B.13. The impact of tropical nights on commuting accidents involving excessive speed (female drivers under 30)

	(1)	(2)	(3)	(4)	(5)	(6)	(7)	(8)
$>$ 20°C (tropical night)	-0.194	-0.176	-0.399	-0.383	-0.0055	0.0143	-0.283	-0.293
	(0.799)	(0.793)	(0.855)	(0.865)	(0.826)	(0.818)	(0.902)	(0.906)
Weather controls	✓	✓	✓	✓	✓	✓	✓	✓
Mun. & week-year FE	✓	✓	✓	✓	✓	✓	✓	✓
Prov. × month FE	✓	✓						
Prov. × week FE			✓	✓				
Mun. × month FE					✓	✓		
Mun. × week FE							✓	✓
Day-of-week FE		✓		✓		✓		✓
Mean dep. var.	0.002	0.002	0.005	0.005	0.012	0.012	0.041	0.041
Observations	133,667	133,667	69,527	69,527	27,179	27,179	7,668	7,668

Notes: The dependent variable is the number of female commuting drivers under 30 involved in traffic accidents for which excessive speed was recorded as a contributing factor. All columns are estimated by PPML and report the coefficient on the tropical-night indicator (daily minimum temperature above 20°C). Temperature bins are defined using daily minimum temperature; the omitted category is 15°C–20°C. Weather controls include precipitation, maximum temperature, and maximum wind speed. Standard errors clustered by municipality are reported in parentheses. Mean dep. var. is the column-specific mean of the municipality-day outcome. Significance levels: * $p < 0.10$, ** $p < 0.05$, *** $p < 0.01$.

As an additional suggestive exercise, Table B.13 estimates the speeding-related regression for the subset of female commuting drivers under 30—an age group for whom child-related responsibilities are likely less prevalent, as discussed above. The point estimates range from -0.399 to 0.014, exhibit no consistently positive (or negative) pattern, and are statistically indistinguishable from zero across all specifications. These estimates are also substantially smaller in magnitude than the corresponding estimates in Table B.12 (Panel A). This contrast is consistent with the proposed caregiving-related time-pressure

mechanism, as the estimates provide no evidence of increased speeding-related accident involvement among women for whom caregiving responsibilities are likely less prevalent.

Table B.14. The impact of tropical nights on commuting accidents among female drivers by age group

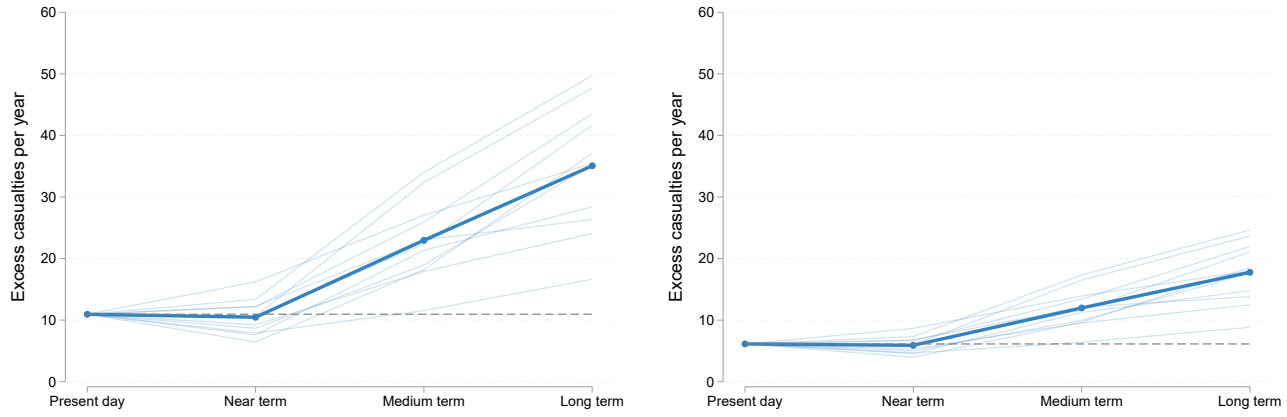
	(1)	(2)	(3)	(4)	(5)	(6)	(7)	(8)
				Panel A. Female drivers aged $[45, 48)$				
$>20°$C (tropical night)	-0.0255	-0.0414	-0.116	-0.114	-0.0362	-0.0555	-0.226	-0.227
	(0.287)	(0.294)	(0.288)	(0.296)	(0.286)	(0.290)	(0.303)	(0.312)
Mean dep. var.	0.002	0.002	0.004	0.004	0.010	0.010	0.035	0.035
Observations	269,938	269,938	151,467	151,467	60,486	60,486	17,321	17,321
				Panel B. Female drivers aged $[48, 51)$				
$>20°$C (tropical night)	0.568**	0.567**	0.541**	0.550**	0.691***	0.673***	0.701**	0.718**
	(0.238)	(0.237)	(0.271)	(0.269)	(0.243)	(0.242)	(0.275)	(0.280)
Mean dep. var.	0.002	0.002	0.004	0.004	0.010	0.010	0.036	0.036
Observations	243,022	243,022	127,748	127,748	53,303	53,303	14,778	14,778
				Panel C. Female drivers aged $[51, 54)$				
$>20°$C (tropical night)	-0.538	-0.517	-0.634	-0.629	-0.593	-0.557	-0.755*	-0.751*
	(0.387)	(0.390)	(0.430)	(0.431)	(0.377)	(0.384)	(0.406)	(0.411)
Mean dep. var.	0.002	0.002	0.005	0.005	0.011	0.011	0.038	0.038
Observations	180,998	180,998	86,149	86,149	39,717	39,717	11,331	11,331
				Controls and fixed effects (all panels)				
Weather controls	✓	✓	✓	✓	✓	✓	✓	✓
Mun. & week-year FE	✓	✓	✓	✓	✓	✓	✓	✓
Prov. × month FE	✓	✓						
Prov. × week FE			✓	✓				
Mun. × month FE					✓	✓		
Mun. × week FE							✓	✓
Day-of-week FE		✓		✓		✓		✓

Notes: The dependent variable is the number of female commuting drivers in the corresponding age group involved in traffic accidents. Panel A reports estimates for drivers aged 45–48; Panel B reports estimates for drivers aged 48–51; Panel C reports estimates for drivers aged 51–54. All columns are estimated by PPML and report the coefficient on the tropical-night indicator (daily minimum temperature above 20°C). Temperature bins are defined using daily minimum temperature; the omitted category is 15°C–20°C. Weather controls include precipitation, maximum temperature, and maximum wind speed. Standard errors clustered by municipality are reported in parentheses. Mean dep. var. is the column-specific mean of the municipality-day outcome. Significance levels: * $p < 0.10$, ** $p < 0.05$, *** $p < 0.01$.

A complementary mechanism that may contribute to the larger point estimates among women in Table 3 is sex-specific variation in thermoregulation. Prior physiological research documents differences between women and men in sweating and skin-blood-flow responses (Kaciuba-Uscilko and Grucza, 2001; Charkoudian et al., 2017), and shows that hormonal changes during the menopausal transition

(perimenopause) can affect temperature regulation and may heighten sensitivity to heat (Monteleone et al., 2018; Charkoudian et al., 2017; Conti et al., 2025). Motivated by this evidence, Table B.14 presents a suggestive age-based exercise for female commuting drivers in three age groups spanning ages commonly associated with the menopausal transition. The tropical-night coefficient is positive and statistically significant across specifications among women aged 48-51—an age cohort associated with the transition into perimenopause and the onset of menopause. By contrast, no positive effect is detected in the adjacent age groups, comprising women aged 45-48 and 51-54. This pattern is consistent with heightened sensitivity around the menopausal transition—although it should be interpreted as suggestive because menopausal status is not observed and age is only an imperfect proxy.

Figure B.2. Projected excess casualties by commuting-driver gender (medium-emissions scenario)



(A) Female drivers **(B)** Male drivers

Notes: The figure shows projected excess casualties per year associated with accidents involving female and male commuting drivers in the sample municipalities, allowing future tropical-night exposure to evolve across horizons and climate models under the medium-emissions scenario (SSP2-4.5), assuming no additional adaptation. Gender refers to the commuting driver whose involvement is modeled. Panel A presents projections associated with female commuting drivers, while Panel B presents projections associated with male commuting drivers. The present-day benchmarks are obtained by applying the gender-specific attributable-share transformation $[1 - \exp(-\hat{\alpha})]$ to the female and male commuting-driver involvements observed on tropical-night days during 2014-2019 and converting the resulting excess involvements into casualties using the observed casualty-per-involvement rate. Future increments use the gender-specific preferred estimates from column (2) of Table 3—Panels A and B, respectively—and are calculated by multiplying the cumulative increase in the annual number of tropical nights relative to the 2014-2019 sample period by each municipality's gender-specific average daily number of commuting drivers involved in accidents and by the implied proportional effect $[\exp(\hat{\alpha}) - 1]$. They are then converted into casualties using the same casualty-per-involvement rate. Near term, medium term, and long term refer to 2011-2040, 2041-2070, and 2071-2100, respectively. Thin lines report projections from the 11 individual climate models, while thick lines report projections based on climate measures averaged across the 11 models.

Next, Figure B.2 complements the aggregate projections in the main text by reporting the corresponding projections separately for female and male commuting drivers, assuming no additional adaptation. For each gender, the calculation applies the estimates from Table 3 to the corresponding municipality-

level baseline incidence during 2014-2019. Across emissions scenarios and horizons, the projected increase is substantially larger among female drivers, reflecting the gender heterogeneity documented in Table 3—note that, since the coefficients for male drivers are imprecisely estimated and statistically indistinguishable from zero, the male series should be interpreted as the mechanical implications of the corresponding point estimates rather than as precise forecasts. Overall, the projections document that, absent further adaptation, the additional commuting burden associated with rising tropical-night exposure would fall disproportionately on female drivers.

Appendix B.5. Income: additional results and robustness checks

Finally, Table 4 in Section 4.3 reports estimates of an extension of equation (2.1) that allows the effect of tropical nights to differ between low- and high-income municipalities. In the main analysis, these groups are defined using municipality-level net household income from INE. As an additional robustness check, Table B.15 repeats the exercise using gross household income to classify municipalities. Across all specifications, the point estimate for low-income municipalities exceeds the corresponding estimate for high-income municipalities. However, the low-income estimates are less precise: two are statistically significant at the 10 percent level, while several others have p-values just above 0.10. Thus, the estimates closely mirror the qualitative pattern in the main text—although the evidence of income heterogeneity should be interpreted as suggestive.

Table B.15. The impact of tropical nights on commuting accidents by gross household income

	(1)	(2)	(3)	(4)	(5)	(6)	(7)	(8)
$>$ 20°C (low income)	0.210	0.235	0.200	0.233*	0.209	0.232	0.216	0.249*
	(0.148)	(0.149)	(0.142)	(0.143)	(0.152)	(0.152)	(0.147)	(0.150)
$>$ 20°C (high income)	0.144***	0.132***	0.136***	0.123**	0.150***	0.137***	0.135**	0.120**
	(0.0496)	(0.0465)	(0.0515)	(0.0479)	(0.0499)	(0.0466)	(0.0533)	(0.0496)
Weather controls	✓	✓	✓	✓	✓	✓	✓	✓
Mun. & week-year FE	✓	✓	✓	✓	✓	✓	✓	✓
Prov. × month FE	✓	✓						
Prov. × week FE			✓	✓				
Mun. × month FE					✓	✓		
Mun. × week FE							✓	✓
Day-of-week FE		✓		✓		✓		✓
Mean dep. var.	0.007	0.007	0.008	0.008	0.024	0.024	0.062	0.062
Mean accidents/day	10.61	10.61	10.61	10.61	10.61	10.61	10.61	10.61
				Low-income				
Tropical-night effect (%)	23.4	26.5	22.1	26.2	23.2	26.1	24.1	28.3
Total Δ accidents	43.87	49.76	42.05	49.89	46.89	52.86	49.45	58.05
Total Δ accidents (conservative)	31.30	30.43	28.34	28.07	40.29	38.98	41.03	40.63
				High-income				
Tropical-night effect (%)	15.5	14.1	14.6	13.1	16.2	14.7	14.5	12.7
Total Δ accidents	24.19	21.96	23.54	21.10	27.24	24.71	25.68	22.64
				Comparison across income groups				
Low/high ratio	1.81	2.27	1.79	2.36	1.72	2.14	1.93	2.56
Low/high ratio (conservative)	1.29	1.39	1.20	1.33	1.48	1.58	1.60	1.79
Pseudo-R^2	0.343	0.355	0.347	0.359	0.243	0.258	0.179	0.199
Observations	3,233,997	3,233,997	3,072,155	3,072,155	967,121	967,121	375,833	375,833

Notes: The dependent variable is the number of commuting drivers involved in traffic accidents. All columns are estimated by PPML. The table reports coefficients on the tropical-night indicator interacted with indicators for municipalities at or below (low income) and above (high income) the median of municipality-level household gross income from INE. Temperature bins are defined using daily minimum temperature; the omitted category is 15°C–20°C. Weather controls include precipitation, maximum temperature, and maximum wind speed. Standard errors clustered by municipality are reported in parentheses. Tropical-night effects are computed as $100 \times [\exp(\hat{\alpha}_g) - 1]$, where $\hat{\alpha}_g$ is the income-group-specific coefficient on the $>$ 20°C indicator. Mean dep. var. is the column-specific mean of the municipality-day outcome. Mean accidents/day is the mean number of commuting drivers involved in accidents per calendar day in the column-specific estimation sample. Total Δ accidents for group g is computed as $[\exp(\hat{\alpha}_g) - 1] \times$ mean accidents/day $\times f_g \times (365 \times 6)$, where f_g is the mean across municipality-years in the estimation sample of the within-year mean of the indicator for a tropical night in income group g. The conservative low-income total equals the pooled aggregate estimate underlying the corresponding column of Table 1 minus the high-income total reported here. Low/high ratios divide the respective low-income total by the high-income total. All accident statistics refer to commuting drivers involved in accidents. Formal tests do not reject equality between the low- and high-income coefficients at conventional levels. Significance levels: * $p < 0.10$, ** $p < 0.05$, *** $p < 0.01$.